

The sequence stratigraphic development of the Late Permian Kapp Starostin Formation, central Spitsbergen

Erika Rørvik Njå

Master of Science Thesis
In Sedimentology/Petroleum Geology

June 2016



Department of Earth Science
University of Bergen



Department of Arctic Geology
The University Centre in Svalbard

Abstract

This study investigated the sedimentology and the sequence stratigraphy of the Late Permian Kapp Starostin Formation in the southwestern part of Dickson Land, central Spitsbergen. The underlying Gipshuken Formation and the overlying Triassic Formation, as well as their boundaries to the Kapp Starostin Formation, were also investigated. In the Barents Sea, the Tempelfjorden Group is represented by the Røye and Ørret formations. The measured section in Dickson Land was compared to an age-equivalent spiculitic unit of the Røye Formation from the Loppa High in the Barents Sea. The core section is approximately 50.3 m long and is a part of the reservoir in the Gohta discovery (well 7120/1-3). Fourteen depositional facies have been recognized from the investigated succession in Dickson Land, and another three facies from the core section from well 7120/1-3. The facies have been grouped into 6 facies associations, where FA1 and FA2 comprises the strata of the Gipshuken Formation, FA3, FA4 and FA5 comprises the strata of the Kapp Starostin Formation and FA6 comprises the strata of the Triassic Vikinghøgda Formation. A depositional model with an inner- mid- and outer ramp area is applied for the Kapp Starostin Formation. The inner ramp comprises the intertidal to shallow subtidal areas above the FWFB and is characterized by well-washed and well-sorted sand shoals and shell banks. The mid ramp is the area between the FWFB and SWWB, and was the site of the dominant silica factory of the shelf during the Permian Chert Event. The outer ramp is the area below the SWWB, which was dominated by accumulation of microscleric sponge spicules and siliceous black shale. Based on the facies analysis and the stacking pattern of the facies, three transgressive-regressive sequences were recognized in the Kapp Starostin Formation. Increasingly shallower facies upward in the formation displays the overall regressive development towards the Permian-Triassic boundary. Late Palaeozoic rocks constitute one of the play models in the Barents Sea, and the Permian Røye Formation represents one of the possible reservoir rocks. The main difference between the Røye Formation and the Kapp Starostin Formation was the high degree of dolomitization of the Røye Formation. The karstification and dolomitization is probably due to prolonged subaerial exposure of the Loppa High.

Acknowledgements

This thesis is part of a master's degree in petroleum geology at the Department of Earth Science at the University of Bergen.

First of all, I would like to thank my supervisors Sten-Andreas Grundvåg (University of Tromsø) and William Helland-Hansen (University of Bergen) for providing an interesting and challenging project, and for their critical review of the thesis. Sten-Andreas is especially thanked for arranging the formalities around the fieldwork and for invaluable help during the first days in the field.

I would also like to thank the logistics department at UNIS for training and equipment that made me well prepared for the weeks in the field.

Irina Maria Dumitru was very helpful with the preparation of thin sections. I also have to thank Udo Zimmermann (University of Stavanger) for letting me use the microscopes at UiS. Last, but not least, I want to thank Anne Mette Tholstrup Simonsen for invaluable assistance and company during the fieldwork on Svalbard, and our two polar bear guards, the dogs Storm and Vesla, for keeping us safe during the nights.

This research was funded by ARCEX partners and the Research Council of Norway (grant number 228107).

Erika Rørvik Njå

Bergen 01.06.2016

Table of Contents

1. Introduction	4
1.1 Preface	4
1.2 Objectives	5
1.3 Geographic location and local topography.....	6
1.4 Study area	9
2. Geological framework.....	12
2.1 Tectonic setting	12
2.2 Lithostratigraphy and sedimentary systems.....	17
2.2.1 The Billefjorden Group	21
2.2.2 The Gipsdalen Group	22
2.2.3 The Tempelfjorden Group	25
2.2.4 The Sassendalen Group	27
2.3 Correlation with the Barents Shelf and Bjørnøya	28
2.4 Correlation with Arctic Canada and North Greenland.....	35
3. Methods	38
4. Facies analysis	40
4.1. Introduction.....	40
4.2 Facies of the Gipshuken Formation	43
4.3 Facies of the Kapp Starostin Formation	49
4.4 Facies of the Vikinghøgda Formation.....	74
4.5 Facies of the Røye Formation.....	75
5. Facies associations.....	80
5.1 Facies association 1 (FA1) – Supratidal flat	80
5.2 Facies association 2 (FA2) – Intertidal to subtidal flat.....	80
5.3 Facies association 3 (FA3) – Shoreface deposits (Inner ramp)	81
5.4 Facies association 4 (FA4) – Offshore transition deposits (Mid ramp)	81
5.5 Facies association 5 (FA5) – Offshore shelf deposits (Outer ramp-basin).....	82
6. Depositional models for the Gipshuken and Kapp Starostin formations.....	83
7. Sequence stratigraphy	88
7.1 Transgressive-regressive sequences	96
8. Economic implications	98
8.1 Diagenesis and reservoir potential.....	98
8.2 A Late Palaeozoic play model.....	100
8.3 The Kapp Starostin Formation as an outcrop analogue for the Røye Formation...	104
9. Summary and conclusions.....	106
9.1 Outlook	107
References.....	109
APPENDIX 1 – Lithostratigraphic logs	118
Section A.....	118
Section B.....	124
Section C	126
Section D-D'	127
Section E	139
Gothta core section, Well 7120/1-3	140

1. Introduction

1.1 Preface

The Lower to Upper Permian succession in Svalbard, which is the focus of this thesis, has been the target for many previous studies (Gee et al., 1952; Cutbill & Challinor, 1965; Malkowski & Hoffman, 1979; Cutler, 1981; Malkowski, 1982; Steel & Worsley, 1984; Ezaki et al., 1994; Dallmann et al., 1999; Hüneke et al., 2001). The earliest studies focused on the sedimentology, dating of the strata and correlation to other sections, while more recent studies have tried to interpret the palaeoenvironment and construct sequence stratigraphic models (Ehrenberg et al., 2001; Blomeier et al., 2011; Blomeier et al., 2013). Several unpublished works have also been important for the understanding of the sedimentary system (Hellem, 1980; Fredriksen, 1988; Henriksen, 1988; Bottolfsen, 1994; Carmohn, 2007; Grundvåg, 2008; Goode, 2013). Much work have also been done on the similar and age-equivalent successions on the Finnmark Platform, the Loppa High, Bjørnøya (Larssen et al., 2002; Stemmerik & Worsley, 2005; Worsley, 2008), and in the Canadian Arctic and North Greenland (Beauchamp & Desrochers, 1997; Stemmerik, 1997; Beauchamp & Baud, 2002; Gates et al., 2004; Reid et al., 2007). Dating of the Upper Palaeozoic successions in Greenland, Svalbard and the Barents Sea have been based on many fossil groups, including fusulinids, conodonts, foraminifers and palynomorphs (Piasecki, 1984; Nakamura et al., 1987; Nakrem, 1988; Nilsson, 1988; Stemmerik, 1988; Nakrem, 1991; Stemmerik et al., 1991; Nakrem et al., 1992; Nilsson, 1993; Mangerud, 1994).

Svalbard is located at the northwestern edge of the Eurasian plate, and forms the subaerially exposed NW margin of the Barents Shelf. The Barents Sea is considered to be a frontier petroleum province and the demand for detailed knowledge about the regional-scale and prospect-scale geology in the area is increasing despite decades of research and exploration. The Norwegian Petroleum Directorate (NPD) has estimated the total undiscovered resources in the Barents Sea at 1275 mill Sm³ o.e (2014). NPD has also proposed Middle and Upper Permian rocks as one of the play models, and the recent Gohta and Alta discoveries on the Loppa High proved that the Late Carboniferous and Permian rocks have a significant reservoir potential in the Barents Sea.

Consequently, there has been an increased interest for the age-equivalent Kapp Starostin Formation. Svalbard and the Barents Shelf share parts of the same tectonic evolution and depositional history. Thus, well-exposed outcrops on Svalbard is the key to understanding some of the most important petroleum systems on the Barents Shelf, including amongst others several Upper Palaeozoic play models.

1.2 Objectives

The aim of this study has been to investigate the facies variability and the sequence stratigraphic development of the Late Permian Kapp Starostin Formation in the Dickson Land area in central Spitsbergen. The underlying Gipshuken Formation and the overlying Vikinghøgda Formation were also investigated, as well as the boundaries between the formations. The sedimentary facies of the Gipshuken Formation, Kapp Starostin Formation and Vikinghøgda Formation are fundamentally different; the Gipshuken Formation represents deposition in a semi-arid to arid sabkha environment, the Kapp Starostin Formation represents deposition on a cool-water carbonate-siliciclastic shelf, whereas the Vikinghøgda Formation represents deposition on an open-marine siliciclastic shelf. Although the Kapp Starostin Formation has been the focus of many previous studies, there are still some uncertainties regarding the facies and facies transitions, as well as what processes were active during deposition. The facies and facies associations were used to construct a sequence stratigraphic model for the Kapp Starostin Formation. This study is based on sedimentary logs measured in the field and thin section analysis of samples collected during fieldwork. The data collected during fieldwork in Svalbard has been compared to a core section (50.3 m) from an age-equivalent succession (well 7120/1-3, Røye Formation) on the Loppa High in the Barents Sea. The Middle to Upper Permian successions in the Barents Sea has been proposed as possible geological plays and this thesis will investigate if the Kapp Starostin Formation can be used as an outcrop analogue for the Permian rocks in the Barents shelf.

The explicit objectives of this thesis are:

- Investigate the sedimentology and the sequence stratigraphic architecture of the Kapp Starostin Formation.

- Conduct a detailed facies investigation of samples collected during fieldwork.
- Present field observations in a digital lithostratigraphic log.
- Compare outcrop-data with core data from the Barents Sea (well 7120/1-3).

1.3 Geographic location and local topography

Svalbard is a Norwegian archipelago situated in the Barents Sea between 74° – 81°N latitude and 10° – 4°E longitude (Fig. 1). The archipelago comprises numerous of islands and skerries, with Spitsbergen, Nordaustlandet, Edgeøya, Barentsøya, Prins Karls Forland, Kong Karls Land, Kvitøya and Bjørnøya being the major islands. The total land area comprises 62,700 km², of which glaciers and inland icecaps cover about 60% (Worsley et al., 1986).

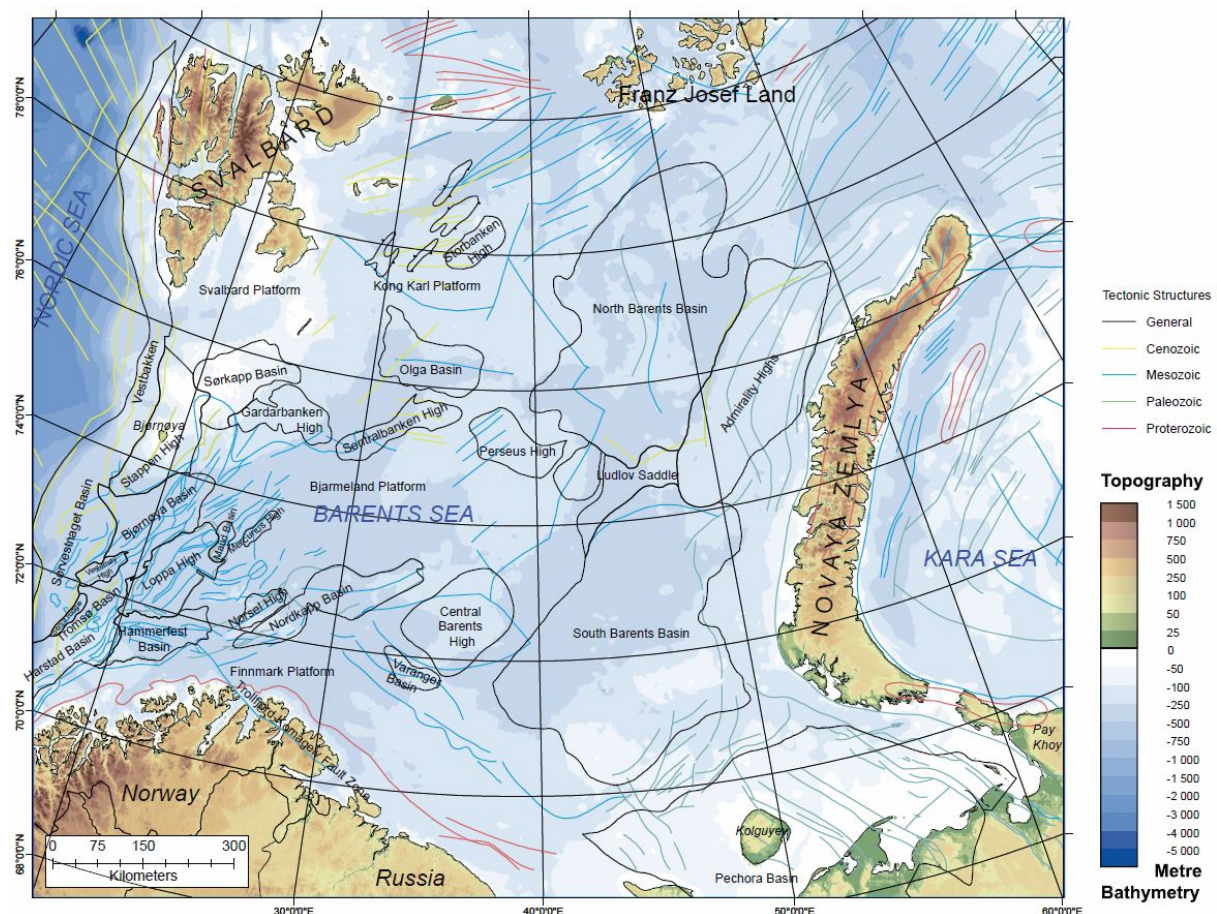
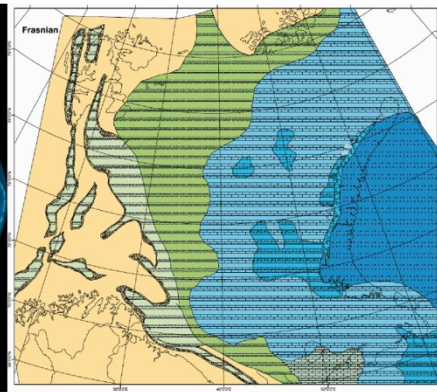
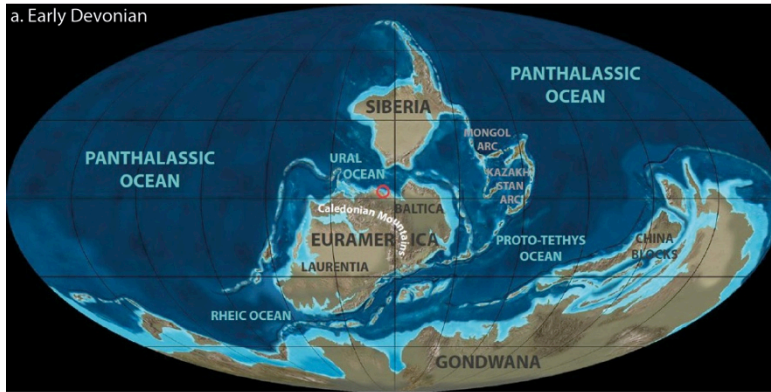


Figure 1: Map showing the geographic location of Svalbard relative to the Norwegian mainland and the main structural elements of the Barents Shelf (Smelror et al., 2009). This study focus on Lower to Upper Permian rocks in Svalbard and on the Loppa High.

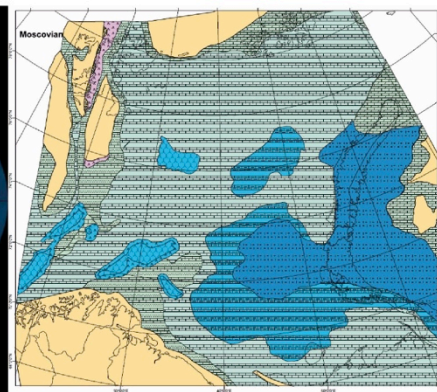
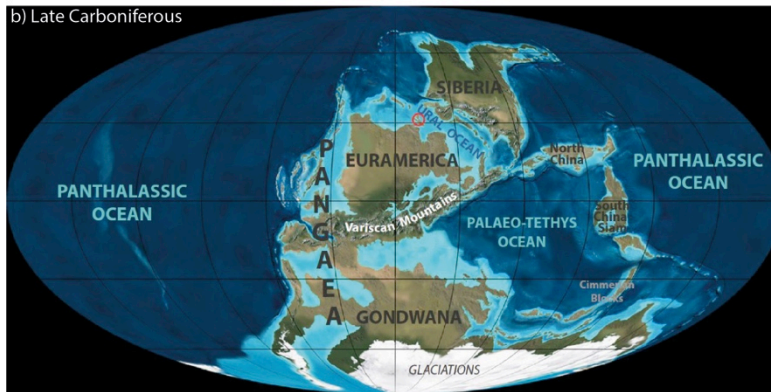
Svalbard forms the subaerially exposed northwestern part of the Barents Shelf, which emerged when the area was uplifted due to crustal movements in the Mesozoic and Cenozoic (Dallmann et al., 1987). The shelf extends northwards from the coasts of Norway and northwestern Russia and is made of a mosaic of rift basins, platforms and structural highs, covered by the shallow waters (average 230 m) of the epicontinental Barents Sea (Fig. 1) (Faleide et al., 1993; Doré, 1995). West of Svalbard, a 40-80 km wide shelf separates Spitsbergen from a structurally complex area and the deep and narrow Norwegian-Greenland Sea. Fifty to hundred km north of Svalbard, the northern continental margin of the shelf plunges steeply (up to 10°) into the Arctic Ocean (Dallmann et al., 1999).

Because Svalbard is an uplifted part of the Barents Shelf, the area provides insight to its geological history and stratigraphic development. Before late Mesozoic and Cenozoic uplift, Svalbard was located in an area with substantial subsidence, which resulted in generation of accommodation space and allowed continuous sedimentation. The stratigraphic succession in Svalbard therefore shows a more or less complete record from the Devonian through to the Paleogene (Worsley et al., 1986). During Carboniferous and Permian Svalbard also drifted northwards, and the paleolatitude increased from around 20°N to 45°N (Fig. 2) (Stemmerik & Worsley, 2005). This gradual paleolatitudinal shift was followed by an environmental change from tropical and humid in the Early Carboniferous to warm and arid in the Late Carboniferous-Early Permian to cold-temperate in the Late Permian (Stemmerik & Worsley, 2005). These latitudinal and climatic changes are reflected in the deposits, as changes in the sedimentary facies and faunal assemblages.

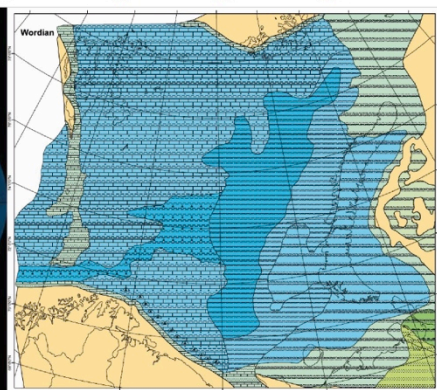
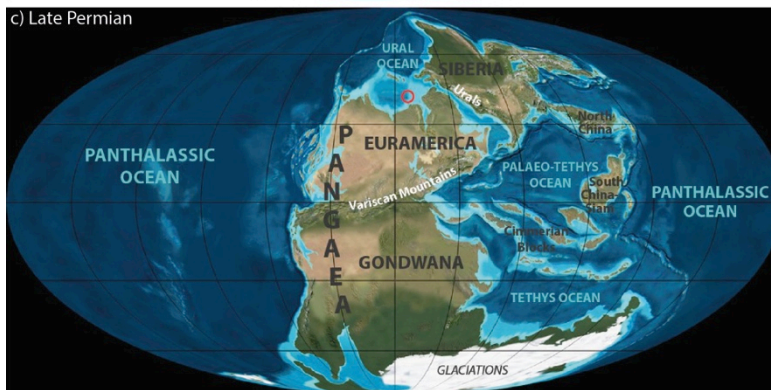
a. Early Devonian



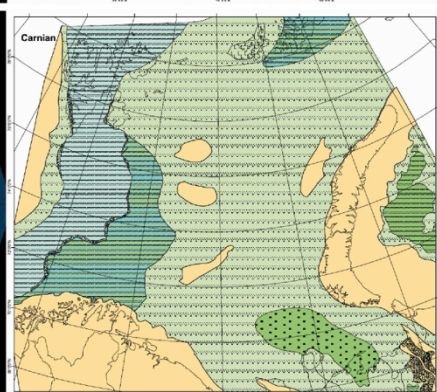
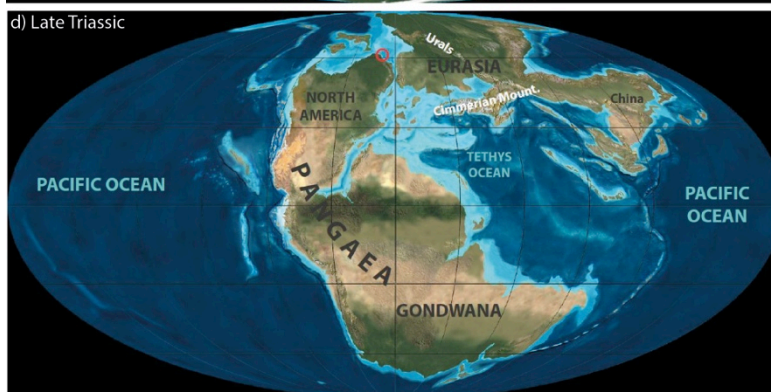
b) Late Carboniferous



c) Late Permian



d) Late Triassic



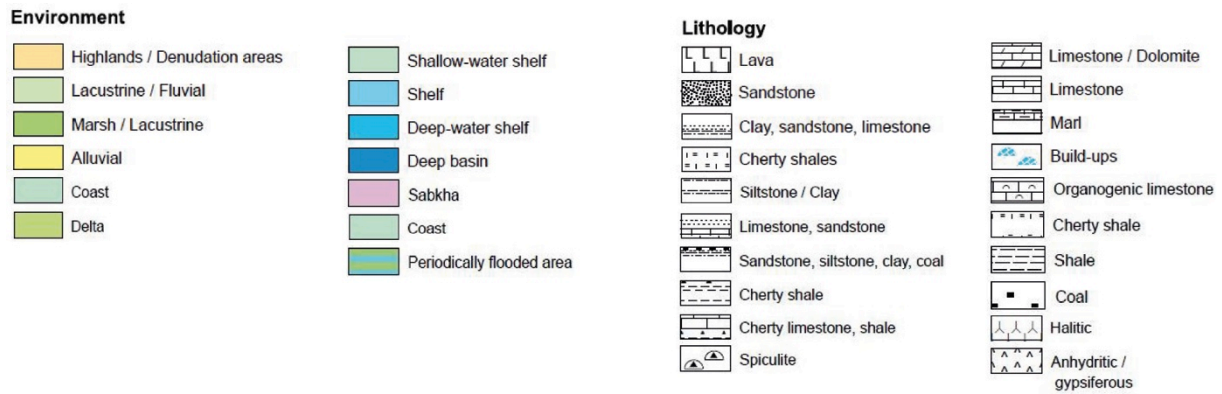


Figure 2: Global palaeogeography and location of the Svalbard area (encircled) and prevailing depositional environment on the Barents Shelf during the **a)** Left: Early Devonian (Emsian, ca 400 Ma), right: Late Devonian (Frasnian, ca 380 Ma), **b)** Left: Late Carboniferous (Pennsylvanian, ca. 300 Ma), right: Moscovian (ca 310 Ma). Svalbard is located around the 30th northern latitude at the northern margin of Pangaea, **c)** Left: Late Permian (Lopingian, ca. 260 Ma), right: Woridan (ca 266 Ma). Svalbard is located around 45°N, at the northern margin of Pangaea. Time of the “Permian Chert Event” and extensive deposition of sponge spicules, **d)** Left: Late Triassic (ca. 200 Ma), right: Carnian (ca 230 Ma). Svalbard is located around 55°N, on a vast epicontinental shelf. Palaeogeographic illustration by R. Blakely, modified from Dallmann et al. (2015b). Barents Shelf environments modified from Smelror et al. (2009).

1.4 Study area

The topography in central Spitsbergen is characterised by flat, table-like mountains separated by river valleys (Fig. 3c). The mountain plateaus generally have an elevation of about 400-500 m in the area, and represent an uplifted and warped Tertiary peneplane (Harland et al., 1997). Erosion has continued to sculpture the land and created steep cliffs, talus cones, ravines and valleys. The Kapp Starostin Formation, which is the main focus of this study, commonly forms cliffs and is often associated with waterfalls and steep canyons, as opposed to the underlying Gipshuken Formation, which is characterized by gentler angles and scree-covered slopes (Fig. 4). Due to the steep slopes and sparse vegetation, the Kapp Starostin Formation is superbly exposed. In the lowlands, tundra vegetation dominates all the way to the gravelly shoreline.

The fieldwork was conducted from 14.-30. august 2015 in the southwestern part of Dickson Land, the land area between Billefjorden and Dicksonfjorden in central Spitsbergen (Fig. 3). Geologically, this area is dominated by nearly flat lying strata of Late Palaeozoic age. Most of the measured outcrops are located in Esperantodalen between Heimenfjellet and Bredsdorffberget (Figs. 3c, 4). This location was chosen due to its good exposure and vertical and lateral extent. Some outcrops on the southern and western side of Heimenfjellet were also measured. The measured succession is about

280 m thick and the outcrops are located between 75m and 365m above sea level. The outcrops were reached by hiking from the camp location at Esperantonset.

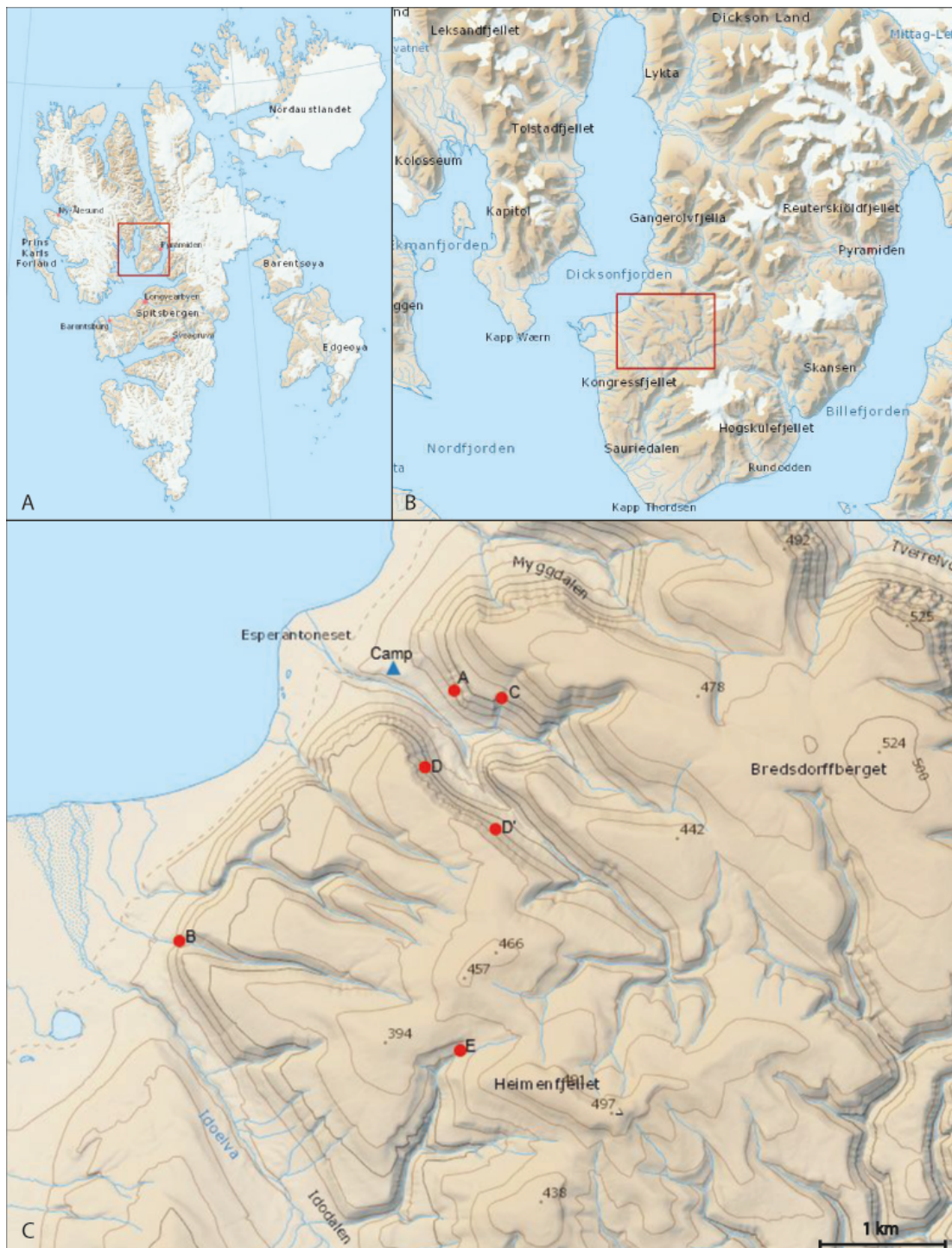


Figure 3: a) Map showing the location of the study area in central Spitsbergen. b) The study area is located in Dickson Land, the land area between Dicksonfjorden and Billefjorden. c) Map showing the location of the camp and the location of the measured sections (A-E).



Figure 4: Outcrop picture of section D, the most lateral and vertical continuous section. The Gipshuken Formation constitutes the lower part of the succession, which is mostly covered by scree. The overlying Kapp Starostin Formation has steeper slopes and is superbly exposed.

2. Geological framework

2.1 Tectonic setting

The tectonic history of the Barents Sea is complex and not fully understood (e.g. Smelror et al., 2009). The tectonic evolution of the area has played an important role in controlling the sedimentation patterns of the post-Caledonian strata, which is reflected in changing depositional patterns, depositional breaks, provenance and transport directions (Steel & Worsley, 1984; Dallmann et al., 1999; Smelror et al., 2009). The Late Palaeozoic history of the SW Barents Shelf can be divided into four simplified episodes: 1) consolidation of the basement during the Caledonian Orogeny, 2) extensional and compressive events during the Devonian, 3) extensive rifting during the Carboniferous and Permian, and 4) regional subsidence in Permian (Faleide et al., 1993; Gudlaugsson et al., 1998). This geological history is similar for both Svalbard and the south-western Barents Sea (Fig. 5).

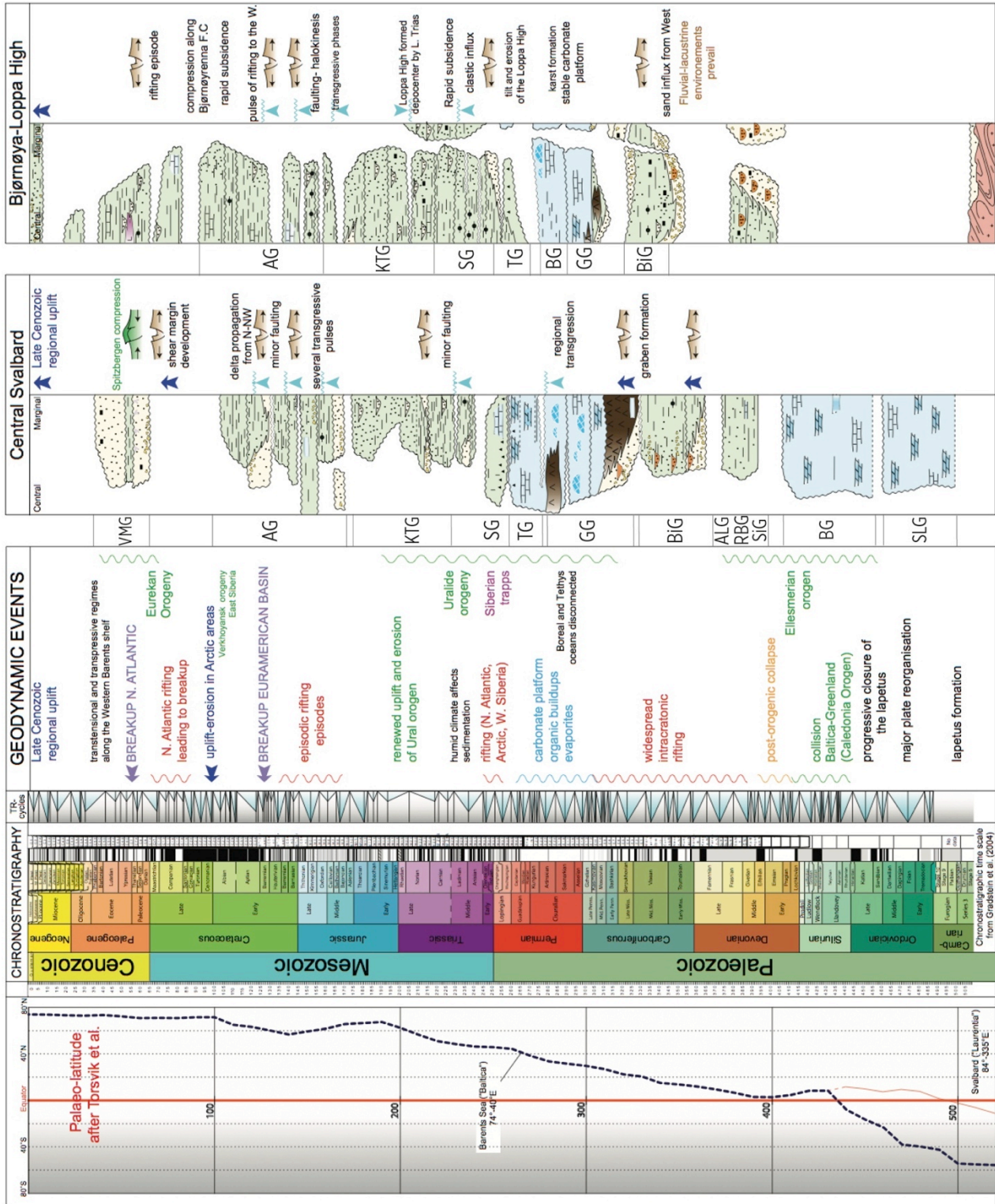
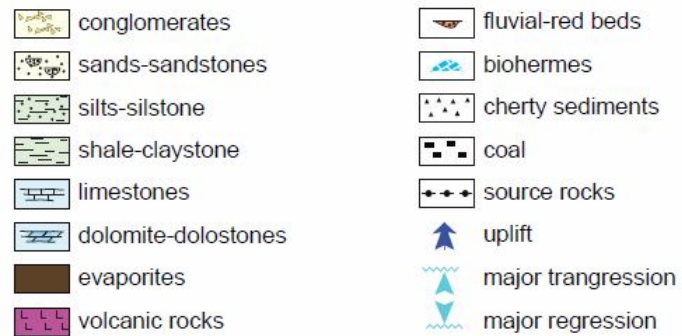


Figure 5: Lithostratigraphic development and correlations of Svalbard and the Bjørnøya-Loppa High area in the Barents Sea. The columns represent an average lithology and tectonic history of each area. SLG: Sørkapp Land Group, BG: Bullbreen Group, SiG: Siktefjellet Group, RBG: Red Bay Group, ALG: Andrée Land Group, BiG: Billefjorden Group, GG: Gipsdalen Group, BG: Bjarmeland Group, TG: Tempelfjorden Group, SG: Sassendalen Group, KTG: Kapp Toscana Group, AG: Adventdalen Group, VMG: Van Mijenfjorden Group.



The Precambrian basement of Svalbard show evidence of a multi-orogenic development with prominent events of Grenvillian (Precambrium), Caledonian (Ordovician-Silurian), Ellesmerian/Svalbardian (Late Devonian), Variscan (middle-Carboniferous), and West Spitsbergen and Eureka (Paleogene) orogenies (Dallmann et al., 1999). In contrast to the pre-Devonian rocks, rocks younger than Devonian have been deformed relatively little (Gee et al., 1952). Following the Caledonian orogeny, the compressional regime changed into a regime characterized by crustal extension, collapse of the Caledonian orogeny and extensive erosion of the hinterlands (Smelror et al., 2009; Dallmann et al., 2015b). Thick deposits of molasse sediments accumulated in the western Barents Sea and on Svalbard (Smelror et al., 2009). These deposits are commonly called the Old Red Sandstone and are represented by the Siktefjellet, Red Bay and Andrée Lang groups on Svalbard (Fig. 5) (Dallmann et al., 2015b). Both the Siktefjellet and Red Bay groups were deposited during active rifting (syn-rift stage) and is lying unconformably on deformed basement rocks, whereas the Andrée Land Group was deposited after the tectonic movements ceased (post-rift stage) (Dallmann et al., 2015b). All three groups are separated from one another by phases of tectonic activity, which deformed parts of the strata (Dallmann et al., 2015b). The Svalbardian phase, which is thought to be a final convulsion of the Caledonian orogeny, was initiated in the Late Devonian (Famennian) and resulted in compressional tectonics, which led to the development of an angular unconformity between the Old Red Sandstone and the overlying strata (Hellem, 1980; Dallmann et al., 2015b). In the Late Devonian to Early Carboniferous this compressional regime changed to a left-lateral shear regime with major strike-slip movements and intracratonic rifting (Faleide et al., 1984; Dallmann et al., 2015b). Transpressional

deformation of the East Greenland and Norwegian margins and the western Barents Sea formed intramontane basins filled with molasse sediments (e.g. Old Red Sandstone) (Golonka et al., 2003). Two rift arms started to develop; the Atlantic rift arm followed the old Caledonide suture between Greenland and Norway and continued northeast across the central Barents Sea, whereas the Arctic rift arm formed between Greenland and Spitsbergen and eventually linked with the Sverdrup Basin rift in the west (Stemmerik, 1997; Golonka et al., 2003). Additional rift-phases occurred during the middle-Carboniferous (Bashkirian) and Middle to Late Permian (Artinskian-Kazanian) time (Stemmerik et al., 1991; Stemmerik, 1997). This Carboniferous to Permian rifting resulted in fault-controlled subsidence and development of several structurally controlled depocenters, such as the Bjørnøya, Hammerfest, Tromsø, Nordkapp and Sverdrup basins (Beauchamp & Desrochers, 1997; Gudlaugsson et al., 1998; Henriksen et al., 2011b) (Fig 1). On Svalbard, rift basins developed along several pre-existing fault zones (e.g Billefjorden Fault Zone, Lomfjorden Fault Zone, Figs. 6 and 7), and led to the formation of a number of horst-and-graben structures (e.g. St. Jonsfjorden, Billefjorden and Inner Hornsund troughs and Wedel Jarlsberg Land, Ny-Friesland, Nordfjorden and Sørkapp-Hornsund highs, Fig. 7) (Gee et al., 1952; Henriksen et al., 2011b; Dallmann et al., 2015b). At the onset of the Carboniferous period, Svalbard was located just north of equator (20°-30°N) and the Barents Sea was part of a vast area stretching from Northern Greenland and Arctic Canada in the west, to Novaya Zemlya in the east (Torsvik et al., 2002; Worsley & Nøttvedt, 2008). Sedimentation occurred in fluvial, lacustrine and eolian systems, and resulted in deposits ranging from coal-bearing alluvial plain and red desert sediments belonging to the Billefjorden Group (Torsvik et al., 2002; Worsley & Nøttvedt, 2008).

Uplift of the northern margin of Pangaea during the Serpukovian resulted in a depositional break and is evident as an erosional unconformity in most of the northern north Atlantic and the western Barents Sea (Steel & Worsley, 1984; Stemmerik, 2000; Stemmerik & Worsley, 2005; Worsley, 2008). The uplift was followed by renewed rifting and fault block movement during Bashkirian-Moscovian, which resulted in a new configuration of troughs and half-grabens (Gjelberg & Steel, 1981). A regional sea-level rise during the Moscovian was accompanied with a climatic shift from humid to arid (Worsley, 2008). The tectonic movements waned later in the Carboniferous and the

fault block tectonism transformed into a stable shelf with small differences between earlier troughs and intermediate platform areas, except from the Inner Hornsund Trough and Sørkapp-Hornsund High (Bugge et al., 1995; Gudlaugsson et al., 1998; Dallmann et al., 1999). A vast post-rift carbonate platform that stretched westward to present-day Alaska developed (Worsley, 2008). With these changes the sedimentation changed from siliclastic-evaporitic during the fault-block tectonism, to carbonate production on the stable platform and deposition of the Gipsdalen Group (Hüneke et al., 2001). These conditions lasted until Late Permian, when siliclastic input again became dominant (Hüneke et al., 2001).

Reorganisation of the of the central Pangaeian shelf during the late Sakmarian-Artinskian, led to marginal uplift and the formation of a hiatus (Stemmerik & Worsley, 2005). Sediments of this age are missing in most of North Greenland, Spitsbergen and Bjørnøya (Worsley et al., 2001a; Stemmerik & Worsley, 2005). Structural highs, like the Loppa and Stappen highs (Fig. 1 for location), in the western Barents Sea were also uplifted during Early Permian and continued to be tectonically active until the Middle-Permian (Worsley, 2008). The plate-reorganization and development of a marine seaway between Norway and Greenland connected to Boreal Realm to the central European Zechstein Basin, which resulted in changes in the oceanic circulation (Stemmerik et al., 1999; Stemmerik & Worsley, 2005; Worsley, 2008). This led to a drastic change in water temperature and depth during the mid-Sakmarian, and resulted in a facies shift from warm-water carbonates to cool-water carbonates and spiculites (Worsley, 2008). This was the beginning of the Permian Chert Event (PCE), which was a 30 Ma long episode of chert accumulation along the northwestern margin of Pangaea (Fig. 2c) (Beauchamp & Baud, 2002). Outcrops with strata deposited on this vast shelf are found in various circum-Arctic regions (e.g. Loppa High, Wandel Sea Basin, Sverdrup basin and Timan-Pechora Basin) (Dallmann et al., 2015b). The extensional tectonism waned completely in the late Artinskian-early Kungurian (Beauchamp & Desrochers, 1997). The development of the Uralide orogeny to the east resulted in increased subsidence rates in the entire Barents Sea and formation of foreland basins (Golunka et al., 2003). The subsidence allowed continuous sedimentation and the Upper Palaeozoic to Palaeogene strata locally exceeds 15 km in thickness (Faleide et al., 1993; Gudlaugsson et al., 1998). Such thick accumulations are found in the Uralian foredeep

zone, which worked as a major catchment zone for sediments eroded from the Uralian orogeny (Smelror et al., 2009). Where subsidence rates were lower, the sedimentary succession is substantially thinner. The sediment transport had previously been from the west, but uplift to the east induced by the formation of the Uralide orogeny in Late Permian-Early Triassic, shifted the transport direction towards the west (Henriksen et al., 2011b). The Barents Sea region received sediments from the Urals in the east, the Fennoscandian Shield in the south and possibly local exposed areas to the west and northwest (Mork, 1999; Smelror et al., 2009). Areas like the Finnmark Platform and Stappen and Loppa highs (Fig. 1 for location) were sites of slower subsidence and carbonate production from the mid-Carboniferous onwards (Stemmerik, 1997). During the Wordian, these highs were emergent or shallow-marine and dominated by banks of bryozoans and brachiopods (Smelror et al., 2009). Even though these platforms had a similar depositional evolution, they show different depositional trends related to their tectonic history (Stemmerik, 1997). The subsidence that characterized the Middle Permian waned throughout the Triassic and gave rise to a more stable area with deposition of repeated clastic successions of delta-related coastal and shallow shelf sediments.

2.2 Lithostratigraphy and sedimentary systems

The basement in Svalbard is made up of igneous and metamorphic rocks of Precambrian to Lower Silurian age and is commonly called the Hecla Hoek series (Hjelle & Brekke, 1993). These rocks are exposed in a NNW-SSE trending belt along the west coast and in the northern part of Spitsbergen, and on Nordaustlandet (Fig. 6). Devonian Old Red molasse sediments are confined to a major graben, the so-called Old Red Basin in the northern part of Spitsbergen (Blomeier et al., 2003). The Upper Carboniferous to Paleogene succession is remarkably complete and constitutes the platform sediments in the central and eastern parts of the archipelago. The Late Palaeozoic rocks crop out in Western, Central and Northeastern Spitsbergen, Bjørnøya and on the western coast Nordaustlandet (Fig. 6). On the west coast of Spitsbergen the rocks occur in a narrow elongated NNW-SSE zone as part of the West Spitsbergen fold-and-thrust belt, and they are commonly folded and tilted vertically as a result of the Palaeogene orogeny (Bergh et al., 1997). The rocks in the study area are less influenced by this deformation, but

they are dipping gently by some few degrees towards southwest. The dip variations is due to the asymmetric character of deformation and down-warping that occurred during the orogeny that formed the Spitsbergen fold-and-thrust belt (Worsley et al., 1986).



During the Late Palaeozoic (Early Carboniferous to mid-late Permian), the North Greenland-Barents Sea region formed a complex rift-related system with subsiding basins and more stable platforms (Stemmerik, 1996, 1997; Ahlborn et al., 2014). This period was characterized by glacioeustatic driven sea-level variations, long-term with superimposed short-term climatic changes, and tectonic activity related to rifting and basin subsidence that together controlled the sedimentation patterns and stratigraphic development. The uppermost Devonian-lowermost Serphukovian sedimentation was non-marine, except for on the Finnmark Platform where marine sediments were deposited during a brief interval in the Visean (Stemmerik, 2000). The mid-Carboniferous to Middle Permian sediments were deposited in a warm and arid climate during a period with high-frequency and high-amplitude glacioeustatic sea-level fluctuations, and was dominated by warm-water carbonates, evaporites and locally siliciclastic deposits (Steel & Worsley, 1984; Stemmerik & Worsley, 1989). Up to 100 m thick deposits of palaeoaplysiniid-phyllloid algal buildups developed on structural highs during sea-level highstands, while carbonate mud accumulated in the deeper basins (Henriksen et al., 2011b). During sea-level lowstands, structural highs were exposed, which led to karstification of the carbonates (Stemmerik et al., 1995; Elvebakk et al., 2002). A regional sea-level rise during the Early Permian led to transgression and deposition of aggradational to retrogradational successions of bryozoan- and crinoid-dominated limestones (Stemmerik, 2000). The deep-water temperate environment that existed in the westernmost part of the Barents region during the Wordian created perfect conditions for sponge colonies and led to widespread blooming of various sponge species (Smelror et al., 2009).

Following the stratigraphic scheme of Cutbill & Challinor (1965), the Upper Palaeozoic strata is divided into three groups; The Billefjorden Group, the Gipsdalen Group and the Tempelfjorden Group. Each group represent a second-order sequence with a duration of about 15-30 million years (Stemmerik & Worsley, 2005). Below follows a brief geological summary of the three groups.

2.2.1 The Billefjorden Group

The Lower Carboniferous Billefjorden Group comprises clastic sedimentary rocks of late Famennian to early Serpukhovian age (Worsley, 2008). Sedimentation first occurred in separate troughs, but became widespread during the Early Carboniferous (Steel & Worsley, 1984). Extensional tectonics during mid-Carboniferous led to development of several narrow rift basins and adjacent highs in the Billefjorden area, in inner Hornsund and on Bjørnøya (Johannessen & Steel, 1992). The rift basins have half-graben geometries and follow the NNW-SSW trend of the Caledonian and Svalbardian fracture lines (Johannessen & Steel, 1992). The deposits of the Billefjorden Group are preserved in these middle Carboniferous troughs (e.g. the Inner Hornsund, St. Jonsfjorden, Billefjorden and West Bjørnøya trough) (Fig. 7). The earliest syn-rift sediments were deposited in a humid terrestrial environment and include fluvial orthoquartzites and conglomerates, shale and local coal seams (Dallmann et al., 1999; Maher & Braathen, 2011). The later syn-rift sediments includes a wide range of facies, such as evaporites, fluvial and shallow marine sediments. Clastic wedges and alluvial fans shed from the Nordfjorden High interfingers with basin-centre evaporites (Eliassen & Talbot, 2003b). The depositional environment changed from a humid and warm terrestrial early syn-rift environment, to a warm marine-influenced late syn-rift environment. As this group is not a part of this study it will not be further discussed. However, note that coals and coaly shales in this group is considered possible source rocks in many of the play models in the Barents Sea.

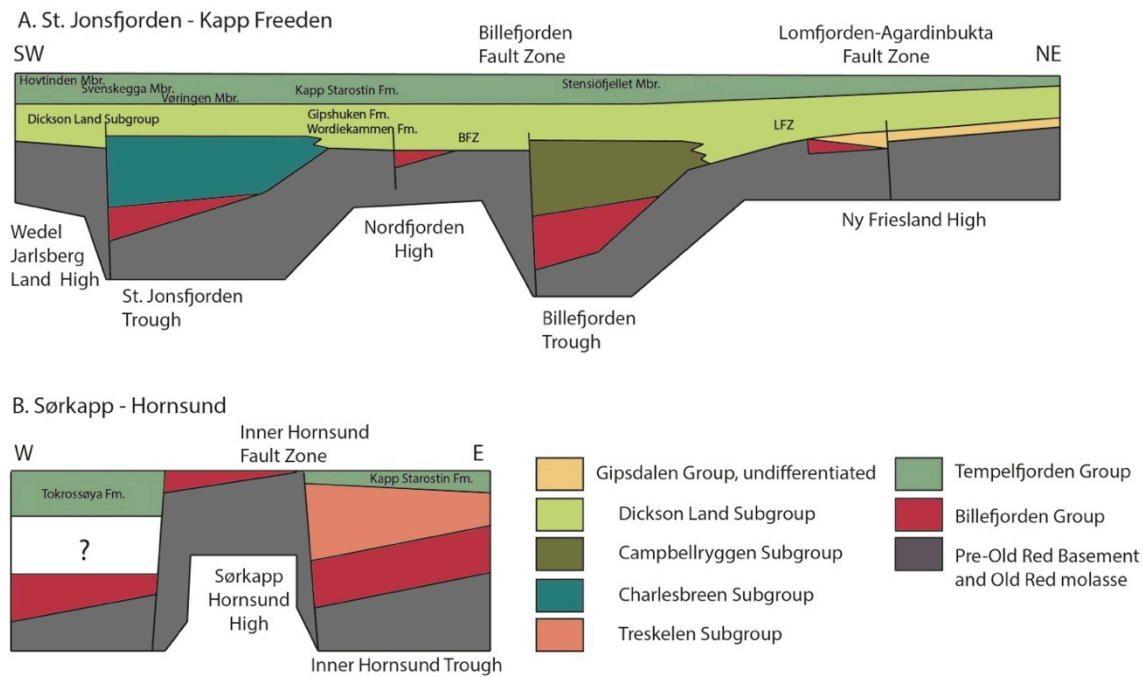


Figure 7: Cross sections showing the Late Palaeozoic strata between **a)** St. Jonsfjorden and Kapp Fredeen, and **b)** Sørkapp and Hornsund. The Billefjorden Group is confined to the Middle Carboniferous rift-basins. The Gipsdalen Group unconformably overlies the Billefjorden Group and onlaps structural highs due to a regional transgression during the Moscovian. The Treskelen, Charlesbreen and Campbellryggen subgroups are confined to individual troughs, whereas the Dickson Land Subgroup (the Wordiekammen and Gipshuken formations) was deposited on a vast Late Palaeozoic platform. The Tempelfjorden Group is deposited on the same platform. The group thins towards the east across structural highs and has its maximum thickness in the basins, e.g. 460 m in the St. Jonsfjorden Trough. See Fig. 6 for location of the fault zones.

2.2.2 The Gipsdalen Group

The Gipsdalen Group unconformably overlies the Billefjorden Group and comprises strata of Serpukhovian to Artinskian age (Dallmann et al., 1999). The unconformity resulted from a regional uplift during the Serpukovian and is associated with a significant paleoclimatic change from warm and humid to warm and arid/semi-arid (Stemmerik & Worsley, 2005). The uplift was followed by renewed rifting of the already existing half-grabens and a major sea-level rise (Worsley, 2008; Blomeier et al., 2009). Deposition took place in these half grabens, but as the region was transgressed, sediments started to onlap structural highs and the marginal parts of the basin (Fig. 7) (Stemmerik, 2000). During this period Svalbard was situated between 20°N and 40°N latitude and the deposits display the result of the climatic change; red clastics and sabkha sediments represent the humid non-marine environment and evaporites and warm-water carbonates represent a shallow-marine platform (Scotese & McKerrow,

1990; Harland et al., 1997). The clastic redbeds therefore make up the lower part of the succession, and are found in the same fault-controlled basins as the underlying Billefjorden Group (Fig. 7) (Steel & Worsley, 1984). The middle Carboniferous syn-rift sedimentation was gradually replaced by post-rift evaporites and shallow marine to lagoonal carbonates as the marine influence increased through the Bashkirian and into the Moscovian (Dallmann et al., 1999). Structural highs, such as Wedel Jarlsberg Land High, the Sørkapp-Hornsund High and the Nordfjorden High, were all progressively transgressed during the Moscovian, and became the sites of platform carbonate development (Dallmann et al., 1999). The area then developed into a stable shelf characterized by uniform subsidence and widespread deposition of warm-water carbonates (Blomeier et al., 2009).

The Gipsdalen Group is divided into four subgroups, which previously was addressed to associate the various strata with underlying troughs or basins (Dallmann et al., 1999). The four subgroups are; the Charlesbreen Subgroup, the Campbellryggen Subgroup, the Treskelen Subgroup and the Dickson Land Subgroup (Fig. 7). The successions show a complex depositional history due to tectonic activity and climatic changes, and several formations have not been assigned to any of the subgroups, due to lack of correlative data. This especially applies to the formations in eastern Spitsbergen and on Bjørnøya (Dallmann et al., 1999). Only the Dickson Land Subgroup is relevant for this work. The Dickson Land Subgroup comprises the two uppermost formations of the Gipsdalen Group, namely, the Wordiekammen Formation (early Moscovian to Sakmarian) and the Gipshuken Formation (Sakmarian to Artinskian). These formations were not deposited in individual troughs, but on the Late Palaeozoic carbonate platform that covered vast areas of Svalbard (Fig. 7) (Dallmann et al., 1999). The lower Wordiekammen Formation is dominated by marine limestones deposited in open to semi-restricted shallow subtidal marine and restricted intertidal to supratidal environments (Blomeier et al., 2009), whereas the upper Gipshuken Formation is dominated evaporites in addition to dolomite/limestone units (Dallmann et al., 1999; Blomeier et al., 2011). The evaporites represent arid lagoonal, tidal flat and supra-tidal sabkha deposits and are primarily found in central Spitsbergen (Blomeier et al., 2011). Eastwards, limestones and dolomites replace the evaporites and the formation becomes more similar to the Wordiekammen Formation (Harland et al., 1997).

The Gipshuken Formation crops out across large parts of central Spitsbergen along the margins of the Central Tertiary Basin. It is commonly missing on structural highs, like the Sørkapp-Hornsund High (Fig. 8) (Dallmann et al., 1999). The formation is composed of rhythmic sequences of limestone/dolomite and gypsum/anhydrite, in addition to carbonate breccia, and includes a photozoan biotic association (Harland et al., 1997; Hüneke et al., 2001). Deposition took place in warm, shallow seas and tidal flats with high salinity (Harland et al., 1997). The upper boundary of the formation is marked by an erosional unconformity locally on top of a caliche succession. This unconformity marks the end of a period of cyclic sabkha and carbonate platform deposition driven mainly by glacio-eustacy (Dallmann et al., 1999; Blomeier et al., 2011). The Gipshuken Formation is subdivided into six members; the Vengeberget, Zeipelodden, Kloten, Skansdalen, Templet and Sørfonna members (Fig. 8) (Dallmann et al., 1999). The Skansdalen and Templet members interfingers laterally, and it is the Skansdalen member that forms the upper part of the Gipshuken Formation in the western and central areas of Spitsbergen, including the study area in Dickson Land (Dallmann et al., 1999). It is therefore only the Sakmarian to Artinskian strata of the Skansdalen Member that was investigated during this study. The Skansdalen Member has a thickness up to 150 m in the type-section, but only 90 m were measured in the study area.

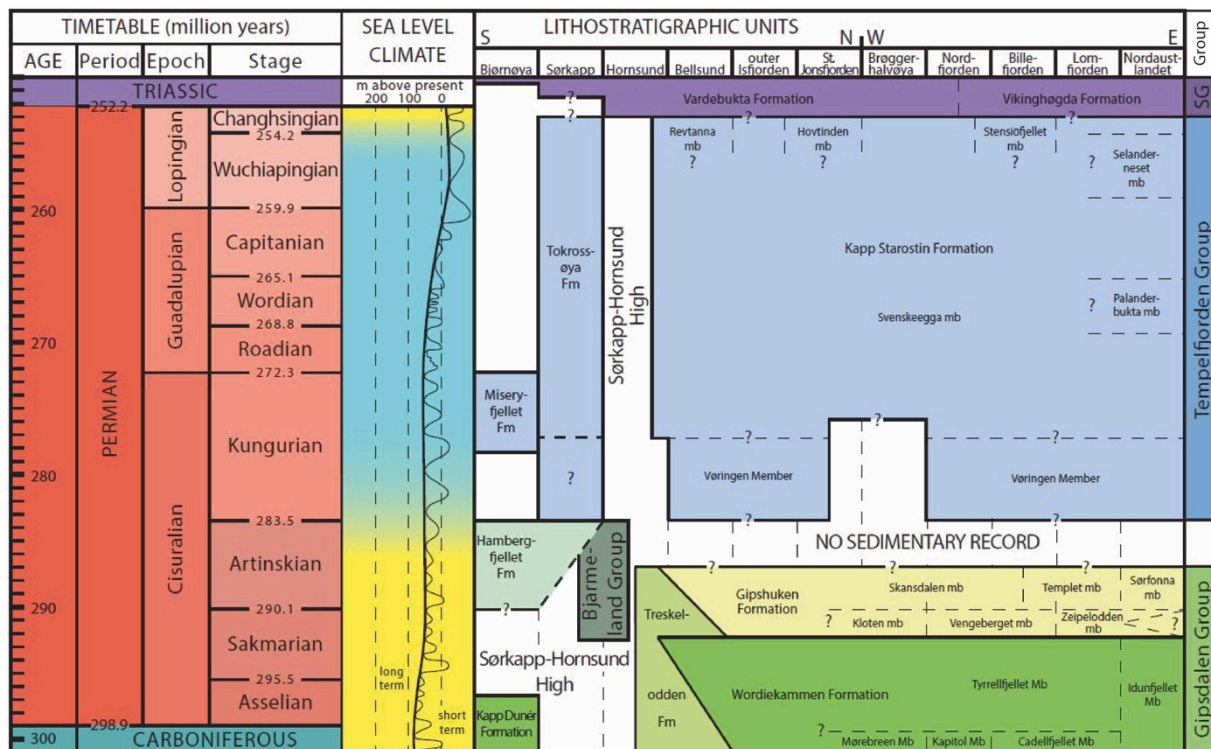


Figure 8: Lithostratigraphic overview of the Permian strata of Svalbard.

2.2.3 The Tempelfjorden Group

The Tempelfjorden Group comprises rocks of Middle to Late Permian age (Fig. 8) (Dallmann et al., 1999). The succession consists mainly of dark and light spiculites, spiculitic cherts, siltstones and shales, but locally also carbonates and glauconitic sandstones (Dallmann et al., 1999; Ehrenberg et al., 2001; Blomeier et al., 2013). The fauna includes a heterozoan biotic assemblage of brachiopods, bivalves, sponges, bryozoans and crinoids (Nakamura et al., 1987; Ezaki et al., 1994; Nakrem, 1994). The bio- and litho-facies strongly contrasts with that of the underlying Gipshuken Formation and clearly indicates a shift to a cooler and deeper environment (Worsley, 2008; Blomeier et al., 2011). The group overlies a significant subaerial unconformity on platform areas, whereas basins and basin margins show abrupt deepening (Fig. 8) (Worsley et al., 1986; Worsley, 2008). Due to imprecise dating of the Upper Permian rocks the magnitude of the hiatus is not known, and may be from <1 to as much as 15 m.y. (Hellem, 1980; Ehrenberg et al., 2001). Deposition occurred all over Svalbard, except on the Sørkapp-Hornsund High where the strata pinches out (Fig. 8) (Hellem & Worsley, 1978; Dallmann et al., 1999). The group is lateral extensive, thins toward the structural highs and have maximum thicknesses in the basins (e.g 460 m in the St. Jonsfjorden Trough) (Fig. 7) (Larssen et al., 2002).

The Tempelfjorden Group comprises three laterally equivalent formations; the Kapp Starostin Formation in northern and central Spitsbergen, the Tokrossøya Formation on Sørkappøya and the Miseryfjellet Formation on Bjørnøya (Fig. 8). The Kapp Starostin Formation is present along western Spitsbergen, parts of central to northeastern Spitsbergen and Nord-Austlandet, and was first named by Cutbill & Challinor (1965). The formation had previously been referred to as “Brachiopod Formation” (Nordenskiöld, 1863), “Brachiopod Cherts” (Gee et al., 1952) and “Starostin Formation” (Burov et al., 1965). The formation is composed of chert, spiculites, limestones, shale and sandstone, and was deposited during the late Artinskian to Kazanian (Dallmann et al., 1999). The Kapp Starostin Formation is divided into seven members; the basal Vøringen Member, and the Svenskegga, Hovtinden, Revtanna, Stensiöfjellet, Palanderbukta and the Seleanderneset members (Fig. 8). The Vøringen Member (Late Artinskian-Kungurian) is the lowermost unit of the Kapp Starostin Formation and has earlier been called Spirifer Limestone due to the high content of

large thick-shelled spiriferid brachiopods (Nakamura et al., 1987; Ezaki et al., 1994; Blomeier et al., 2013). The Vøringen Member is a massive, grey bioclastic limestone-unit that often forms cliffs over the more easily weathered Gipshuken Formation, and is easily seen in the field. The base of the unit is sharp and erosive and marks the boundary between the dolomitic, warm-water carbonates of the Gipshuken Formation and the spiculites and cool-water carbonates of the Kapp Starostin Formation (e.g. Blomeier et al., 2011). The bioclastic limestone of the Vøringen Member was probably deposited during a regional transgression and represent a barrier sequence that retreated over the restricted marine platform and sabkha environments of the Gipshuken Formation (Steel & Worsley, 1984; Worsley et al., 1986). The Vøringen Member is present over large areas of Spitsbergen and Nordaustlandet and has a maximum thickness of about 40 m (Dallmann et al., 1999). In the study area this member has a thickness of about 15 m.

The Svenskegga and Hovtinden members are both present in the Isfjorden area and form the middle and upper part of the Kapp Starostin Formation. The Svenskegga member (Kungurian-?Kazanian) is directly overlying the Vøringen Member and is composed of spiculitic shale, chert, siltstone and limestone and generally has a thickness of about 150-230 m (Dallmann et al., 1999). The Hovtinden member (?Kazanian) comprises silicified shale, siltstone and sandy limestone, and the lower boundary is defined where shales, sandy cherts or cherty sandstones conformably overlie the bioclastic limestone interval in the upper part of the Svenskegga member (Dallmann et al., 1999). This member make up the major part of the Kapp Starostin Formation and generally have a thickness of about 200-230 m (Dallmann et al., 1999). The Svenskegga and Hovtinden members have only been defined in their type section at Kapp Starostin in outer Isfjorden, however they are also believed to occur at Vinodden and Marmierfjellet (Grundvåg, 2008). In the type section, the biota is dominated by sponge spicules, brachiopods, bryozoans and trace fossils (e.g. Zoophycos) and a bioclastic limestone marker bed occur uppermost in the Svenskegga Member. The observations in the study area concur with the descriptions from the type section, and it is therefore assumed that the Svenskegga and Hovtinden members also can be defined there.

The Tokrossøya Formation crops out on a small island close to the southernmost tip of Spitsbergen, and represents the Tempelfjorden Group on the southwestern side of the Sørkapp-Hornsund High (Dallmann et al., 1999). The formation was deposited in a separate basin, but as a lateral equivalent to the Kapp Starostin Formation it is also composed of similar lithologies (Harland et al., 1997). The Tokrossøya Formation is subdivided into three informal units; the Lower- and Upper Tokrossøya Formation and the Sandhamna beds. The lower unit is mainly composed of calcareous spiculitic cherts, while the upper unit is composed of siltstones, sandstones and cherty limestones. The Sandhamna beds in an informal unit in the middle part of the Tokrossøya Formation, composed of thick sandstone beds (up to 20 m beds), intercalated by cherty limestones (Dallmann et al., 1999).

The Miseryfjellet Formation crops out on Bjørnøya and is dominated by sandy limestones and a rich fauna of brachiopods, bryozoans and crinoids similar to that of the equivalents on Spitsbergen (Dallmann et al., 1999).

2.2.4 The Sassendalen Group

The transition between the Tempelfjorden Group and the overlying Triassic Sassendalen Group is marked by an abrupt change of facies, from late Permian fossiliferous lithologies to homogeneous soft and dark Triassic shales and siltstones. The boundary may in some places be represented by a hiatus of uncertain magnitude, particularly on highs and platforms (Steel & Worsley, 1984; Stemmerik & Worsley, 1989; Stemmerik, 1997; Mørk et al., 1999). However, the presence of this unconformity is highly debated and it has also been suggested that sedimentation was continuous, but very slow (Mangerud & Konieczny, 1993; Wignall et al., 1998). A generally transgressive trend throughout the early Triassic led to the onlap and submergence of positive features such as the Sørkapp-Hornsund and Stappen highs (Worsley, 2008). The sea-level rise was followed by oceanic anoxia, indicated by lower biotic diversity and increasing TOC (total organic carbon) (Dustira et al., 2013). Gradual increase in TOC values corresponds with the declining oxygen-levels. This trend has also been recorded in other sections on the western and northern Pangaeian margins (Wignall & Newton, 2003; Bond & Wignall, 2010a). It is estimated that approximately 90% of all marine

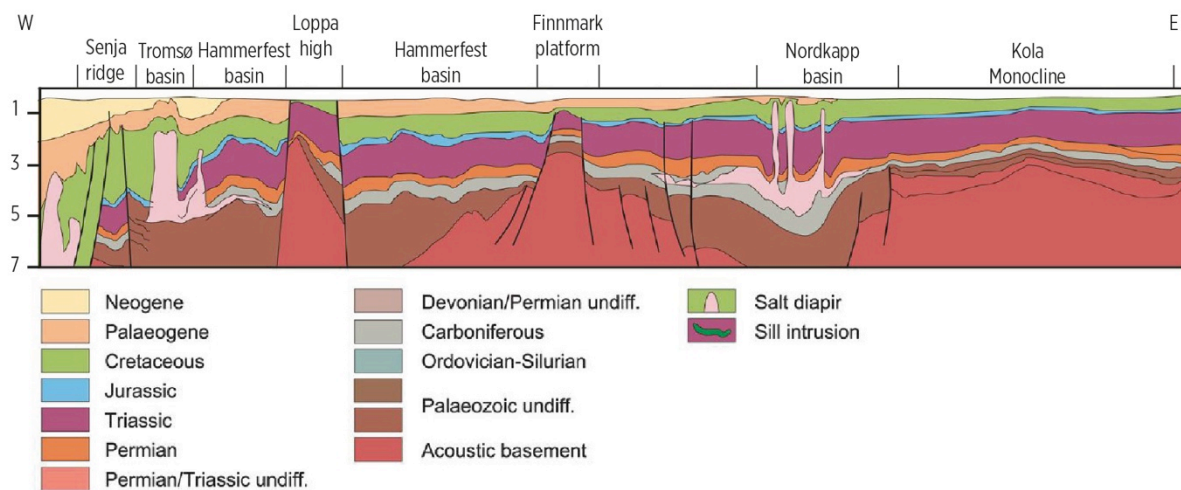
species and 70% of terrestrial vertebrate species were exterminated during the Permian-Triassic environmental crisis (Erwin, 2006). Several factors have been proposed as driving forces behind this mass extinction, e.g. cooling (Stanley, 1984), hyposalinity (Stevens, 1977), volcanism (Renne et al., 1995; Kozur, 1998; Reichow et al., 2002), anoxia (Wignall & Hallam, 1992; Wignall & Twitchett, 1996) and extraterrestrial impact (Becker et al., 2001; Kaiho et al., 2001). The Triassic strata of the Sassendalen Group and the Permian strata of the Tempelfjorden Group are therefore highly different. The entire group is dominated by non-siliceous finegrained clastics, such as shales, siltstones and sandstones. The Vikinghøgda formation makes up the lowermost part of the Sassendalen Group in central Spitsbergen, and comprises shales, siltstones and sandstones (Harland et al., 1997). In the study area this group is often covered by scree, however a few outcrops can be found on the mountain plateaus. A small outcrop (about 1 m) was measured immediately above the Kapp Starostin/Vikinghøgda formation boundary.

2.3 Correlation with the Barents Shelf and Bjørnøya

Comparison of cores, well logs and seismic data from the southwestern Barents Sea with outcrop data from Svalbard show that the stratigraphic successions show strong similarities in term of lithologies, depositional architecture and tectonic development (Dallmann et al., 1999). The Late Palaeozoic succession extends across the southwestern Barents Sea, from the Finnmark Platform to the Atlantic margin (Fig. 9b). Stratigraphic equivalents to the Billefjorden, Gipsdalen and Tempelfjorden groups have been identified in several exploration wells (Nøttvedt et al., 1993; Bugge et al., 1995). Where correlation between penetrated offshore successions and the onshore successions on Svalbard is possible, the same lithostratigraphic group names have been applied. Between Svalbard and Bjørnøya, the Finnmark Platform and the southern Barents Sea, the data coverage is poor, and thus separate group names have been established. In previous works, the late Palaeozoic succession in the Barents Sea has been referred to by a wide range of names; Ehrenberg et al. (1998a) divided the succession into nine units, L1-L9, where unit L9 corresponds to the Late Permian Tempelfjorden Group, whereas Samuelsberg et al. (2003) divided the succession into five seismic sequences (SS), where seismic sequence five corresponds to the

Tempelfjorden Group. Colpaert et al. (2007) divided the Late Palaeozoic succession of the Finnmark Platform into six seismic units (SU1-SU6), where SU1-SU4 correspond to the Ugle, Falk and Ørn formations of the Gipsdalen Group, SU5 corresponds to the Ulv and Isbjørn formations of the Bjarmeland Group and SU6 corresponds to the Røye and Ørret formations of the Tempelfjorden Group. Ahlborn et al. (2014) subdivided the Gipsdalen Group into three seismic units, where unit 1 comprises the Ugle, Falk and Minkinfjellet formations, unit 2 comprises the Wordiekammen and Ørn formations and unit 3 comprises the Gipshuken Formation and the Fafner succession.

A



B

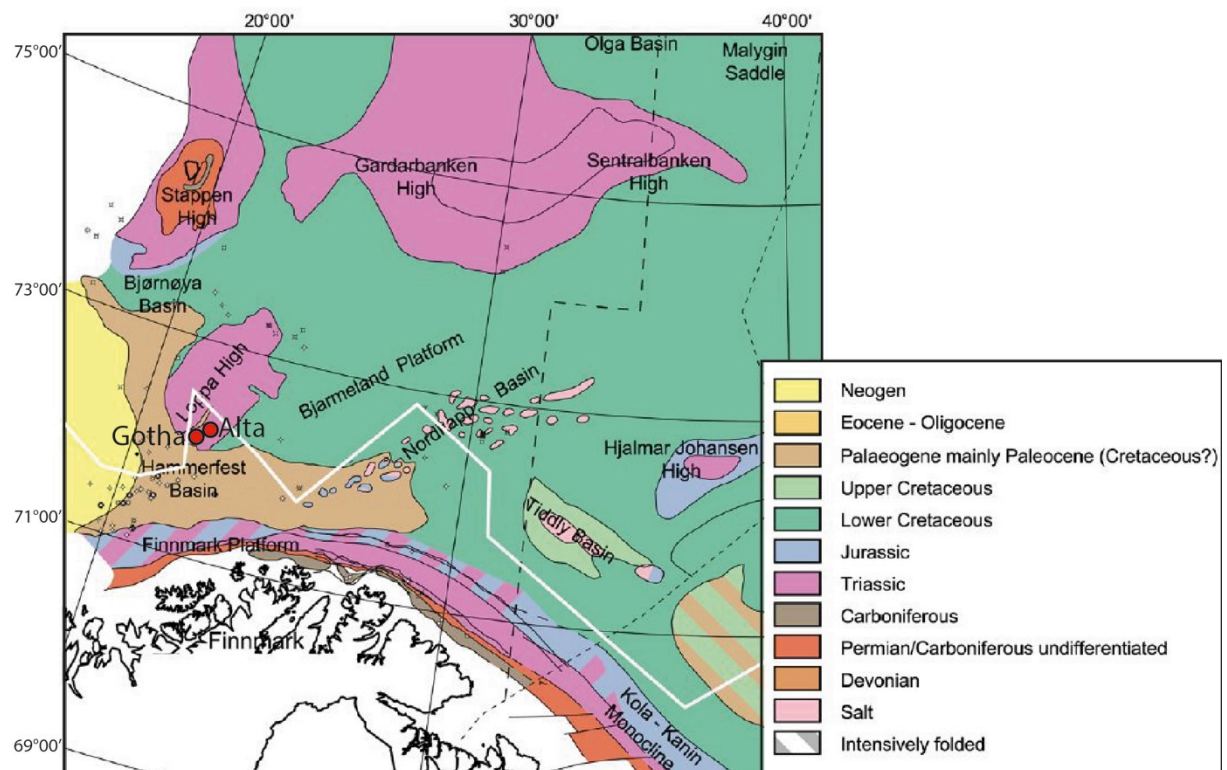


Figure 9: a) Regional geoseismic profile running from the Atlantic margin in the west to the Kola Monocline in the east. The profile shows the distribution of Late Palaeozoic rocks in grey and orange colours. The location of the profile is shown in figure 6b **b)** Regional subcrop map of the western Barents Sea region. Late Palaeozoic rocks are most common on the Finnmark Platform and the Stappen High. The white solid line indicates the location of the geoseismic profile. The Gohta (well 7120/1-3) and Alta (well 7120/11-1) discoveries were made in karstified Permian rocks on the Loppa High. Modified from Henriksen et al. (2011a).

The Gipsdalen Group is divided into three formations in the southern Barents Sea; the Ugle, Falk and Ørn formations. On Bjørnøya we find the equivalents Landnøringvika, Kapp Kåre, Kapp Hanna and Kapp Dunør formations. A newly described succession, the Fafner succession on northern flank of the Loppa High, is suggested to be an offshore equivalent to the Gipshuken Formation (Ahlborn et al., 2014). The Gipsdalen Group has been penetrated by several wells in the southern Barents Sea, e.g. wells 7229/11-1, 7128/6-1, 7128/4-1 and 7130/4-1 on the Finnmark Platform, wells 7220/6-2, 7120/1-1, 7120/2-1 and 7121/1-1 on the Loppa High, and wells 7124-3-1 and 7226/11-1 on the southern margins of the Bjarmeland Platform (Fig. 10)(Larssen et al., 2002). The shallow cores (7029/03-U-02, 7030/03-U-01 and 7129/10-U-02) were drilled close to the Finnmark coastline (Larssen et al., 2002). The same lithologies and rhythmic sequences found onshore Spitsbergen are also seen in the Barents Sea cores; redbeds, siltstones, conglomerates, mixed carbonates-siliciclastics, limestones and dolomites (Larssen et al., 2002). The thickest successions are more than 1000 m thick (well 7121/1-1, Fig. 10) and are found in the basinal areas (e.g. the Nordkapp Basin, Fig. 1 for location). Towards structural highs, e.g. the Loppa High and mainland Norway, the succession thins. Deposition of the basal non-marine Ugle Formation occurred during active rifting in the late Serpukhovian to Bashkirian in an alluvial-fluvial environment, while deposition of the overlying Falk Formation occurred in a shallow marine environment when siliciclastics still were supplied from emergent highs (Larssen et al., 2002). The uppermost Ørn Formation was deposited in shallow- to deeper marine environments during a warm and arid climate (Steel & Worsley, 1984; Larssen et al., 2002).

Gipsdalen Group

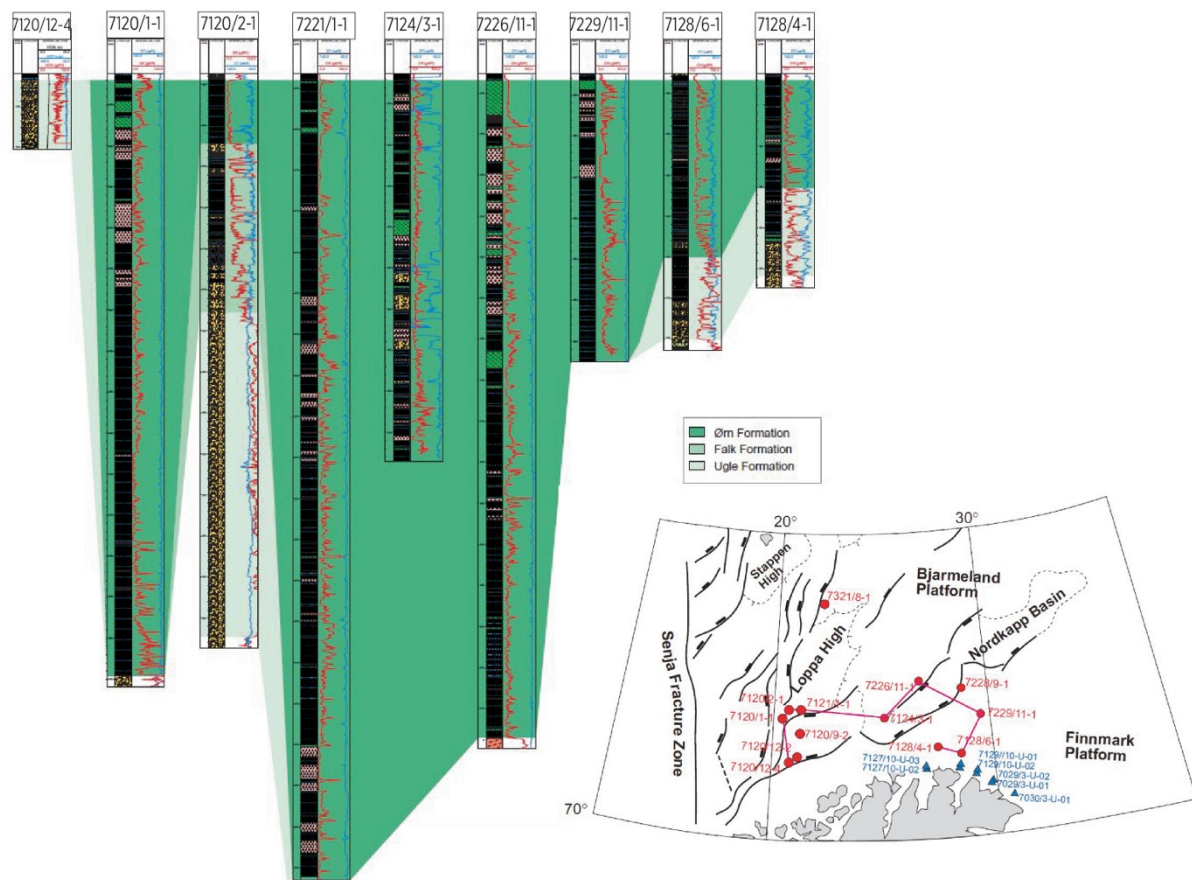


Figure 10: Correlation of the Ørn, Falk and Ugle formations of the Gipsdalen Group in wells on the Finnmark Platform, the Bjarmeland Platform and the Loppa High. The thickest developments are found in the basinal areas and the thinnest developments occur across structural highs. Location of the wells is shown on the map. Modified from Larssen et al. (2002).

The late Sakmarian-Artinskian successions of Svalbard and the southern Barents Shelf are rather different and therefore a new group, the Bjarmeland Group, has been established there (Dallmann et al., 1999). The Bjarmeland Group has been penetrated by several wells, including 7229/11-1, 7128/6-1 and 7128/4-1 on the Finnmark Platform, wells 7120/1-1 and 7121/1-1 on the Loppa High, and wells 7124-3-1 and 7226/11-1 on the southern margins of the Bjarmeland Platform (Fig. 11). The thickest penetrated succession is 488 m thick and is found in well 7121/1-1 on the Loppa High (Fig. 11) (Larssen et al., 2002). On the Bjarmeland Platform the thickness varies between 233 and 271 m (Wells 7226/11-1 and 7124/3-1), and on the Finnmark Platform the succession thins from 312 to 89 m (Wells 7229/11-1, 7128/4-1 and 7128/6-1)(Larssen et al., 2002). In the offshore areas, the Bjarmeland Group is represented by three formations; the Polarrev, Ulv and Isbjørn formations. The

Bjarmeland Group has one thin representative formation on Bjørnøya, the Hambergfjellet Formation, which lies stratigraphically below the Tempelfjorden Group and possibly is a condensed equivalent of the Isbjørn Formation (Dallmann et al., 1999). The base is marked by a major flooding surface, which marks the transition from a shallow warm water fauna to a cool water fauna of crinoids, bryozoans, brachiopods and siliceous sponges. The Bjarmeland Group is thin or absent over inner platforms and structural highs, such as on Spitsbergen and the southern Finnmark Platform, and is thickest at the eastern flank of the Loppa High and eastward across the Bjarmeland Platform (Larssen et al., 2002). The Bjarmeland Group may have lateral equivalents on Spitsbergen. It has been suggested that the lower Sakmarian to lower Artinskian part of the group may correlate to the uppermost Gipshuken Formation of Spitsbergen, whereas the uppermost Artinskian part, including the Hambergfjellet Formation of Bjørnøya, may be correlated to the Vøringen Member of the Kapp Starostin Formation (Dallmann et al., 1999; Worsley et al., 2001b; Larssen et al., 2005). If that is the case, there may be a hiatus between the Vøringen Member and the overlying Svenskegga member. This boundary was often covered by scree, however, at section B (Fig. 3c for location) dark spiculite was lying directly above the Vøringen Member. Although the boundary was very distinct, it was neither possible to confirm or disprove such.

Bjarmeland Group

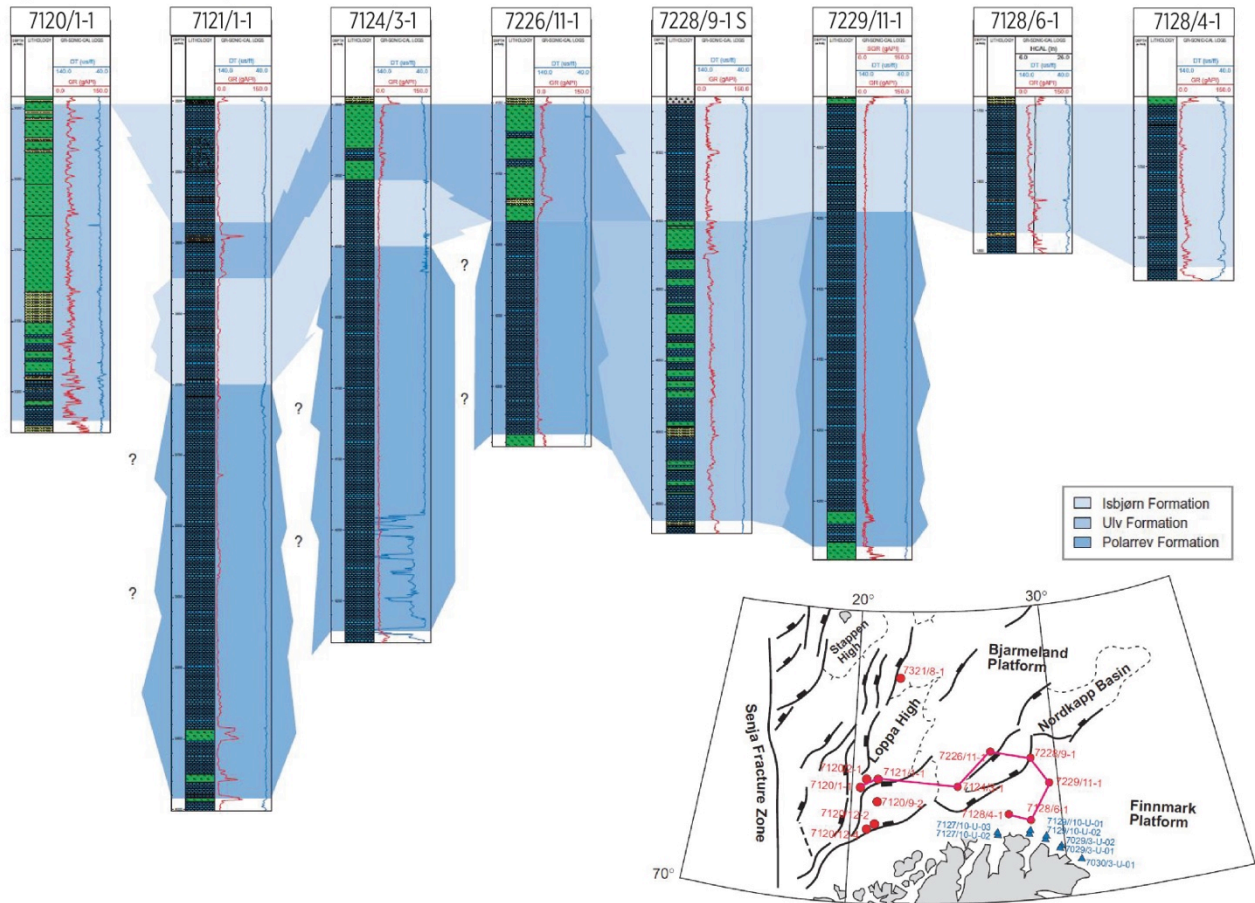


Figure 11: Correlation of the Isbjørn, Ulv and Polarrev formations of Bjarmeland Group in wells on the Finnmark Platform, the Bjarmeland Platform and the Loppa High. Location of the wells is shown on the map. Modified from Larssen et al. (2002)

In the Barents Sea, the Tempelfjorden Group lies on top of the Bjarmeland Group, except for a few known places where it lies directly on top of the Gipsdalen Group (wells 7120/12-1 and 7120/12-4) (Larssen et al., 2005). The group is divided into two formations, the Røye Formation and the Ørret Formation, which are both lateral equivalents to the Miseryfjellet Formation of Bjørnøya and the Kapp Starostin Formation of Spitsbergen. The group is thickly developed along the southern margin of the Loppa High, where a thickness of 509-591 m has been recorded (wells 7121/1-1 and 7120/1-1) (Larssen et al., 2002). However, the thickest developments are found on the southern margin of the Hammerfest basin where 752-901 m of the succession has been penetrated (wells 7120/12-2 and 7120/12-4, Fig. 12). On the Bjarmeland Platform the group thins to 425 m (well 7124/3-1) and 226 m (well 7226/11-1), whereas on the Finnmark Platform the group thins from 180 m (well 7228/9-1) on the northern margin to 135 m (wells 7128/4-1 and 7128/6-1) (Larssen et al., 2002). The lithologies are

similar to the equivalent successions on Svalbard, except for in the southwestern Hammerfest Basin (wells 7120/12-4 and 7120/12-2), where coarse siliciclastics also occur (Larssen et al., 2002). The Røye Formation comprises silicified mudstones, limestones and spiculites, whereas the overlying Ørret Formation is composed of less silicified mudstones and coarser siliciclastics (Larssen et al., 2002).

The Tempelfjorden Group thins over structural highs, also across the Loppa High, where it thins and is truncated upflank due to repeated Permian-Early Triassic uplift (Fig. 9a) (Larssen et al., 2002). The uplift and subaerial exposure has led to karstification of the carbonate deposits on the crest of the high (Stemmerik et al., 1999). On the southern margin of the Loppa High wells have penetrated the Røye Formation (7121/1-1) and interfingering of successions Røye and Ørret Formation (7120/1-1, 7120/12-2 and 7120/12-4)(Fig. 12)(Larssen et al., 2002). The Røye Formation is laterally continuous from the eastern Finnmark Platform to the Loppa High, whereas the Ørret Formation is laterally passing into the Røye Formation updip the Finnmark Platform and the Loppa High (Fig. 12) (Larssen et al., 2002)

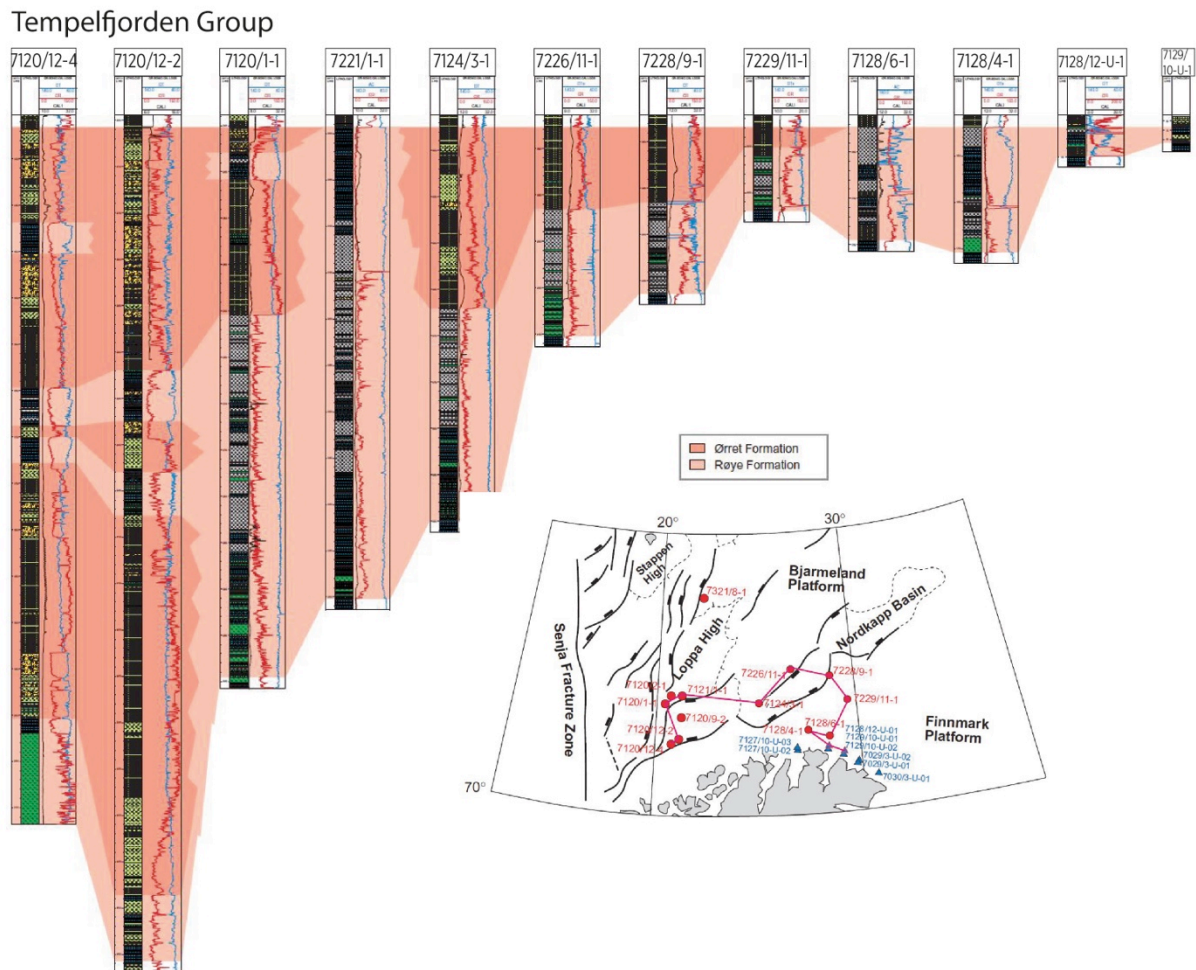


Figure 12: Correlation of the Ørret and Røye formations of the Tempelfjorden Group in wells on the Finnmark Platform, the Bjarmeland Platform and the Loppa High. Location of the wells is shown on the map. Modified from Larssen et al. (2002).

2.4 Correlation with Arctic Canada and North Greenland

The Late Palaeozoic succession of Svalbard and the Barents Sea show strong similarities to the time-equivalent successions of North-East Greenland, Arctic Canada and the Sverdrup Basin in particular (Cutbill & Challinor, 1965; Worsley et al., 1986). Plate tectonic reconstructions indicates that these areas was located close to each other during the Late Palaeozoic to early Mesozoic times, and that Svalbard possibly was connected to Ellesmere Island as an eastern extension of the Sverdrup Basin (Worsley et al., 1986). During the Late Carboniferous and Permian, Svalbard and the Barents Sea was part of a large province extending from the Canadian Arctic to northern Russia and southward to the Caspian Sea (Faleide et al., 1984; Stemmerik & Worsley, 1989). Outcrops with similar facies development as the Tempelfjorden Group are found throughout this province, in a depositional belt extending for more than 3,000 km

(Beauchamp & Desrochers, 1997). In all of these regions the Carboniferous lies discordant on the older rocks, and the Lower Carboniferous strata contains coal seams (Cutbill & Challinor, 1965). Over that, there is a succession of warm-water carbonates, evaporites and clastics of middle Carboniferous to Early Permian age, and a succession of shales, sandstones, cool-water carbonates and spiculites of Late Permian age (Fig. 13). The increasingly cooler-water facies are a result of the gradual northwards drift of the region together with changing oceanographic circulation (Reid et al., 2007). Plate tectonic reconstructions indicates a gradual northwards drift of the Sverdrup Basin and Barents Sea area from a latitude of about 25°N -35°N during the Bashkirian-Sakmarian, to just north of 35°N during the Artinskian and 40°N during the Kungurian-Kazanian (Golonka et al., 1994). Dating and correlation of the Artinskian-Kazanian successions in Greenland, Svalbard and the Barents Sea is based on fossils like fusulinids, conodonts, palynomorphs and small foraminifera (Piasecki, 1984; Stemmerik et al., 1991; Nakrem et al., 1992; Mangerud, 1994; Bugge et al., 1995; Stemmerik, 1996).

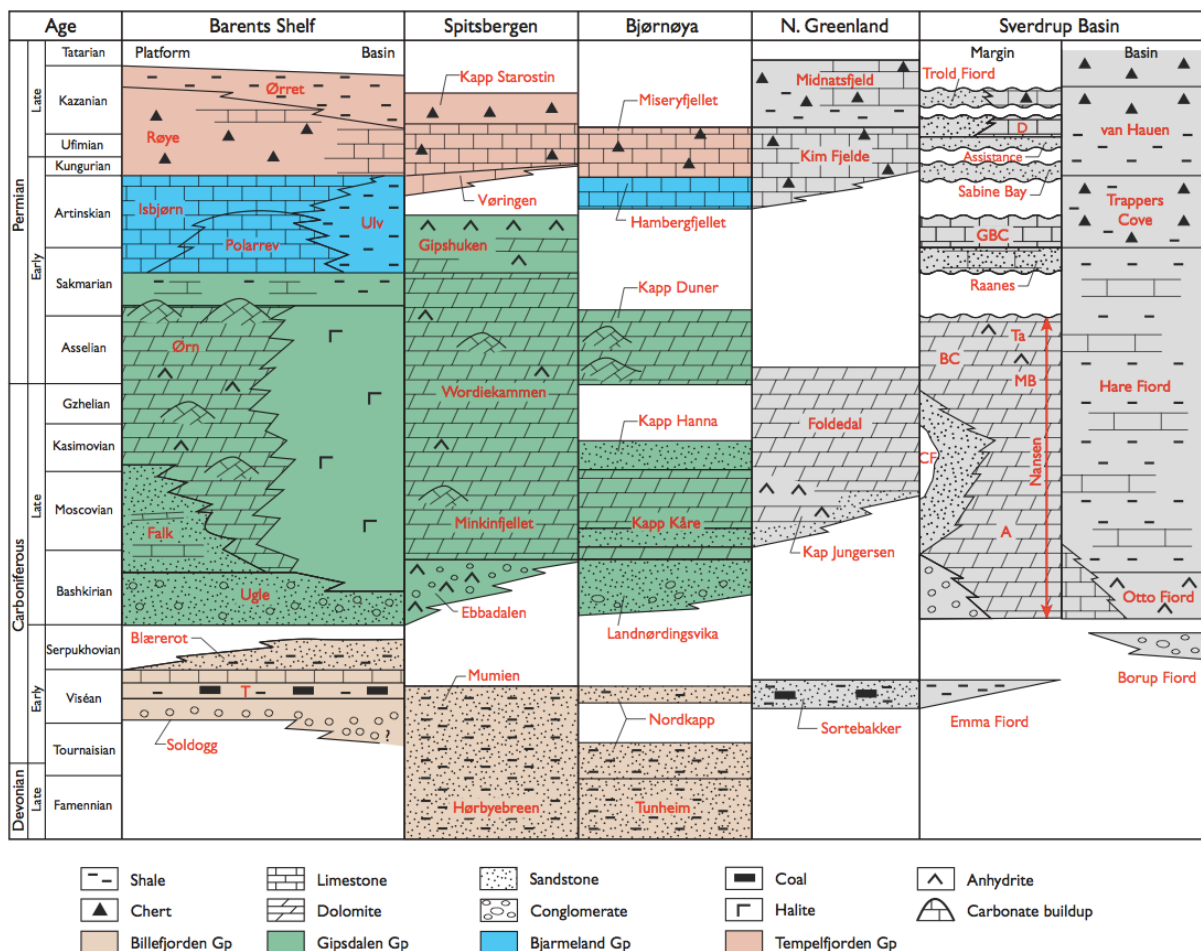


Figure 13: Correlation of the Late Palaeozoic strata of the Sverdrup Basin, North Greenland, Barents Shelf, Bjørnøya and Spitsbergen. This study focus mainly on the Late Permian succession on the Barents Shelf and Spitsbergen. A:Antoinette, D:Degerbøls, T:Tettegras, BC:Belcher Canyon, CF:Canyon Fiord, MB:Mount Bayley, Ta= Tanquary, GBC:Great Bear Cape. Larssen et al. (2005).

The Moscovian to Sakmarian sediments are characterized by widespread carbonate deposition (Fig. 13) (Larssen et al., 2005). The Gipsdalen Group on Spitsbergen can be correlated with the Kap Jungersen and Foldedal formations in North Greenland, and with the Borup fiord, Otto Fiord, CanyonFiord, Nansen, Antoinette, Tanquary, Belcher Fiord and Hare Fiord formations in the Sverdrup Basin (Beauchamp et al., 2001). The succession in North Greenland is stratigraphically incomplete and only records the Moscovian to Gzelian development on a carbonate-dominated shelf, whereas the Sverdrup Basin succession is stratigraphically complete and lithologically complex (Larssen et al., 2005). Large parts of the shelf were subjected to uplift and erosion during the latest Sakmarian. This erosion is evident from missing stratigraphy on Spitsbergen, Bjørnøya, North Greenland and the marginal parts of the Sverdrup Basin (Fig. 13)(Larssen et al., 2005). The sedimentation was only continuous in the deep basins, such as basins on the Barents Shelf and the deeper parts of the Sverdrup Basin (Larssen et al., 2005). The Isbjørn, Polarrev and Ulv formations of the Bjarmeland Group can be correlated to the lower Kim Fjelde Formation in North Greenland, and the Raanes, Great Bear Cape and Trappers Cove formations of the Sverdrup Basin (Fig. 13) (Beauchamp et al., 2001). The Tempelfjorden Group can be correlated to the Sabine Bay, Assistance, Trolld Fiord, Degerbøls and van Hauen formations of the Sverdrup Basin, and the upper Kim Fjelde and Midnatsfjeld formations on North Greenland (Fig. 13)(Beauchamp et al., 2001). The Miseryfjellet Formation on Bjørnøya and the main part of the Kapp Starostin Formation on Spitsbergen are dated as Kungurian-Ufimian (Nakrem, 1991). This age is also suggested for the upper part of the Kim Fjelde Formation, the lower part of the Van Hauen Formation and the Sabine Bay, Assistance and Degerbøls formations in the Sverdrup Basin, and for parts of the Røye Formation in the Barents Sea (Mangerud, 1994; Stemmerik, 1996). The Midnattfjeld Formation in North Greenland, the uppermost part of the Kapp Starostin Formation on Spitsbergen and the Røye Formation in the Barents Sea are dated Kazanian (Stemmerik, 1997), whereas the Trolld Fiord and Degerbøls formations in the Sverdrup Basin are dated Roadian to Wordian (Beauchamp et al., 2001).

3. Methods

The main data for this thesis was obtained during conventional fieldwork involving sedimentological measurements of vertical outcrop sections and collection of samples. The data is based on five sections (A-E) that were all measured within a 10 km² area; section A through the upper part of the Gipshuken Formation, section B through the uppermost part of the Gipshuken Formation and the boundary to the Kapp Starostin Formation, section C through the Vøringen Member, section D through the major part of the Kapp Starostin Formation and section E through the uppermost part of the Kapp Starostin Formation and the boundary to the overlying Triassic Vikinghøgda Formation (Fig. 3c for location). Due to the steepness of the outcrops, several lateral shifts along sections A and D had to be made. However, lateral continuity of the strata made it possible to do these lateral shifts by following distinct beds. The glauconitic sandstone of what is inferred to be the Hovtinden member was usually covered by scree, which made it difficult to find exposures. Although a few small exposures were found, description of this lithofacies is mainly based on cobbles found in rivers and ravines.

The description of the outcrops resulted in a composite lithostratigraphic log with parameters like bed thickness, lithology, grain size, structures, fossils and bioturbation. The lithostratigraphic logs measured in the field were digitalized in a 1:50 scale to give a visual impression of the section. The digitalization was done by the use of Adobe Illustrator. The individual logs from section A-E are included in Appendix 1., whereas a composite log is shown in Fig. 40. Carbonates were classified after Dunham (1962), modified by Embry & Klovan (1972), while siliclastic rocks were classified after Pettijohn et al. (1972). Component percentages were determined semi-quantitatively as abundant (>80%), frequent (80-50%), common (50-20%), occasional (20-1%) or rare (<1%). The grain size was determined visually after the Udden-Wentworth scale by the use of a hand lens. Spiculites were classified as either dark or light. Megascleres are defined as spicules having diameters greater than 3 microns (Scholle & Ulmer-Scholle, 2003) or lengths greater than 63 microns (Gammon & James, 2001). Supplementary thin section analysis ensured correct classification and were used to establish the facies. Rock samples were collected systematically for each facies and also at several levels throughout the investigated succession in order to produce thin sections for microfacies

investigation. In total, 37 samples were collected, whereby 22 of them were carefully cut with a water-cooled circular rock saw. The samples were then made into thin sections with a thickness of approximately 30 microns. Thin section analysis was done to determine the mineralogical and textural composition. The thin sections were analysed in plain- and polarized light by the use of a polarizing light microscope (Nikon Eclipse e200). A Zeiss AxioCam ERc5s was used to make the thin section photographs.

Standard equipment like hand-lens, measuring stick, geological hammer, grain size chart, GPS, compass and a digital Canon EOS 400D camera was used in the field. Altitude measurements were obtained by GPS and may be uncertain, due to the weather dependency of the system. This altitude uncertainty also makes the thickness estimation for the gaps between the different sections in the composite log uncertain. Some parts of the studied outcrops were scree-covered or inaccessible, so small parts of the composite log is based on description of loose boulders, poorly exposed stream-sections and observations from a distant. Although this may create some minor errors, the composite log is representative of the actual outcrops.

A core section (50.3 m) from the Gohta discovery (well 7120/1-3) on the Loppa High was compared with the outcrop data from Spitsbergen. Although the observed facies were similar to those defined on Spitsbergen, they were divided into separate facies. This separation was done due to the lack of thin sections from the core section and thus not sufficient information to confirm microscopically similarity. The lithostratigraphic log from the core section is included in Appendix 1.

4. Facies analysis

4.1. Introduction

A significant shift from photozoan to heterozoan carbonate associations is recorded across the boundary between the Gipshuken and the Kapp Starostin formations. This change represents a change from a warm-water, shallow and periodically evaporitic basin to cool-water, fully open-marine conditions (Ehrenberg et al., 2001; Blomeier et al., 2011). The recognized facies are therefore presented formation-wise and reflect decreasing energy conditions. Facies descriptions are based on field observations from the study area in Dickson Land and thin section analysis of 22 samples collected during fieldwork. Outcrop observations include lithology, colour, texture, structures and macrofossils. The facies are distinguished based on their macroscopical and microscopical components, including grain size, mud-content, density and type of fossils and degree of bioturbation. Fourteen depositional facies have been recognized from the investigated succession in Dickson Land (Facies 1-14), and another three facies from the core section from well 7120/1-3 (Facies 15-17). Summary of lithofacies descriptions and interpretations are provided in Table 1.

Table 1: Facies and facies associations

Facies association	Facies	Lithology	Description	Sedimentary process/Depositional environment
FA1	1	Intraclast conglomerate	Rock composed of cm-sized micritic intraclasts. Extensive fractures are filled with blocky calcite cement.	Formed by desiccation and in-situ brecciation of upper intertidal or supratidal mudflats in a warm and arid to semi-arid environment.
FA2	2	Microbial mudstone	Biolaminated mudstone with alternating microcrystalline micritic laminas and coarser laminas with abundant silt sized quartz grains.	Formed by filamentous and unicellular micro-organisms, which traps and binds sediments on the surface of microbial mats, typically in a restricted, lagoonal to tidal-flat environment of a warm-water carbonate platform.
FA2	3	Dolomitic mudstone	Light grey to dark grey mudstone with wavy and continuous bedding planes. Cracks and fissures are filled with gypsum and primary sedimentary structures have been obliterated due to the dolomitization.	Probably formed by dolomitization of microbial mudstones and/or by dolomitization of carbonate mudstones deposited in low-energy environments on a protected inner platform.
FA2	4	Argillaceous limestone	Light brownish to grey carbonate mudstone with a considerable amount of clay minerals (<20%).	Formed by deposition in a low-energy environment, like a protected lagoon or on the distal ramp below SWWB. The argillaceous material is of terrigenous origin and deposited through suspension fallout.
FA3	5	Glauconitic sandstone	Well-sorted sandstone composed of sub-angular to sub-rounded fine sand sized quartz grains and rounded to sub-rounded glauconite grains. The sandstone is extensively bioturbated by <i>Zoophycos</i> and contains occasional fractured brachiopod shells.	Deposited in the high-energy environment of the shoreface zone (above FWWB). The quartz grains are derived from a terrestrial source, whereas the glauconite grains were formed within the sediments.
FA3	6	Brachiopod dominated pack- to rudstone	Massive, medium- to thick bedded limestone with abundant skeletal fragments and shells. Brachiopods dominate, but bryozoans and crinoids are also common. Pores are filled with a sparry calcite cement. Erosive bases and graded beds are common.	Deposited in the high-energy environment of the shoreface zone (above FWWB). The erosive lower boundaries and normal grading are due to storm-related erosion and deposition. Proximal tempestites.
FA4	7	Light spiculite	A massive to nodular yellowish (grey in fresh fractures) rock with abundant dark grey silica nodules and trace fossils of the <i>Planolites</i> , <i>Nereites</i> , <i>Phycosiphon</i> and <i>Zoophycos</i> ichnotaxa. The rock is composed of monaxone megascleritic siliceous sponge spicules.	Formed by accumulation of siliceous sponge spicules in well-oxygenated conditions between the FWWB and SWWB. Intense post-depositional silicification.
FA4	8	Chert breccia	Composed of dark grey angular chert fragments in a blueish-white	Formed by brecciation of light spiculite, either by gradual

			cement of microcrystalline quartz. Vugs and fractures are common.	dissolution and collapse or by the impact of a short-lived high-energy event. See facies description for different theories.
FA5	9	Bryozoan dominated floatstone	Massive and thin-bedded limestone with a mud-supported fabric. Trepostome and fenestellid bryozoans dominate. The micritic matrix contain quartz grains, glauconite grains and sponge spicules.	Resulting from storm reworking of the mid-ramp colonies and transport of the bioclastic material to low-energy environments below the SWWB. Distal tempeste.
FA5	10	Bryozoan-Echinoderm dominated pack- to rudstone	Coarse-grained bioclastic limestone dominated by bryozoans and echinoderms. The matrix is dominated by dolomitic micrite.	Bioclastic material transported from the outer mid ramp to the mud dominated outer ramp below SWWB by relaxation flows or partly by storm wave-supported gravity flows. Distal tempestites.
FA5	11	Bryozoan dominated pack-to rudstone	Coarse-grained bioclastic limestone dominated by cystoporate, trepostome and fenestellid bryozoans. The micritic matrix contains abundant sponge spicules.	Bioclastic material was probably transported from the outer mid-ramp to the low-energy environments below the SWWB, where it was embedded in the micritic matrix. Distal tempestites.
FA5	12	Dark spiculite	A nodular, dark grey to black rock composed of monaxone microclerical siliceous sponge spicules. The spicules are embedded in a dark brown dolomitic, micritic matrix. Bioturbation is common and dominated by <i>Nereites</i> and <i>Phycosiphon</i> .	Deposited in a low-energy, oxygen deficient environment below SWWB.
FA5	13	Black shale	Dark grey to black laminated shale composed mainly of micrite and silt- and sand sized quartz grains. Occasional skeletal fragments and a few whole sponges of the Lithistida order.	Deposited by suspension fallout in the low-energy environments below SWWB, allowing organic material to be preserved.
FA6	14	Laminated siltstone	Homogeneous brown to grey shaly siltstone with planar parallel lamination. No bioturbation or bioclastic material.	Deposited in a low-energy anoxic environment of a siliciclastic shelf.
Gohta core	15	Light spiculite	Tightly cemented light grey spiculite intensely bioturbated by <i>Nereites</i> , <i>Zoophycos</i> and <i>Phycosiphon</i> . Some dark grey silica nodules <3cm in diameter.	Deposited in well-oxygenated conditions between the FWB and SWWB.
Gohta core	16	Dolomitic light spiculite	Light brown to brownish grey dolomitic light spiculite. Some areas are brecciated with angular fragments <6 cm embedded in a dark brown matrix.	Formed by accumulation of siliceous sponge spicules and subsequent diagenetic alteration in terms of silicification, dissolution and dolomitization.
Gohta core	17	Black shale	Dark grey to black laminated shale occurring as thin layers (<2 cm) and laminae within the dolomitic light spiculite. <i>Chondrites</i> trace fossils.	Deposited in low-energy, oxygen-deficient environments far below the SWWB.

4.2 Facies of the Gipshuken Formation

Facies 1: Intraclast conglomerate

The following description is based on observations at section B (Fig. 16b), and detailed analysis of thin section no. 4 (Fig. 14).

Description: This facies comprises a dark brown fine-grained rock with several calcite filled fractures (Fig. 16b). The rock is composed of dark brown intraclasts up to 2,25 cm long. The clasts are sub-angular to rounded and have an internal homogeneous micritic fabric, except for a few clasts, which have internal horizontal to wavy lamination and may be intraclasts of microbial mudstone (Fig. 14). Micritic peloids also occur, and are probably smaller intraclasts. Most of the contacts are sutured. Extensive fractures and secondary pores are filled with blocky sparite cement. Opaque minerals are scattered throughout the facies and many of the intraclast have micrite coatings/crusts. No fossils are observed.

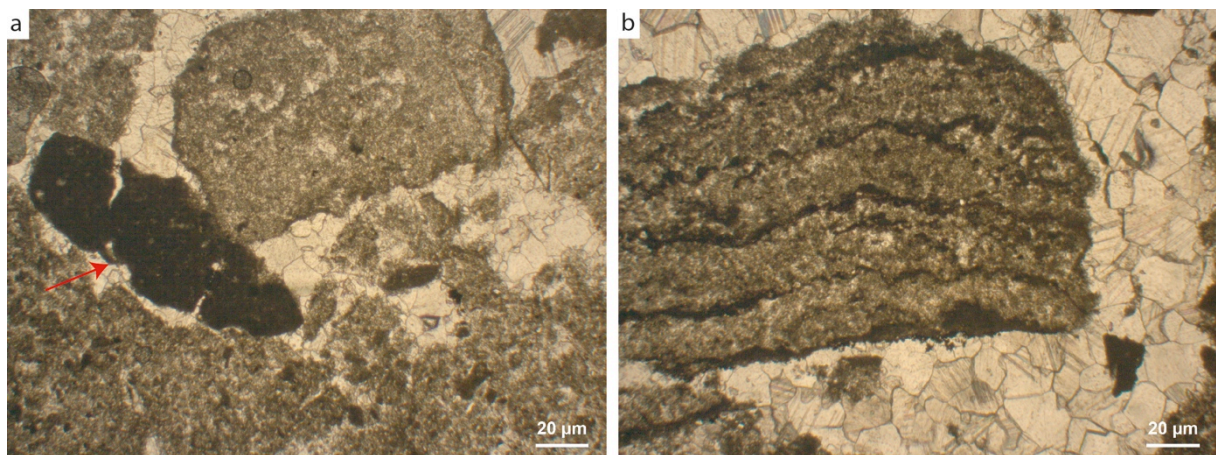


Figure 14: **a)** Intraclasts and micritic peloid (arrow). Fractures are filled with a blocky sparry calcite cement. Thin section no. 4, PPL. **b)** Intraclast with internal horizontal to wavy lamination, probably an altered clast of microbial mudstone. Blocky sparry calcite cement. Thin section no. 4, PPL.

Occurrence and association: The intraclast conglomerate occurs at the top of the Gipshuken Formation, just below the boundary to the Vøringen Member of the Kapp Starostin Formation. The facies is associated with microbial mudstone (F2, Table 1).

Interpretation: Based on the occurrence of micritic peloids, both isolated and in aggregates of clotted micrite, and in situ-brecciation, this facies is interpreted to be

caliche soil profiles (Flügel, 2010). The intraclast conglomerate might have been formed by desiccation of microbial mats, crystallization pressure of evaporites and/or by currents with plasticlasts (Buggisch et al., 2012). Although no fossils are observed and the environment probably was hostile (dry, saline), the micritic coatings represent microcrystalline cement, which may have been microbially triggered (Flügel, 2010). The formation through desiccation or evaporite crystallization suggests a proximal depositional environment in the platform interior, like an intertidal or supratidal flat, and a warm and dry climate.

Facies 2: Microbial mudstone

The description of the microbial mudstone is based on observations of section A and B (Fig 16), and detailed analysis of thin section no. 3 (Fig. 15).

Description: The microbial mudstone is a bindstone composed of alternating light grey and dark grey laminas (Fig. 16c). The light grey laminas are generally thicker than the dark grey laminas, on average 3 mm and 0.8 mm respectively. The lamination is continuous and horizontal to wavy, and may in some places be incipient stromatolite lamination. On a microscale, the structure of the alternating laminas is visible. The dark laminas consist of dark brown to grey homogeneous micrite with a very fine microcrystalline structure, while the lighter laminas consist of a light grey to brownish heterogeneous micrite with a coarser microcrystalline structure (Fig. 15). Opaque minerals occasionally cement the coarser laminas and Fe-staining sometimes occurs parallel to the lamination. Sponge spicules up to 0.75 mm long are common in both the heterogeneous and homogeneous laminas, and are especially dense along certain horizons. Subangular to subrounded silt sized detrital quartz grains are also scattered around, but are more common in the coarser heterogeneous laminas. Poorly developed stylolitic seams both parallel and perpendicular to bedding are also observed (Fig. 15b).

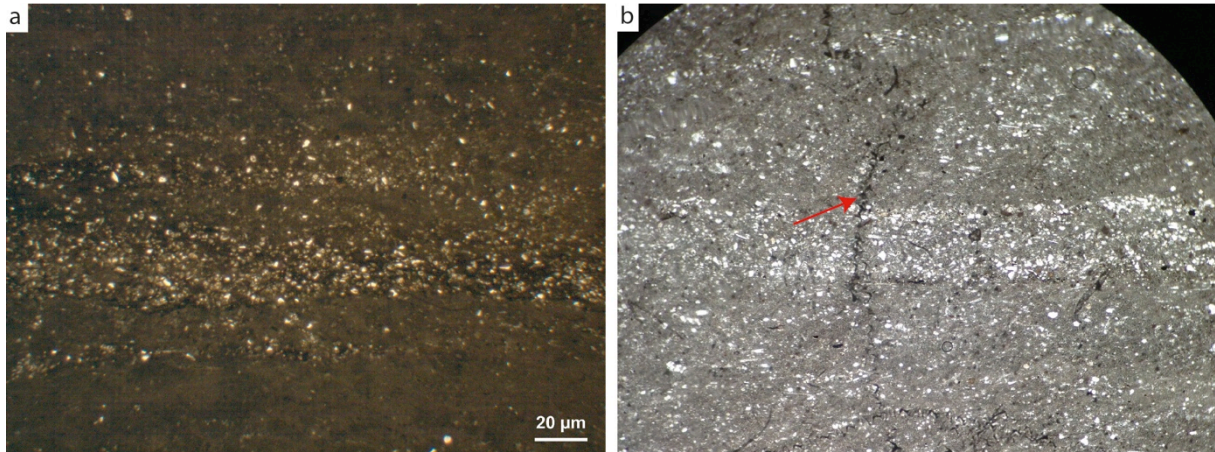


Figure 15: Thin section photos of sample no. 3. **a)** Dark micritic laminae with a fine microcrystalline structure (top and bottom) and a lighter coarser grained lamina with frequent silt sized quartz grains (center). Thin section no. 3, PPL. **b)** Weakly developed stylolites (arrow) in the biolaminated mudstone. Thin section no. 3, PPL.

Occurrence and association: Microbial mudstone is common throughout the Gipshuken Formation and is closely associated with the dolomitic mudstone (F3, Table 1) and intraclast conglomerate (F1, Table 1).

Interpretation: The horizontal to wavy and incipient stromatolite lamination of the mudstone is suggested to be of microbial origin. Although microbial carbonate rocks are known from both marine, marginal-marine, freshwater and terrestrial environments (Flügel, 2010), microbial mats are characteristic for the upper intertidal zone (Kendall & Harwood, 1996). The presence of detrital quartz and the close association with the intraclast conglomerate (F1, Table 1), also suggests a proximal depositional environment, such as a marginal-marine tidal-flat environment. Microbial mats consist of layers of filamentous and unicellular micro-organisms, which trap and bind sediments resulting in the biolaminated sedimentary structures (Tucker et al., 1990). Daily sea level fluctuations control the episodic trapping, binding and precipitation of fine grained carbonate, and thus also the lamination (Blomeier et al., 2011). This facies is therefore interpreted to be a result of cyclic deposition in a restricted, lagoonal to tidal-flat environment of a warm-water carbonate platform (Blomeier et al., 2011).

Facies 3: Dolomitic mudstone

The following description is based on observations at locality A and B.

Description: This facies consists entirely of light grey to dark grey dolomitic mudstone. The fine-grained rock is medium-bedded (approximately 10 cm) with wavy and continuous bedding planes, and has a massive to faintly wavy laminated structure. The rock may be a mixed dolostone/limestone and has many cracks and fissures infilled with gypsum.

Occurrence and association: This facies occurs throughout the Gipshuken Formation and is associated with microbial mudstone (F2, Table 1) and argillaceous limestone (F4, Table 1).

Interpretation: The massive and structureless fabric of this facies makes interpretation of depositional process and environment difficult. However, the presence of wavy lamination in some of the mudstones and the close association to the microbial mudstone (F2) may suggest that the rock was formed by secondary dolomitization of original algal mudstones. Another possibility is that fine-grained carbonate mud settled out of suspension in a low-energy environment seaward of the algal mats and formed a (non-microbial) carbonate mudstone that later was dolomitized. Fine-grained sediments and restricted fauna is typical for carbonate lagoons (Tucker et al., 1990). Dolomitization is a process in which calcium-ions in a carbonate rock are replaced by magnesium. The main considerations in the formation of dolomite are the source of Mg^{2+} ions and the process whereby the dolomitizing fluid is pumped through the carbonate rock (Tucker et al., 1990). Three principal models are proposed for this process: 1) the hypersaline (sabkha, evaporation, reflux) model, 2) the mixed-water (mixing-zone) model, and 3) the sea-water (shallow-subtidal) model (Boggs, 1995a). As deposition of the Gipshuken Formation occurred in a typical sabkha environment, dolomite probably formed as in the hypersaline model. When evaporation exceeded the precipitation, the seawater beneath the sediment became concentrated, so that the Mg/Ca ratio increased (Boggs, 1995a). Dolomitization of the mudstone probably

occurred during early diagenesis when Magnesium-rich water moved through the algal mudstone/carbonate mudstone, which led to replacement of calcium with magnesium.

Facies 4: Argillaceous limestone

The following description is based on observations at locality A, and study of sample no. 2 under a magnifying glass.

Description: This facies is composed of light brownish to grey carbonate mud with a considerable amount of clay minerals (<20%). The rock is massive to slightly fissile and has wavy bedding planes. It is also very loosely packed and easily crumbles.

Occurrence and association: This facies occurs throughout the Gipshuken Formation and is closely associated with dolomitic mudstone (F3, Table 1).

Interpretation: The fine-grained composition of this facies suggests deposition in a low-energy environment, for example a protected lagoon or on the distal ramp below storm-weather wave base (SWWB). The clay-sized argillaceous material is probably of terrigenous origin also indicates deposition in a low-energy environment, where the fine grained material can settle out of suspension. Due to the close association with the dolomitic mudstone (F3), the argillaceous limestone is interpreted to have been deposited in low-energy environments of a protected lagoon.

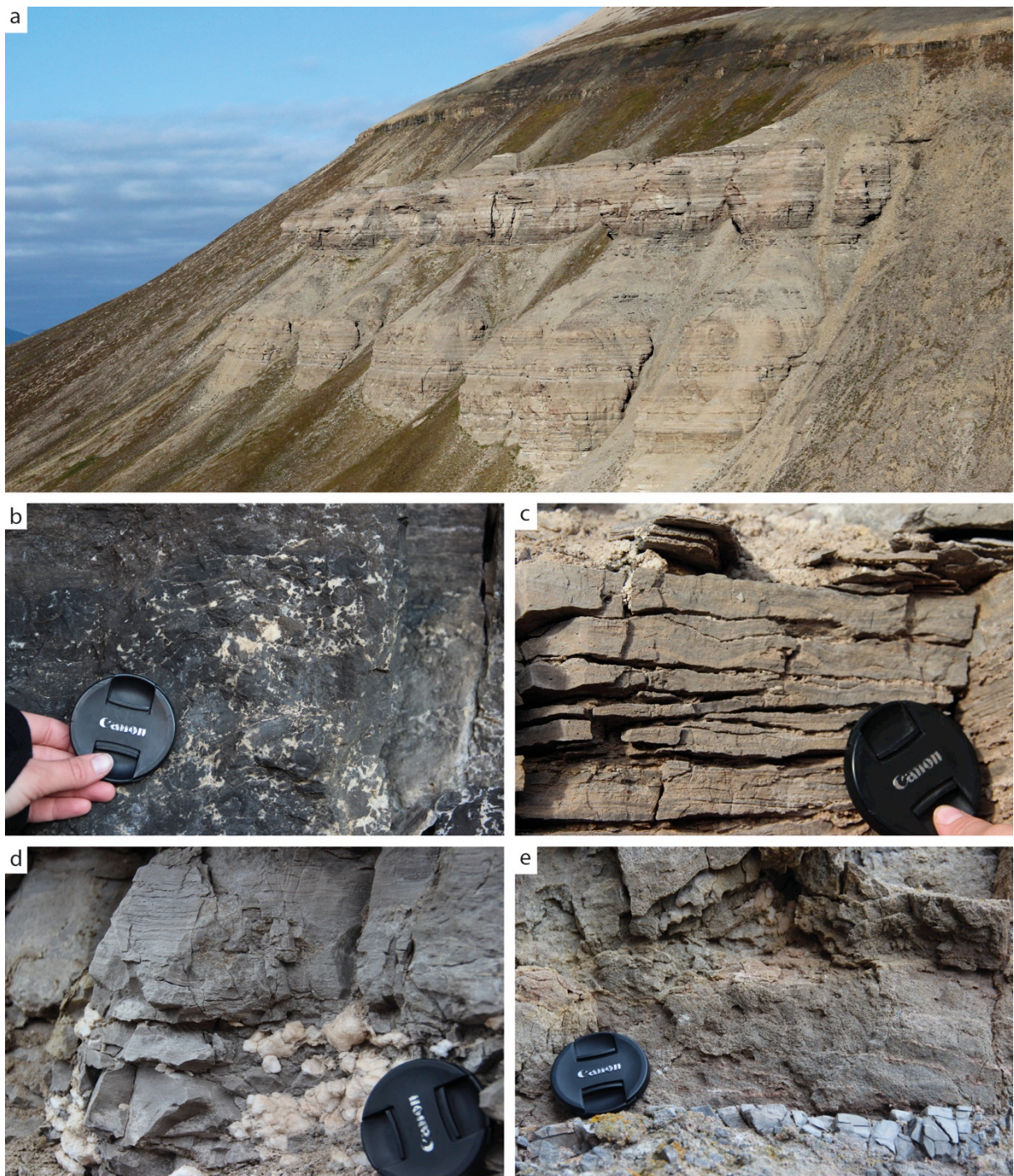


Figure 16: **a)** Overview of locality A (see Fig. 3c for location). Section A was measured on the third cliff from the right (upper and lower cliff). **b)** F1: Lithoclastic rudstone. Fractures are cemented by post-depositional sparry calcite cement. Level 90 m in the composite log (section B). **c)** F2: Microbial mudstone with mm-scale wavy lamination. Level 62 m in the composite log. (section A). **d)** F3: Dolomitic mudstone. The grey rock is massive in the lower part of the picture, but faint lamination can be observed in the upper part of the picture. Gypsum occurs in the middle part. Level 75 m in the composite log (section A). **e)** F4: Argillaceous limestone. A thin layer of dolomitic mudstone can be seen in the lower part of the picture. Level 22 m in the composite log (section A).

4.3 Facies of the Kapp Starostin Formation

Facies 5: Glauconitic sandstone

The following description is based on cobbles found downfall from section D, observations of section E (Fig. 17a), and detailed analysis of thin sections no. 30 and 32.

Description: The sandstone is homogeneous, massive and thin-bedded, and has a high content of glauconite, which gives the rock a clear green colour. The sandstone is well-sorted and is predominantly composed of monocrystalline sub-angular to sub-rounded fine sand sized quartz grains (45%) and fine sand sized rounded to sub-rounded glauconite grains (45%)(Fig. 17d, e). The grains commonly show point contacts, but sometimes also sutured contacts. Micritic matrix fills the pores and also occurs as a few micritic peloids. Opaque minerals and rare to occasional thick-shelled, disarticulated and fractured brachiopods are scattered throughout. This facies is extensively bioturbated by *Zoophycos* trace fossils.

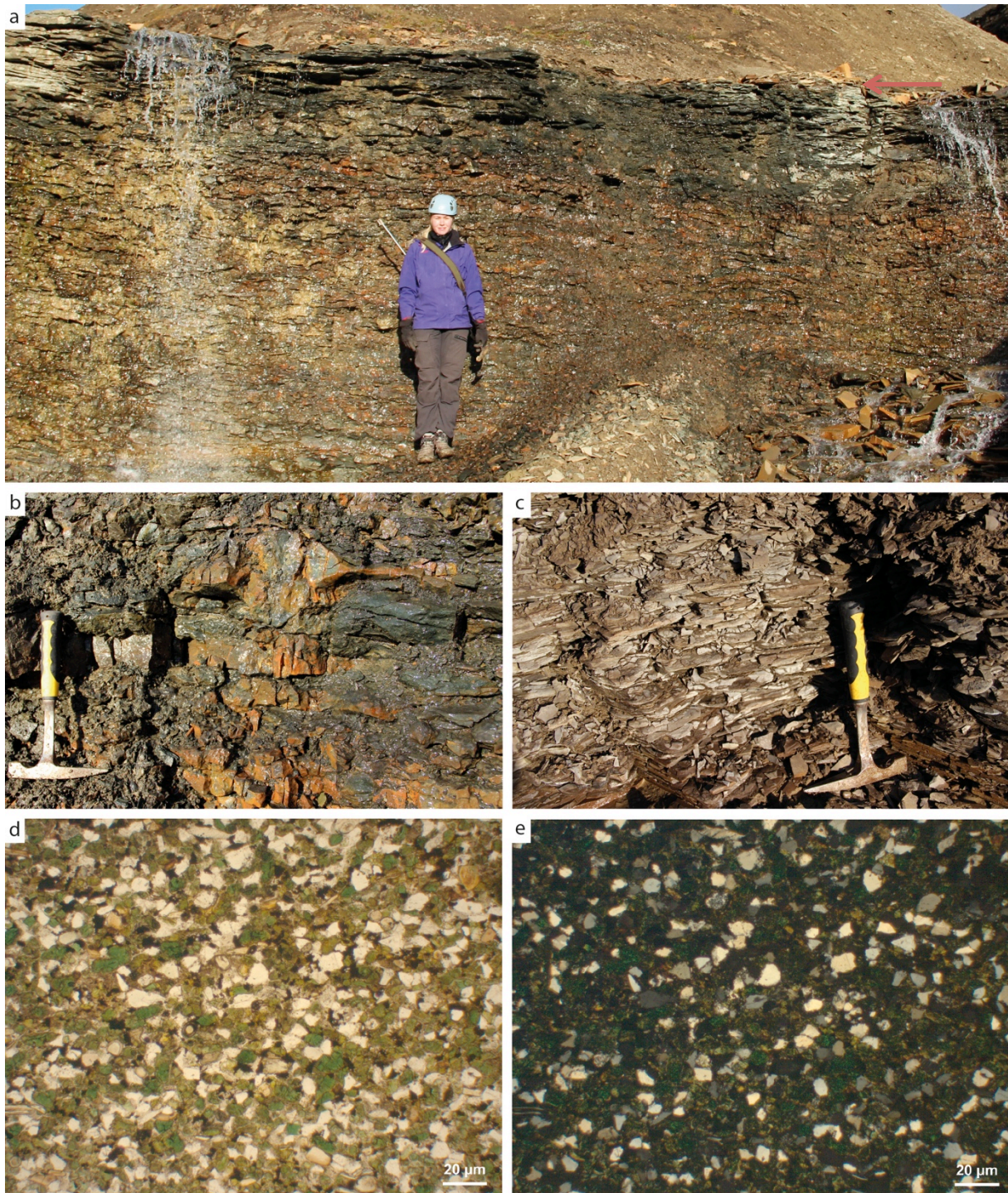


Figure 17: a) Light spiculites interbedded with glauconitic sandstone in the lower part of the picture and 1 m thick glauconitic sandstone unit at the top. The sharp contact on top of the sandstone marks the boundary to the Triassic Vikinghøgda Formation (arrow). Level 278-281 m in the composite log (Section E). **b)** Interbedded glauconitic sandstone (dark green) and light spiculite (reddish). Level 279 m in the composite log (section E). **c)** Triassic siltstone of the Deltadalen Member (Vikinghøgda Formation). Level 281 m in the composite log (section E). **d)** The green, rounded grains are glauconite and the non-coloured grains are quartz. Thin section no. 32, PPL. **e)** Quartz is shown in its characteristic yellowish and grey interference colour. Thin section no. 32, XPL.

Occurrence and association: Glauconitic sandstone occurs within the upper part of the Kapp Starostin Formation (Fig. 18). The facies is prone to weathering and is commonly covered by scree. It is therefore possible that this facies accounts for thicker intervals than reported in the log. The glauconitic sandstone is associated with light spiculite (F7, Table 1).

Interpretation: The high content of detrital quartz and the sub-mature compositional texture, suggests a proximal, high-energy depositional environment. The subrounded quartz grains have probably been rounded and reworked by currents above the fair-weather wave base (FWWB), which resulted in the well-sorted and sub-mature texture. The green colour is due to the high amount of glauconite, a mineral that forms in sediments at the interface of oxidizing seawater and reducing interstitial waters (Odin & Matter, 1981). High content of post-depositional, early diagenetic glauconite implies a combination of continuous reworking of the sediment and low sedimentation rates (Suter, 2006; Blomeier et al., 2011). However, the glauconite grains are rounded and thus appear to have been reworked. It might therefore also be a possible solution that the glauconite grains were reworked by currents and redeposited as a detrital component together with the quartz grains. Although the origin of the glauconite grains is uncertain, the sandstone was most likely deposited in a high-energy, proximal, shallow-marine shoreface environment of the inner ramp. Alternatively, the sandstone represent shelf sand ridges (e.g. Suter, 2006). According to Ehrenberg et al. (2001), sandstone was transported onto the shelf during sea-level lowstand, and subsequently reworked, burrowed and glauconitized during transgression. The prevalence of sandstone increases in the northeastern parts of Svalbard (e.g. Blomeier et al., 2011, 2013), which suggest an uplifted terrestrial source area northeast of Svalbard.

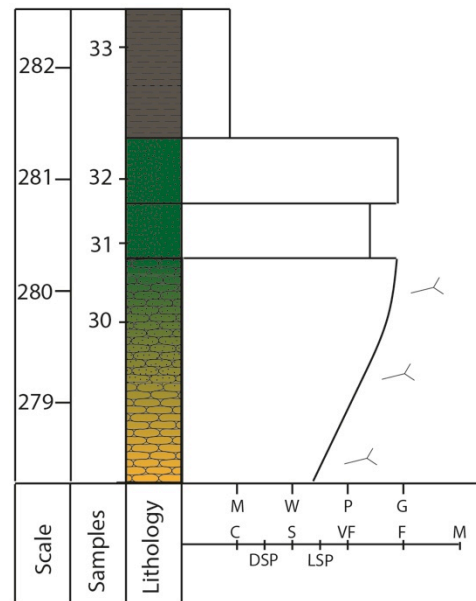


Figure 18: The glauconitic sandstone is most common in the upper part of the formation, and makes up a 1 m thick unit just below the upper formation boundary (section E). Legend is shown in Fig. 40.

Facies 6: Brachiopod dominated pack- to rudstone

The following description is based on observations of the Vøringen Member at section B, C and D, and detailed analysis of thin sections no. 5 and 7.

Description: This facies is a massive, medium- to thick-bedded grey to brown limestone with slightly wavy and continuous bedding planes. Rare cross bedding with skeletal fragments oriented parallel to the bedding also occurs (Fig. 19c). Many beds are normal graded with coarse skeletal fragments along an erosive base. The skeletal fragments are often concentrated in massive shell beds/coquinas (Fig. 19b). Brachiopod shells, whole, disarticulated and abraded, are the dominant fossils of this facies, but bryozoans and crinoids are also common (Fig. 20). Ruditic- and smaller sized impunctate brachiopod shell fragments with internal micro-fibrous structures give the rock a grain-supported texture with a packstone and locally float- to rudstone fabric. Sparry calcite cement fills the pores within the well-washed areas, but micritic matrix is also present in some areas. Micritic intraclasts up to 3 mm long (Fig. 20b), quartz sand, pyrite and glauconite grains are present in varying amount (rare to common). The contacts are mostly point-contacts (some concavo-convex).

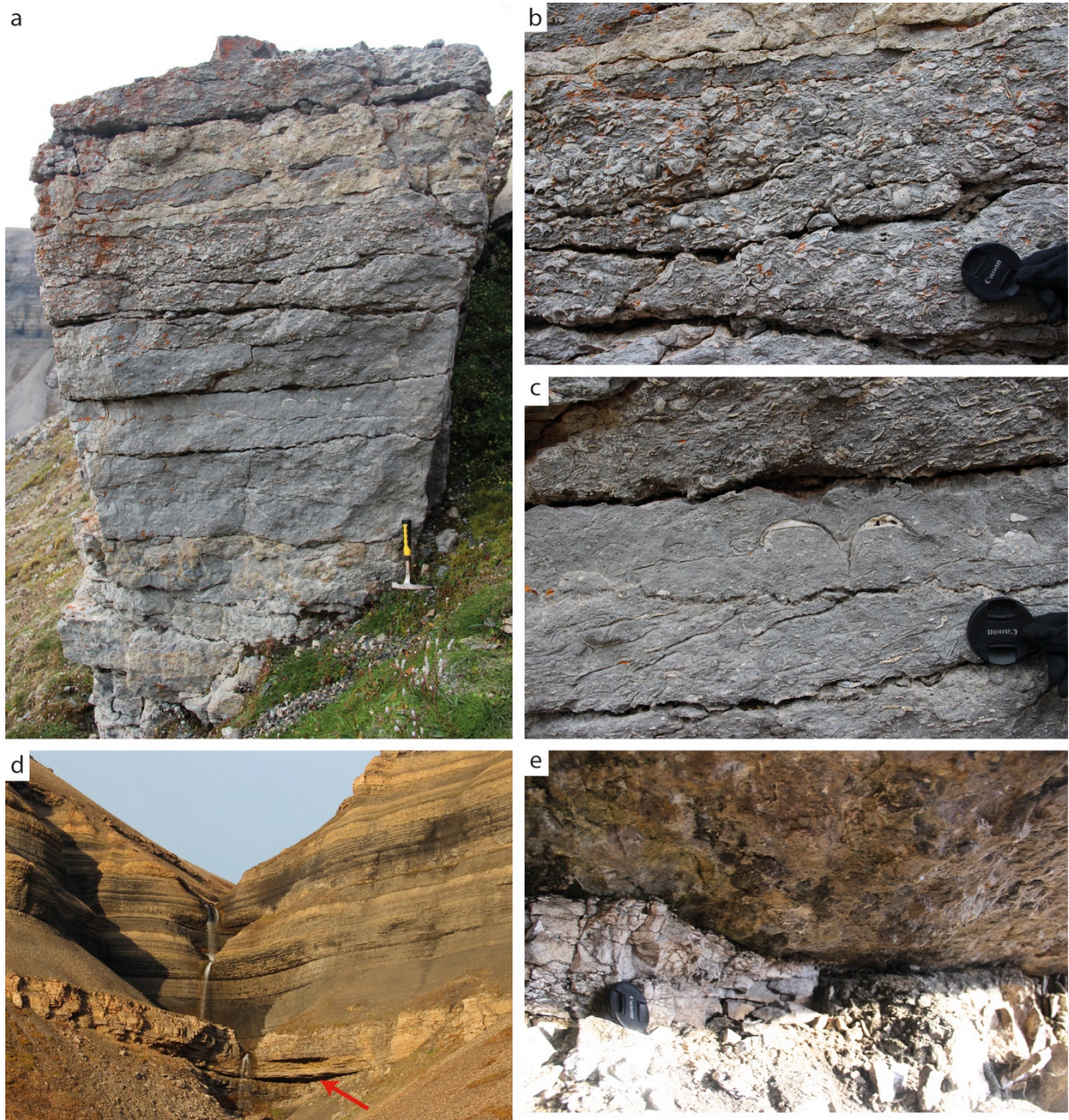


Figure 19: **a)** Well-exposed outcrop of the Vøringen Member at locality C shows well defined beds with erosive bases. **b)** Brachiopod coquina (within section C) with erosive base and high fossil density. Level 5 m in section C log. The fossil assemblage is dominated by brachiopods. **c)** Closeup of some other beds within section C, with much lower fossil density. The lower bed has weak cross-stratification with shell fragments aligned along the beddingplanes. Level 4,5 m in the section C log. **d)** The Vøringen Member at locality B (see Fig. 3c for location). The thickness was measured to 15 m. The upper boundary of the Vøringen Member is mostly covered by scree, but in the waterfall dark spiculite can be seen lying directly on top, separated by a sharp boundary. Arrow points to the boundary between the Gipshtuken Formation and the Vøringen Member. **e)** Close-up of the sharp and undulating boundary between the Gipshtuken Formation (lower part of the picture) and the Vøringen Member (upper part of the picture) (locality B).

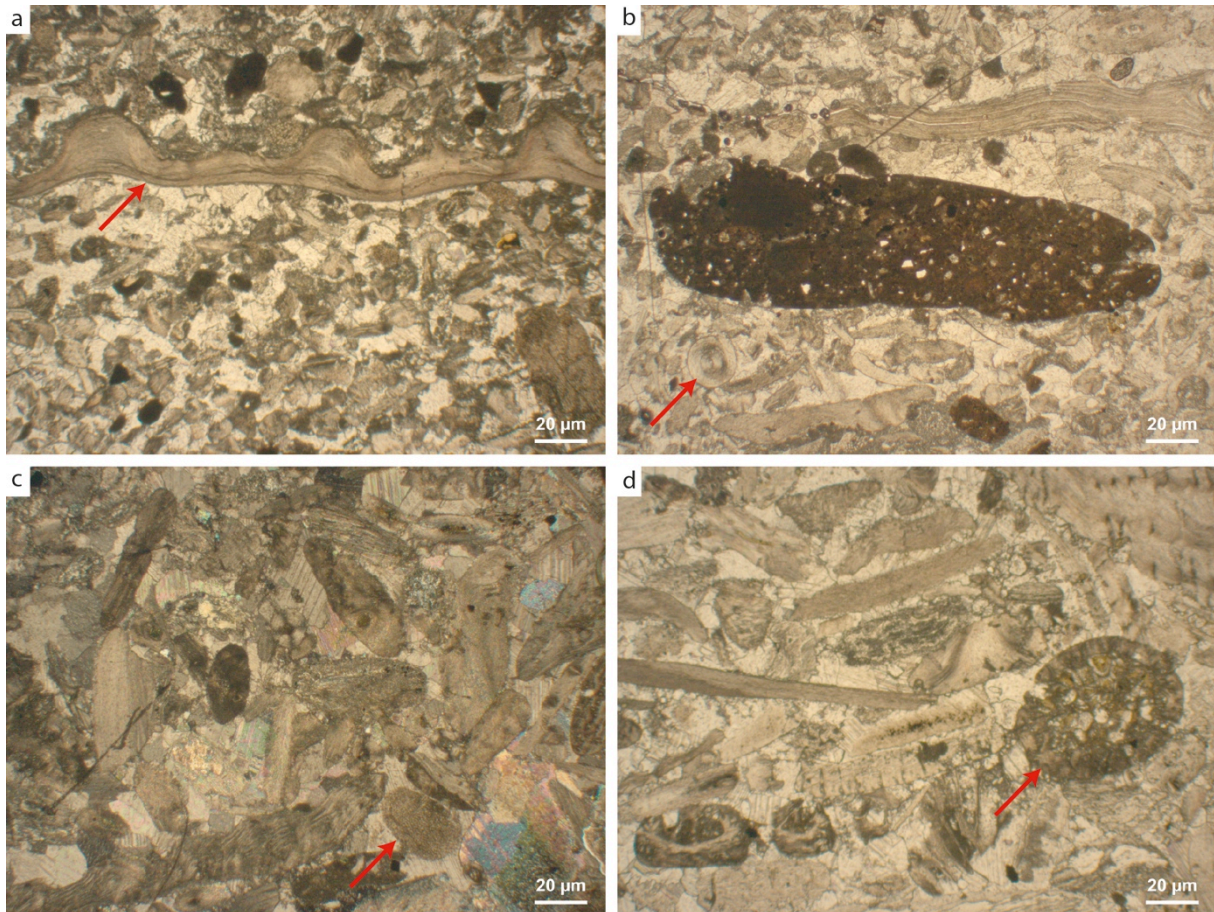


Figure 20: **a)** The sample is composed mostly of fragmented brachiopods and crinoids, but also contain some ruditic sized brachiopods (arrow). Thin section no. 5, PPL. **b)** Micritic peloid, possibly an intraclast from the underlying Gipshuken Formation. Brachiopod spine (arrow). Thin section no. 5, PPL. **c)** Although brachiopod fragments dominate, crinoids (arrow) also occur. Interparticle spaces are filled with blocky sparry calcite. Thin section no. 7, XPL. **d)** Trepustome bryozoans (arrow) are also present. Thin section no. 7, PPL.

Occurrence and association: Brachiopod-dominated pack- to rudstone is the dominating facies of the Vøringen Member (Fig. 21), and is laterally continuous across large parts of the study area. The Vøringen Member was studied in section B, C and D and lies unconformably on top of the Gipshuken Formation. The brachiopod dominated pack- to rudstone is associated with glauconitic sandstone (F5, Table 1).

Interpretation: The grain supported fabric, sparite cement and abraded fossils indicate a

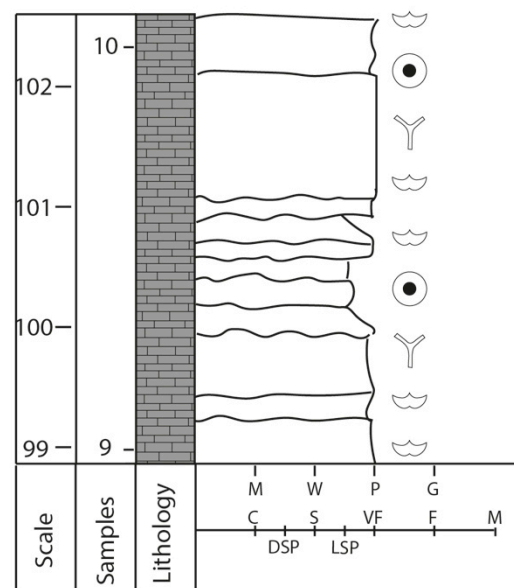


Figure 21: The Vøringen Member at locality B. Characteristic erosive bases and normal graded layers are distinct. Legends is shown in figure Legend is shown in Fig. 40.

high-energy, nearshore depositional environment above the fair-weather wave base (FWWB). A high-energy environment favors organisms that are able to anchor strongly in the substrate, such as thick-shelled brachiopods (Stemmerik, 1997). The density and type of fossils and the reworking of the shells thus indicate a proximal environment of the inner ramp. Higher concentration of micrite, bryozoans and crinoids in some samples might suggest slightly more distal deposition between the FWWB and SWWB (Blomeier et al., 2013). The erosive bases and the graded beds indicate waning flow and may be a result of storm deposition. Storm deposits are typically characterized by an erosive base, a basal lag of shells or other fragments, horizontal to low-angle lamination, wave ripple cross-lamination and bioturbation (Johnson & Baldwin, 1996). The graded beds with erosive bases are therefore interpreted as proximal tempestites. Strongly altered carbonate lithoclasts have previously been described from the Vøringen Member in central Spitsbergen, and may be eroded extraclasts from the underlying Gipshuken Formation (e.g. Ehrenberg et al., 2001; Groen, 2010). Ehrenberg et al. (2001) compared the Vøringen Member to the oyster bank shoreline deposits of the Late Cretaceous-Danian carbonate ramp described by Surlyk (1997). The oyster banks are dominated by cross-bedded sandy skeletal deposits and are thus more similar to the Vøringen Member in NE Svalbard than the Vøringen Member in central Spitsbergen, which contain relatively little detrital quartz (Blomeier et al., 2013). This is probably related to an uplifted terrestrial source area NE of Svalbard (Blomeier et al., 2013), which was also suggested for the glauconitic sandstone (F5).

Facies 7: Light spiculite

The following description is based on outcrops at section D and E, and detailed analysis of thin section no. 12, 13, 14, 15, 16 and 26.

Description: This facies has a characteristic yellowish-light ochre weathering colour with common ochre Fe-staining on the weathering surface. A fresh fracture commonly shows a grey colour. The bedding is thin to thick (5-40 cm) and the bedding planes are wavy and discontinuous, which gives the rock a nodular appearance. Trace fossils, probably of the *Planolites*, *Nereites*, *Phycosiphon* and *Zoophycos* ichnotaxa, are common, whereas skeletal fragments, such as thick-shelled brachiopods rare. Dark grey chert occurs as nodules and layers, where the nodules generally are 0.2-0.5 m in diameter,

but can be up to 1,5 m in diameter. The nodules have an irregular shape and are often elongated parallel to the bedding. Reworked phosphorite nodules are also present within the light spiculite and occur along the top of light spiculitic beds. The phosphorite nodules are commonly draped by thin layers (1-2 cm) of black shale. The light spiculite is dominated by randomly oriented monaxone megascleric siliceous sponge spicules, which give the rock a component-supported fabric (packstone). The megaspicules are up to 0,24 mm long and often have a visible central canal. According to Siedlecka (1970), the siliceous spicules were originally composed of opaline (opal-A), but were altered to opal-CT and eventually microquartz and chalcedony after the organisms died (Boggs, 1995b). Some of the thin sections have matrix free areas with a colorless to brownish material, which may be cryptocrystalline quartz and remnants of opaline silica to be transformed to quartz (Ehrenberg et al., 1998). The spicules are embedded in a micritic matrix, which is occasionally replaced by microquartz. Other skeletal fragments are occasional to common and are strongly altered and often silicified by chalcedony or microcrystalline quartz. Some fragments have an internal fibrous structure and are probably altered brachiopod shells. Various oriented, single tubular burrows filled with glauconite, dense micrite and spicules are common. Fractures are commonly filled with calcite. Rounded to subrounded glauconite grains are occasional to common, but are frequent in samples from the upper part of the Kapp Starostin Formation (sample no. 26). Although glauconitic spiculite is most common in the upper part of the Kapp Starostin Formation, it also occurs in middle part (sample no. 12).

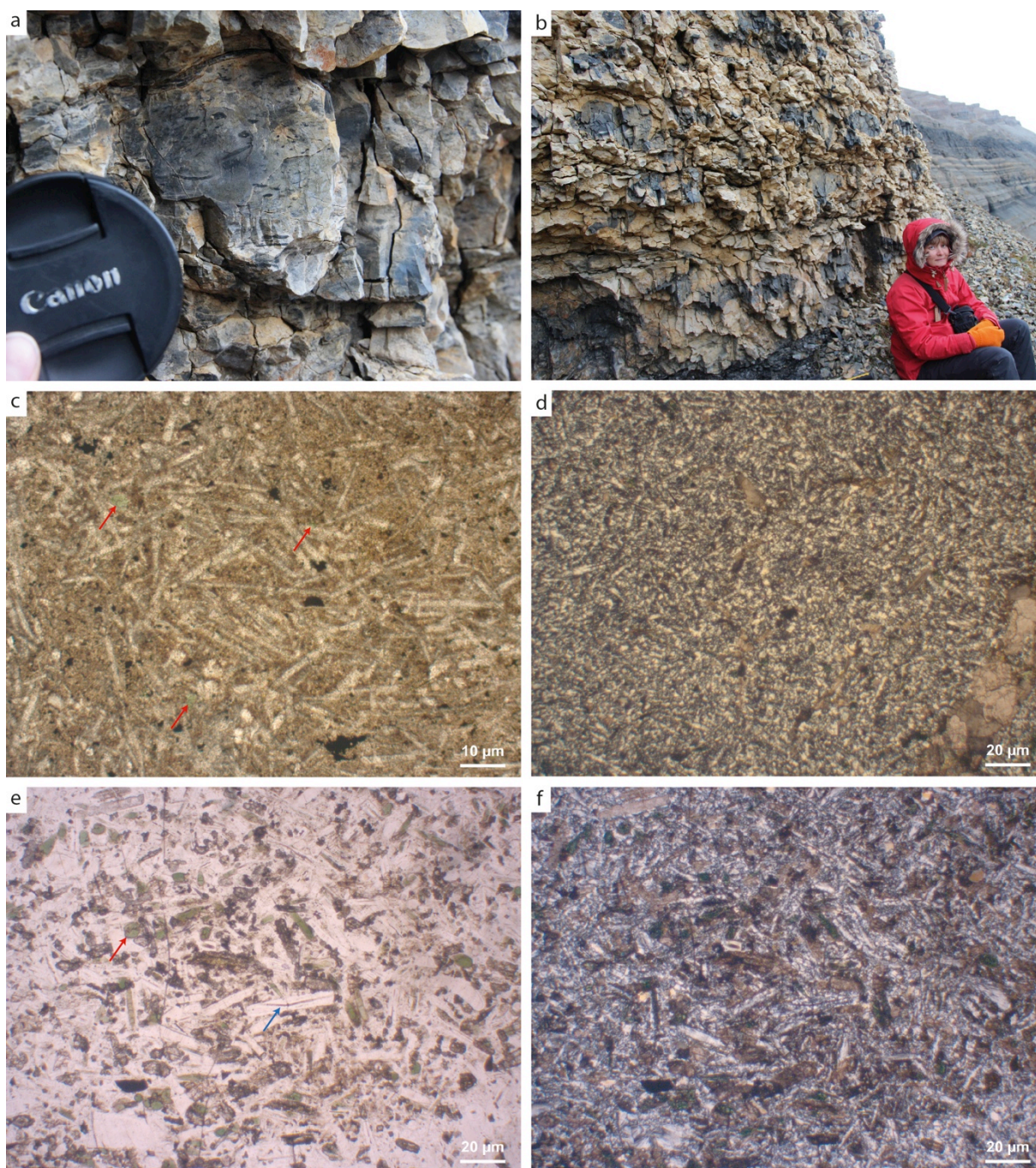


Figure 22: **a)** Light spiculite bioturbated by *Planolites* and *Nereites missouriensis*. Level 143 m in the composite log (section D). **b)** Light spiculite with dark grey silica nodules. Level 150 m in the composite log (section D). **c)** The sample is from a lens of light spiculite within a unit of dark spiculite and contains abundant macroscopic sponge spicules and rounded glauconite grains (arrows). Thin section no. 14, PPL. **d)** Fracture filled with blocky sparry calcite (lower right corner). Thin section no. 15, XPL. **e)** Abundant glauconite grains (e.g. red arrow) and large sponge spicules with visible axial canals filled with micrite (e.g. blue arrow). Thin section no. 16, PPL. **f)** The spiculite is highly silicified by microquartz and the spicules thus show the characteristic yellowish-grey interference colour. Thin section no. 16, XPL.

Occurrence and association: Light spiculite is the most prominent facies of the Kapp Starostin Formation in Dickson Land and is closely associated with the dark spiculite (F12, Table 1). The transition between the dark and light spiculite is often gradual (e.g. at level 158 m in the log, see Fig. 23), although abrupt transitions also occur (e.g. at level 159,8 m in the log, see Fig. 23). The light spiculite also occurs as lenses within the dark spiculite. The lenses are commonly 15-20 cm thick and 50-100 cm long and have channel-shaped lower boundaries (Fig. 31a).

Interpretation: The thick bedding and large size of the spicules suggest a shallower depositional environment with higher sedimentation rates than the dark spiculites (Ehrenberg et al., 2001). Palaeozoic sponges were usually shallow-shelf organisms (Scholle & Ulmer-Scholle, 2003), and despite the random orientation of the spicules, it is hard to determine whether the spicules have been transported from a nearby area or represent in-situ settling of spicules from dissolved sponges. The dense bioturbation have altered any primary sedimentary structures and also indicates that deposition took place in well-oxygenated conditions. Intense bioturbation together with post-sedimentary pressure/solution processes probably gave the chert its massive to nodular appearance (Blomeier et al., 2013). The lack of high-energy sedimentary structures is probably related to bioturbation and strong silicification. During diagenesis, biogenic silica from the sponge spicules was remobilized, which led to silicification of skeletal fragments and the matrix (Blomeier et al., 2013). The sponges grew in the shallow-shelf environment of the mid ramp, which also was the site of the dominant spicule accumulation (Scholle & Ulmer-Scholle, 2003; Blomeier et al., 2013). Currents and storm induced relaxation flows transported the bioclastic material from the inner ramp to the mid ramp, and washed the spicules and bioclastic material together. Formation of glauconite grains probably occurred during periods of slow sedimentation. The reworked phosphorite nodules were probably also formed during periods of slow

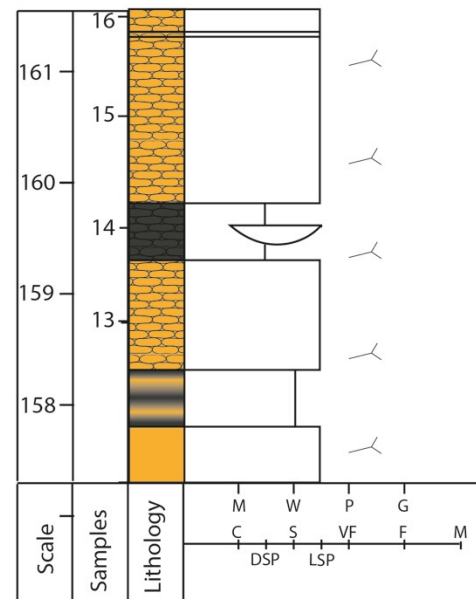


Figure 23: Light spiculite is located at several levels in the succession, both as pure light spiculitic units and interbedded with dark spiculite. Legend is shown in Fig. 40.

sedimentation, when hardgrounds formed by mineralization of minerals such as iron oxides and calcium phosphates, and may reflect periods of sediment bypass due to high current energy (Ehrenberg et al., 2001). The oxygenated, agitated water conditions are probably also the reason for the light colour of this chert, as the energy was too high for fine-grained organic material to settle out of suspension (Blomeier et al., 2013). Due to the component-supported fabric and the content of shallow-shelf fossils (brachiopods), the light spiculite is interpreted to haveing been deposited in oxygenated conditions between the FWWB and SWWB.

Facies 8: Chert breccia

The following description is based on observations of section D, and detailed analysis of thin section no. 24 and 27.

Description: This unit is composed of a massive blueish-silvery chert breccia (Fig. 24). The breccia is composed of light to dark grey angular chert fragments in a blueish-white cement of microcrystalline quartz. The fragments are up to 2 cm long and have no apparent preferred orientation, whereas the fractures are up to 3 mm wide. Brachiopod shell fragments are scattered throughout the brecciated interval. The breccia consists of dolomitic and silicified megaspicules. Vugs and extensive fractures are common (Figs. 24 c-f). Although some fractures are unfilled, most of the fractures are filled with chalcedony. The vugs are up to 5.6 mm² and are usually filled with post-depositional calcite cement. Some vugs, particularly the smaller ones, are filled with chalcedony. The vugs do not seem interconnected, but it is hard to tell as they are only viewed in a cross-section. Occasional skeletal fragments, glauconite grains, opaque minerals and micrite concentrated in small local spots are also present.

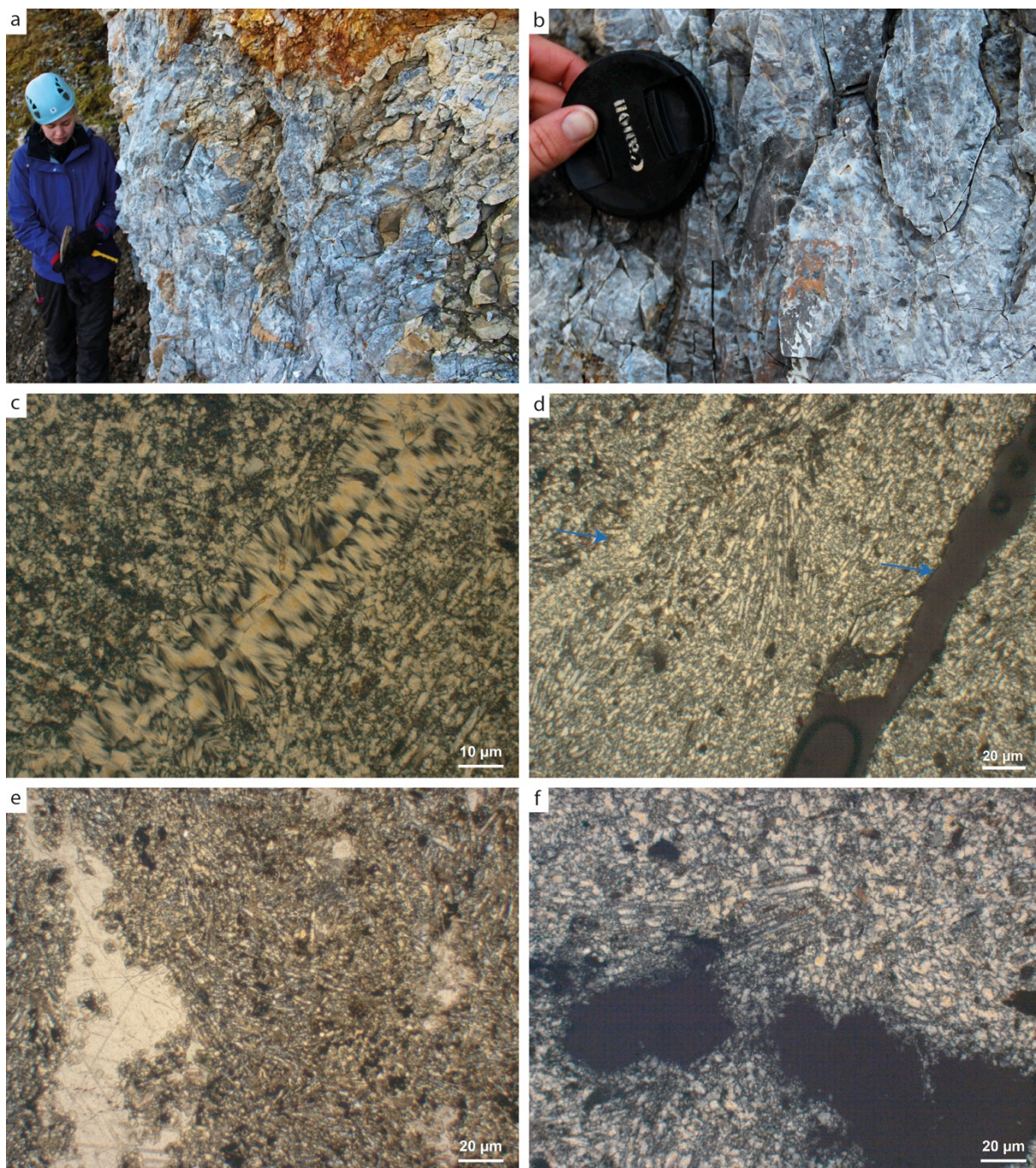


Figure 24: **a)** Outcrop of the blueish-silvery chert breccia at locality D. Level 210 m in the composite log (Section D) **b)** Closeup of the chert breccia. The angular fragments are grey, whereas the silica cement is blueish. Level 210 m in the composite log (Section D). **c)** A fracture filled with chalcedony. Thin section no. 27, XPL. **d)** Fractures in the chert breccia (arrows). The left fracture is filled with microquartz and the right one is unfilled. Thin section no. 27, XPL. **e)** Vug filled with post-depositional calcite. Thin section no. 24, XPL. **f)** Unfilled vugs. Thin section no. 24, XPL.

Occurrence and association: The chert breccia occurs in the upper part of the Kapp Starostin Formation, where it occurs in two approximately 15 m thick units separated by light spiculite (Fig. 25). The chert breccia is closely associated with light spiculite (F7, Table 1).

Interpretation: Due to the component-supported fabric composed of megasclerite sponge spicules, the chert breccia is interpreted to originally have been a light spiculite. As the light spiculite (F7), the chert breccia also contains thick-shelled shallow-shelf fossils. During storms, the thick-shelled brachiopods were probably transported from the inner ramp to the mid ramp, where the bioclastic material and sponge spicules were washed together. There are many theories of how the light spiculite was brecciated. One possibility is that the siliceous sponge spicules were dissolved, which led to the formation of molds and eventually resulted in fracturing and collapse of the spiculite. Such collapses could be triggered by tectonic activity. The angular fragments of the breccia indicate a relatively short transport distance and early silicification by microquartz and chalcedony. Chert breccia is also known from the Mississippian spiculitic strata in south-central Kansas, USA, where the cause of brecciation is believed to be due to one or a combination of three different processes; collapsing of material after karst dissolution, sedimentary reworking and autobrecciation (Watney et al., 2001; Franseen, 2006; Ramaker et al., 2014). The chert in Kansas was subjected to subaerial exposure and meteoric diagenesis, which resulted in dissolution of silica, brecciation and fracturing (Ramaker et al., 2014). Carozzi & Gerber (1978) also studied a Mississippian synsedimentary chert breccia, which they interpreted to having been penecontemporaneously brecciated by a short-lived and high-energy event. This high-energy event was supposedly a tornado, and they therefore interpreted the chert breccia as a tempestite. Kolodny (1969) proposed a model for the chert breccia in the Mishash Formation, based on selective silicification and fracturing due to the load of overlying sediments. A depositional model for the chert breccia on Spitsbergen has

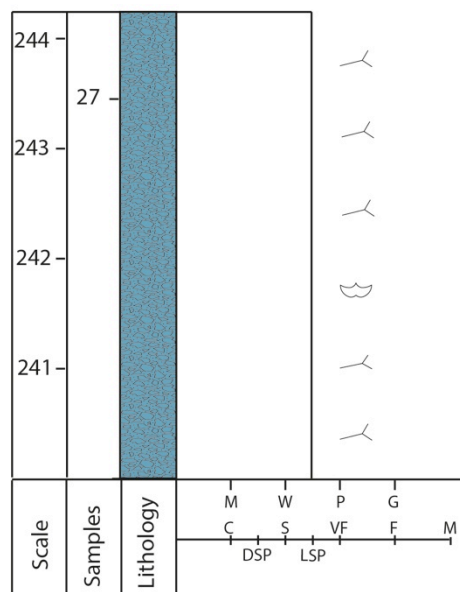


Figure 25: The chert breccia is common in the upper half of the Kapp Starostin Formation. Occasional brachiopod shell fragments occur within the breccia. Legend is shown in Fig. 40.

been proposed by Bottolfsen (1994). He suggested that alternating matrix-poor spiculite and mud-rich sediments were deposited and mixed through bioturbation, and subsequently fractured and cemented by chalcedony during burial. Storm erosion later resulted in further fracturing and removal of the mud, before the sediments eventually were buried and silicified. This model is similar to both the model proposed by Kolodny (1969), as they both include deposition of mixed competent and incompetent lithologies, and the model proposed by Carozzi & Gerber (1978), as they both include brecciation of slightly lithified sediments by a short-lived and high-energy event.

Facies 9: Bryozoan dominated floatstone

The following description is based on observations of outcrop D, and careful analysis of thin section no. 23.

Description: The unit occurs as a massive and thin-bedded brown limestone with wavy upper and lower boundaries. The facies has an overall mud-supported fabric, although some areas are grain-supported. Bryozoans, sponge spicules, brachiopods and crinoids constitute the heterozoan biotic assemblage of this facies, of which cystoporate, trepostome and fenestellid bryozoans dominate (Fig. 26). The fossils are highly fragmented, however some of the crinoids are well preserved and have bored outer surfaces. The matrix is micritic and contain occasional silt sized quartz grains and glauconitic grains. Sponge spicules are especially concentrated in single tubular burrows, where they are silicified by microquartz.

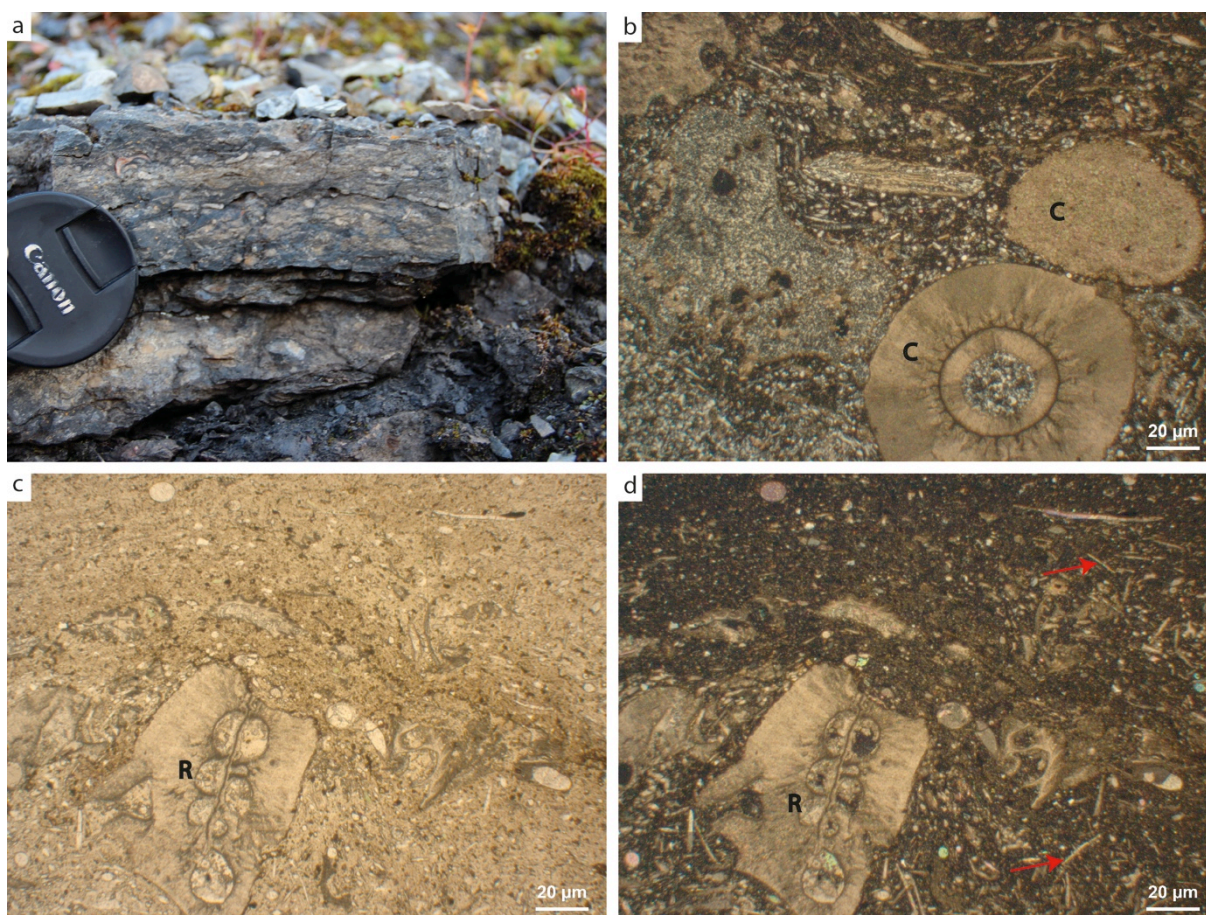


Figure 26: **a)** The bryozoan dominated floatstone occur as a massive thin bed within section D. Level 189 m in the composite log (Section D). **b)** The facies contain several ruditic sized crinoids. The upper crinoid ossicle has pores filled with micrite and the lower crinoid is a well-preserved spine. Thin section no. 23, XPL. **c)** Cystoporate bryozoans are common, here *Ramipora hochstetteri*. Thin section no. 23, PPL. **d)** The micritic matrix contains abundant sponge spicules (arrows). Thin section no. 23, XPL.

Occurrence and association: The bryozoan-dominated floatstone occurs at the top of the thick black shale interval in the middle of the Kapp Starostin Formation, around level 288.5 m in the log (Fig. 27). The floatstone is associated with black shale (F13, Table 1).

Interpretation: The high content of fine-grained micrite and the close association with the black shale suggests a low-energy depositional environment below the SWWB. As trepostome

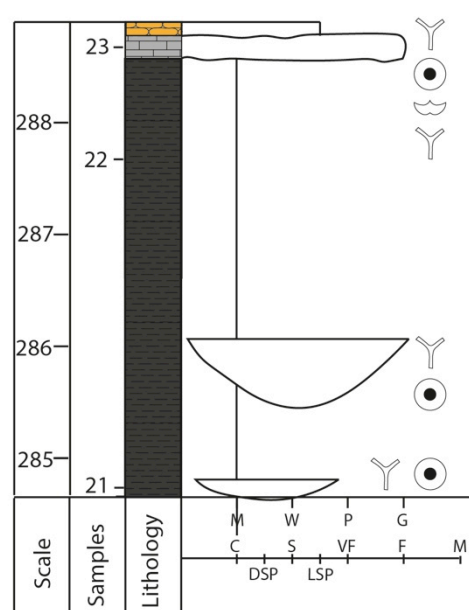


Figure 27: The bryozoan dominated floatstone occur at the top of the thick black shale interval. Legend is shown in Fig. 40.

bryozoans thrive in mid ramp colonies between FWWB and SWWB, whereas the more fragile fenestrate and cyctoporate bryozoans grow in the outer mid-ramp around the SWWB (Nakrem, 1994), the bryozoan dominated floatstone is interpreted to be a result of storm reworking of the mid-ramp colonies and transport of the bioclastic material to low-energy environments below the SWWB. The floatstone is thus a distal tempestite, which is also supported by the irregular upper and lower boundaries.

Facies 10: Bryozoan-Echinoderm dominated pack- to rudstone

The following description is based on observations of section D, and detailed analysis of thin section no. 21.

Description: This facies is present in 10-40 cm thick and a few meters long lenses within the black shale (F13). The lenses have erosive bases and pinch out and interfinger with the shale (Fig. 28b). Large bioclasts up to 10 mm long make up this coarse-grained bioclastic limestone. Cystoporate and trepostome bryozoans and echinoderms dominate the fossil assemblage, but occasional brachiopods and sponge spicules also occur (Figs. 28 d-f). The bioclasts are silicified to various degrees and show point- to sutured contacts. The matrix is dominated by dolomitic micrite, but secondary pore spaces are filled with microquartz and chalcedony. Radially grown length-fast chalcedony fibers with the typical blue-grey to white interference colour have crystallised in a fracture (Fig. 28c). The zooecial apertures of some bryozoans are filled with micrite, and some places with phosphate cement and organic material.

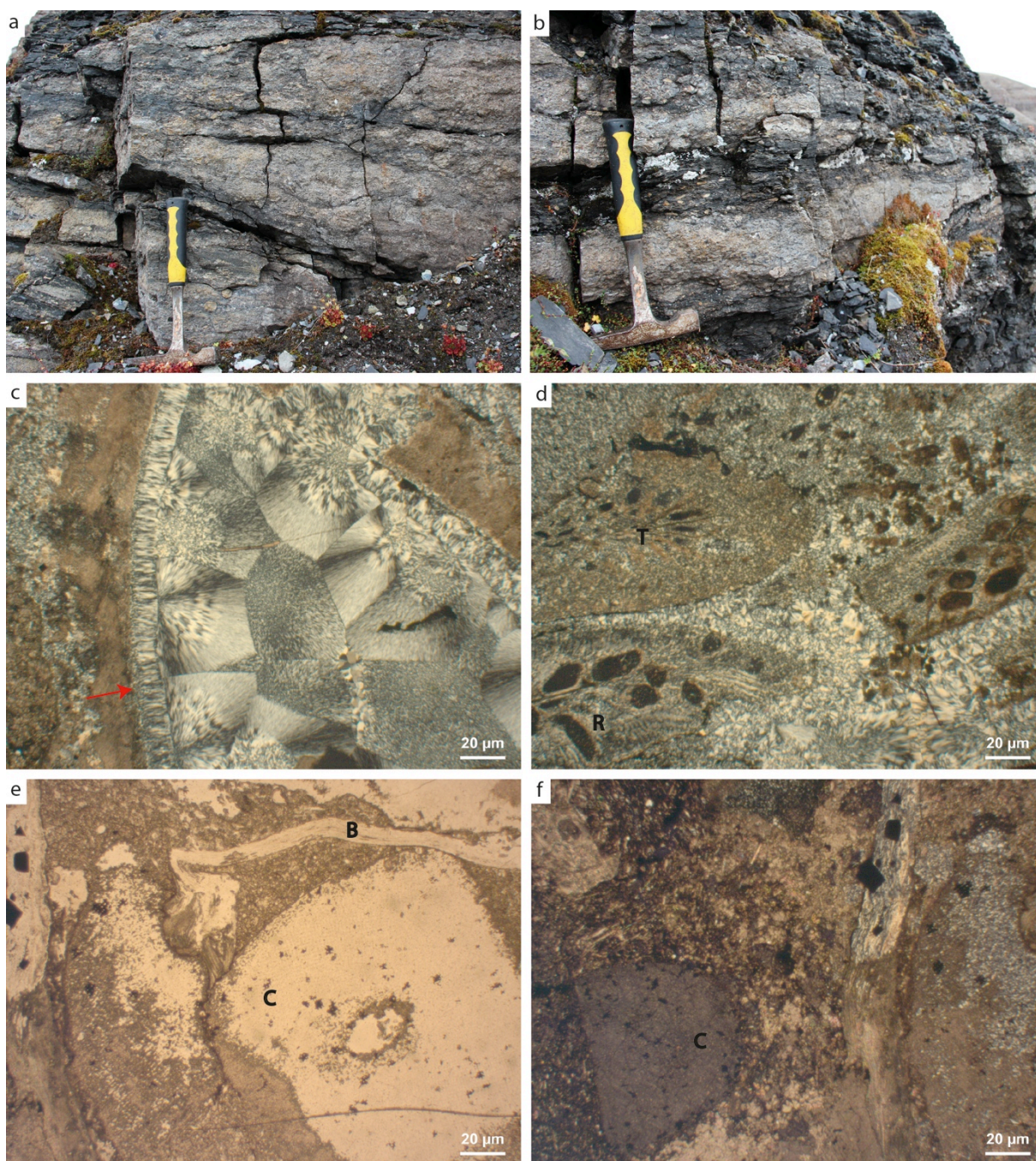


Figure 28: **a)** Bryozoan-Echinoderm dominated pack- to rudstone, section D. Level 185 m in the composite log (Section D). **b)** The limestone interfingers with the shale (F13). Level 185 m in the composite log (Section D). **c)** Parts of the limestone is silicified by chalcedony and microquartz. Here, chalcedony and microquartz has crystallized in a fracture and drusy chalcedony cement is oriented perpendicular to the fracture margin (arrow). Thin section no. 24, XPL. **d)** Cystoporate (*Ramipora hochstetteri*) and trepostome (possibly *Tabulipora*) bryozoans are common. Thin section no. 24, XPL. **e)** Parts of the limestone is dolomitized. Thin section no. 24, PPL. **f)** Crinoid ossicle in a micritic matrix. Thin section no. 24, XPL.

Occurrence and association: The bryozoan-echinoderm dominated pack- to rudstone occurs as lenses within the black shale (F13) in the Kapp Starostin Formation, around

285 m on the log (Fig. 27). The facies is closely associated with black shale (F13, Table 1).

Interpretation: The faunal assemblage of bryozoans and crinoids as well as the micritic matrix suggests a low-energy depositional environment below SWWB. Trepastome bryozoans are robust and mainly thrive in the outer reaches of the mid ramp around the SWWB, whereas the more fragile fenestrate bryozoans generally are found on the outer ramp just below SWWB (Nakrem, 1994; Blomeier et al., 2013). The lenses have probably been deposited during storms, when bioclastic material was transported from the outer mid ramp to the mud dominated outer ramp below SWWB by relaxation flows or partly by storm wave-supported gravity flows.

Facies 11: Bryozoan dominated pack- to rudstone

The following description is based on observations of section D, and detailed analysis of thin section no. 19.

Description: This unit constitutes a massive and thick-bedded coarse-grained limestone dominated by bioclastic fragments of the bryozoan phylum. The ruditic-sized components (up to 17 mm) give the rock a grain-supported fabric and include cystoporate, trepostome and fenestellid bryozoans (Fig. 29). Occasional echinoderms and common ruditic sized impunctate brachiopod shells also occur. The zooecial apertures of the bryozoans are well preserved and filled with micrite. The dolomitic micrite contains abundant sponge spicules and is the dominating matrix, although post depositional sparry calcite cement fills some of the pores. Rare glauconite grains also occur.

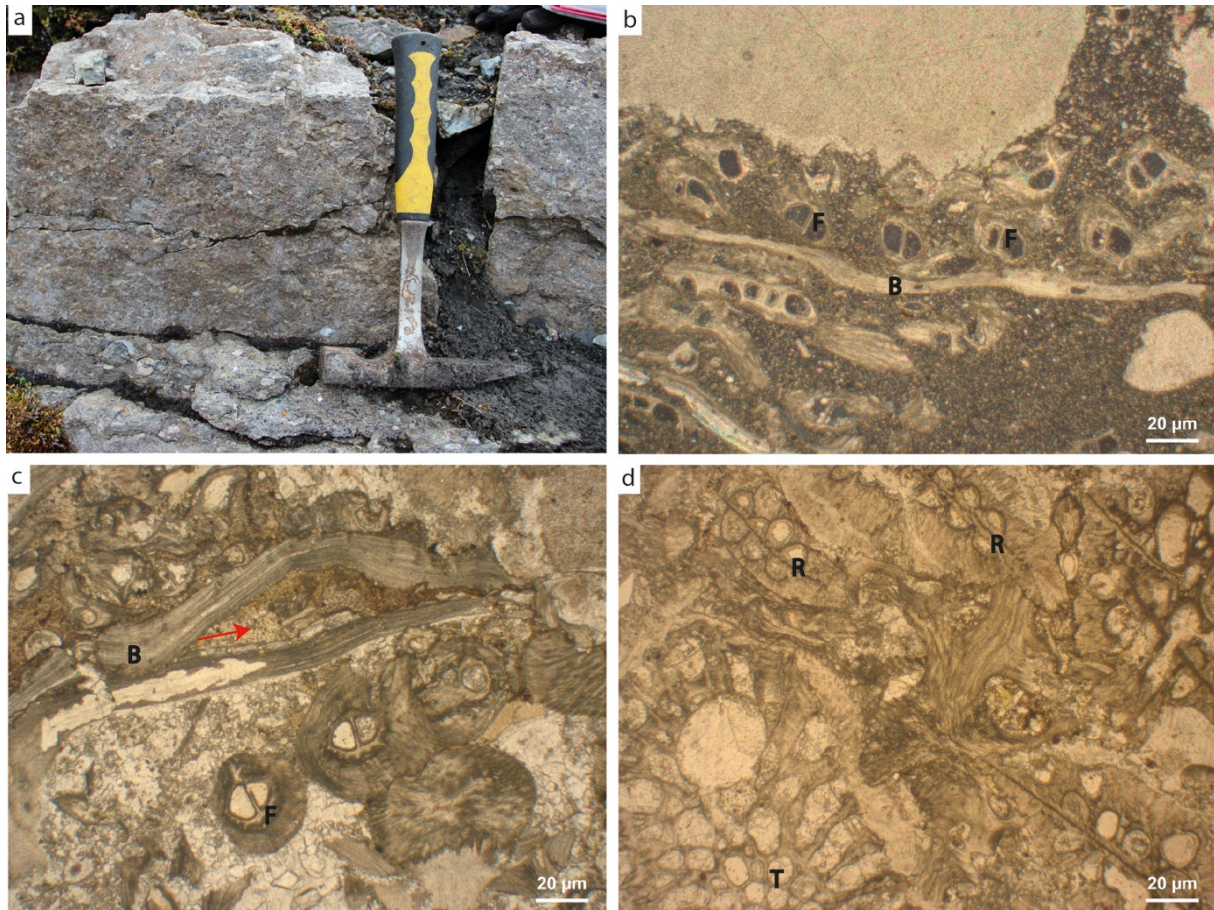


Figure 29: **a)** Bryozoan dominated pack- to rudstone crops out in section D. Level 175 m in the composite log (Section D). **b)** Fenestellid bryozoans are common and are interbedded in a micritic matrix. Thin section no. 19, XPL. **c)** Brachiopod shell with internal micro-fibrous structure. Dolomitic micritic matrix is present within the brachiopod shell (arrow). Thin section no. 19, PPL. **d)** Cystoporate (*Ramipora hochstetteri*) and trepostome (*Tabulipora*) bryozoans. Thin section no. 19, PPL.

Occurrence and association: The bryozoan-dominated pack- to rudstone occurs in the middle of the Kapp Starostin Formation, around 175 m in the log (Fig. 30). The limestone is associated with black shale (F13, Table 1).

Interpretation: The micritic matrix indicates deposition in a low-energy environment. As the fragile fenestrate and cystoporate bryozoans are very well preserved and have well preserved zooecial apertures filled with micrite, they are

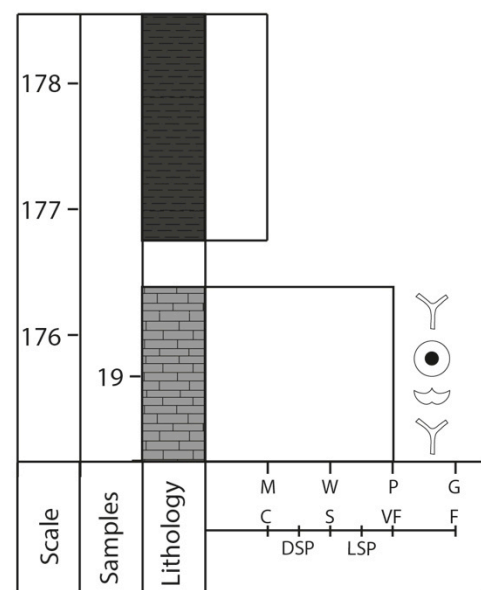


Figure 30: The bryozoan dominated pack- to rudstone crops out around 175 m in the composite log. Legend is shown in Fig. 40.

believed to have been deposited close to their habitat. According to (Nakrem, 1994), fenestrate bryozoans grow in the deeper-marine areas of the outer ramp below SWWB. The bryozoan-dominated pack- to rudstone is therefore interpreted to have been deposited below SWWB in the low-energy environment of the outer ramp, probably by relaxation flows or partly by storm wave-supported gravity flows.

Facies 12: Dark spiculite

The following description is based on observations from section D, and detailed analysis of thin sections no. 10, 11, 18 and 29.

Description: The dark spiculite has a dark grey to black colour, is thinly bedded (1-20 cm) and has a nodular appearance. The bedding planes are wavy and discontinuous and are often draped by thinly laminated shale partings. The rock is composed almost entirely of randomly oriented monaxone microscleritic siliceous sponge spicules, which give the rock a component-supported fabric (packstone) and a well-sorted texture. The spicules are commonly 0.09 mm long, but spicules as long as 0.5 mm occasionally occur. The spicules are embedded in dark brown dolomitic, micritic matrix. Rare and poorly preserved shell fragments and subrounded glauconite grains also occur. The dark spiculite is commonly bioturbated by *Nereites* and *Phycosiphon*. This facies is strongly affected by silicification, as sponge spicules and bioclasts are completely or partially replaced by microquartz.

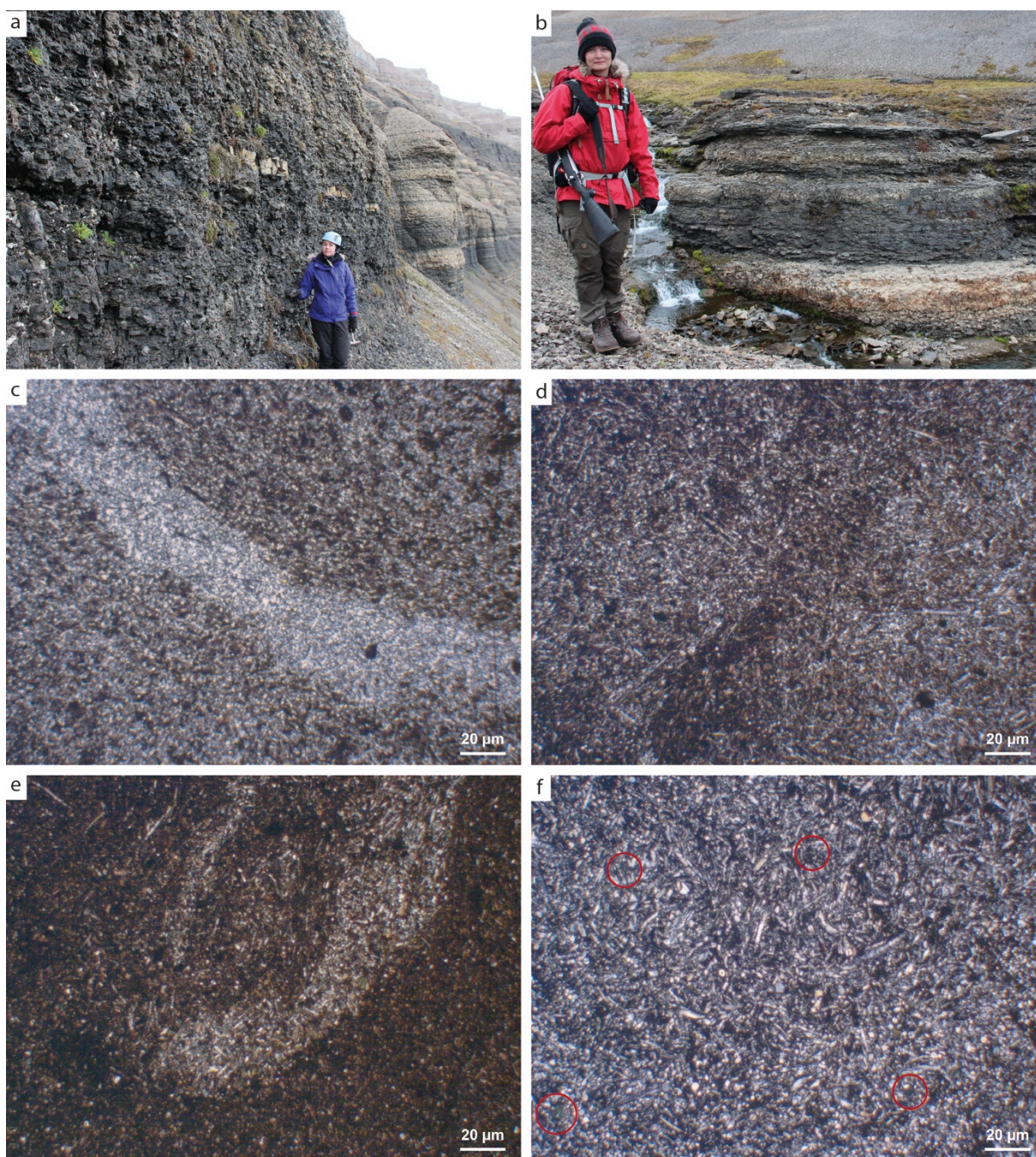


Figure 31: **a)** Dark spiculite is the dominating facies of the lower part of the Kapp Starostin Formation. Lenses of light spiculite is present within the dark spiculite (arrow). Level 122 m in the composite log (Section D). **b)** Dark spiculite is closely associated with light spiculite and the transitions can be both gradual and sharp. Here is a sharp transition between light spiculite (below) and dark spiculite (above) in Myggdalen (see Fig. 3c for location). **c)** Fracture crystallized by microquartz. Thin section no. 10, XPL. **d)** Abundant quartz grains (encircled) in some of the samples, probably a result of the siliciclastic background sedimentation. Thin section no. 11, XPL. **e)** Extensively bioturbated dark spiculite. The burrow is silicified, whereas the surrounding spiculitic matrix is dolomitic. Thin section no. 18, XPL. **f)** Greenish glauconitic dark spiculite with abundant glauconite grains (encircled). Thin section no. 29, XPL.

Occurrence and association: The dark spiculite is the main facies in the lower part of the Kapp Starostin Formation in Dickson Land and forms laterally continuous beds (Fig. 32). The dark spiculite is closely associated with black shale (F13, Table 1), which

commonly forms thin partings on the bedding planes, and light spiculite (F7). The dark spiculite often grades upward into light spiculite, but abrupt boundaries also occur.

Interpretation: The nodular fabric have been suggested to be a result of silica growth around crisscrossing *Thalassinoides* burrows (Henriksen, 1988; Ehrenberg et al., 2001). The intense bioturbation, the low-diversity biotic assemblage, fine-grained matrix and lack of high-energy sedimentary structures suggest a deeper shelf depositional environment below SWWB. The content of organic material (TOC is generally less than 1%) gives the rock its dark colour (Grundvåg, 2008), and is also an indicator of an oxygen deficient depositional environment. The dark spiculite is therefore interpreted to represent deposition in a low-energy environment below the SWWB. The slow sedimentation resulted in thin bedding and formation of glauconitic grains.

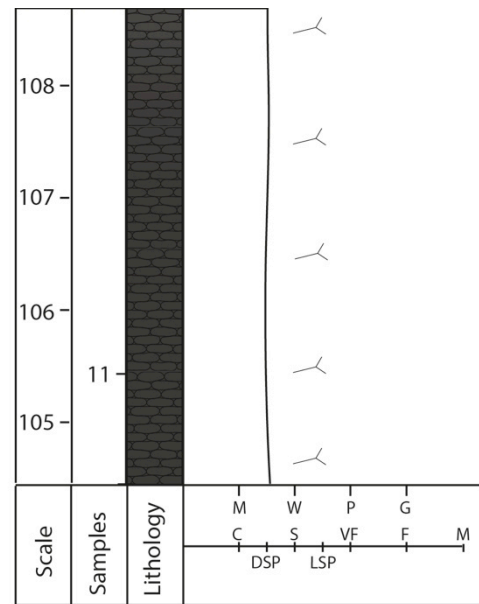


Figure 32: Dark spiculite dominates the lower part of the Kapp Starostin Formation. Legend is shown in Fig. 40.

Facies 13: Black shale

The following description is based on observations of outcrops at section D, and detailed analysis of thin section no. 22.

Description: This facies consists of dark grey to black laminated shale. The rock is fissile and splits into thin mm-scale partings along the laminations. The bedding is parallel and often laterally discontinuous, which may be due to some bioturbation and obliteration of primary structures. Parallel lamination is the main sedimentary structures, but large-scale channel features are also observed. The channel features are approximately 10 m high, 80-90 m long, and occur in the lower part of the shale interval (Fig. 33a). Large-scale cross stratification indicates lateral accretion towards the NE (clinoform migration). The channel and cross-stratification was unfortunately in an area that was inaccessible, so these structures were only observed from a distance. A light bed drapes the bed of the channel and another light bed occurs in the middle of the shale (Fig. 33a).

The middle bed was traced laterally and correlated with the bryozoan dominated pack- to rudstone of facies 11. The black shale is composed of clay- to silt and very fine-grained sand sized quartz grains, micrite, sponge spicules and small brachiopod shell fragments. Although skeletal fragments are sparse, lenses of bioclastic limestone occasionally occur within the shale (Fig. 27). These lenses have erosional lower boundaries and flat upper boundaries and many lenses are typically deposited along the same horizon. Opaque minerals are common and may be pyrite. According to Grundvåg (2008) the TOC value is 0.8 %, which is sufficient to give the shale its dark colour. The shale also contains a few whole sponges, probably of the Lithistida order (Hellem, 1980). According to Siedlecka (1970) the whole sponges have a more rigid skeleton and are not the same as the disintegrated spicules. The sponges usually have a diameter of about 5 cm and the lamination of the shale bends around the sponges.

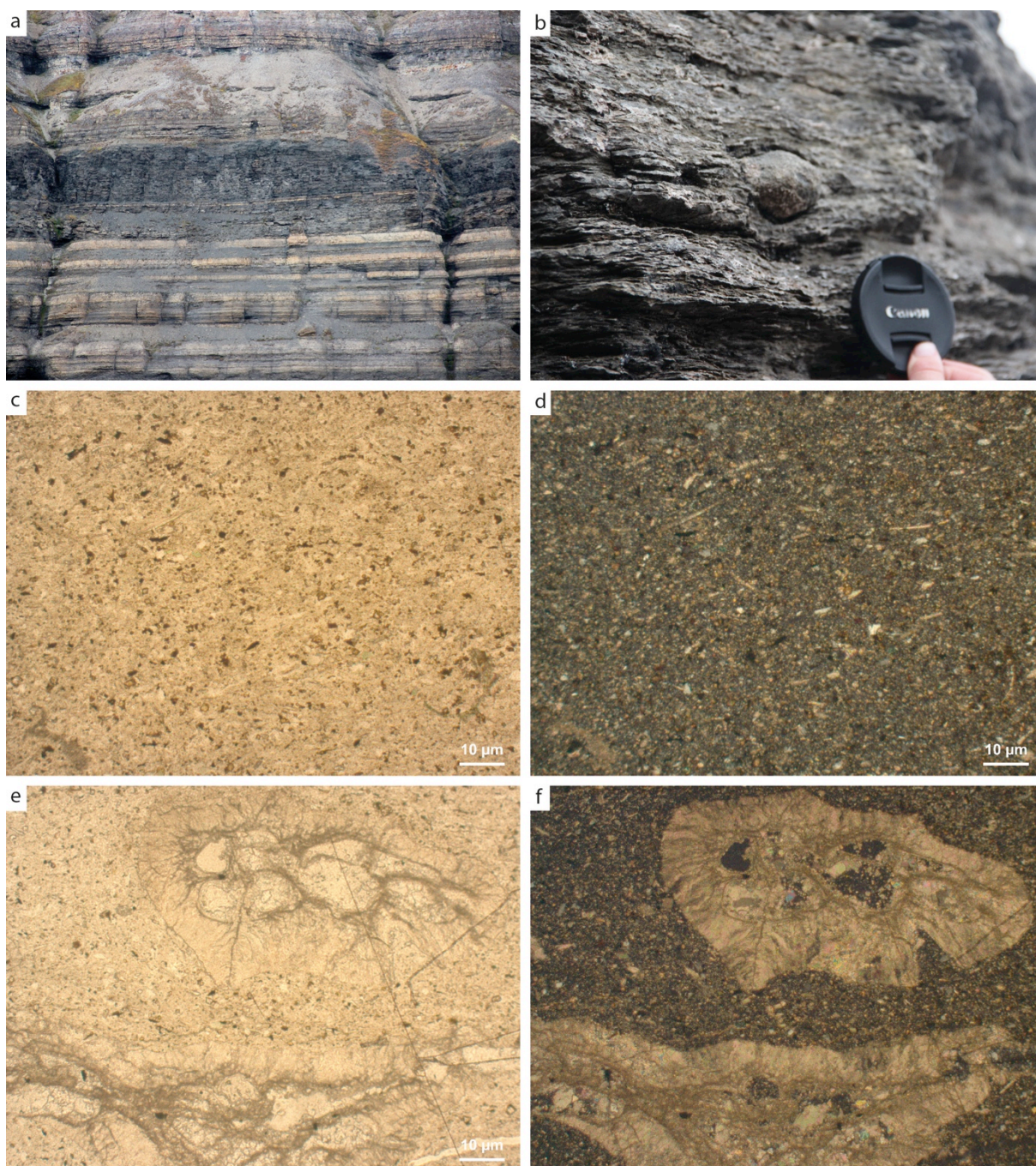


Figure 33: **a)** Black shale occur in an approximately 25 m thick interval in the middle of the Kapp Starostin Formation, as well as thin laminas within the spiculites. A large-scale channel feature is present in the middle of this interval, and is draped by what is interpreted to be bioclastic limestone along the base. SE-NW view. Picture represents approximately level 150 m to 200 m in the composite log (Section D). **b)** A few whole sponges are present within the shale. Level 180 m in the composite log (Section D). **c)** The shale is heterogeneous and includes silt- and very fine sand sized quartz grains, micrite, opaque minerals, glauconite grains and sponge spicules. Thin section no. 22, PPL. **d)** Quartz grains shown in their typical white to grey interference colour. Thin section no. 22, XPL. **e)** Occasional byozoans are also present within the shale. Thin section no. 22, PPL. **f)** The bioclastic material is composed of calcite. Thin section no. 22, XPL.

Occurrence and association: Black shale occurs throughout the Kapp Starostin Formation as 1-3 cm thick drapes on the bedding planes of the dark spiculites (F12), but also occurs in a 19 m thick interval in the middle part of the formation (Fig. 34). The shale is also associated with bioclastic limestone (F9, F10, F11, Table 1), which occurs as lenses and interfingers with the shale. Locally, black shale also occurs as a 2-5 cm thick layer separating the Vøringen Member from the Gipshuken Formation.

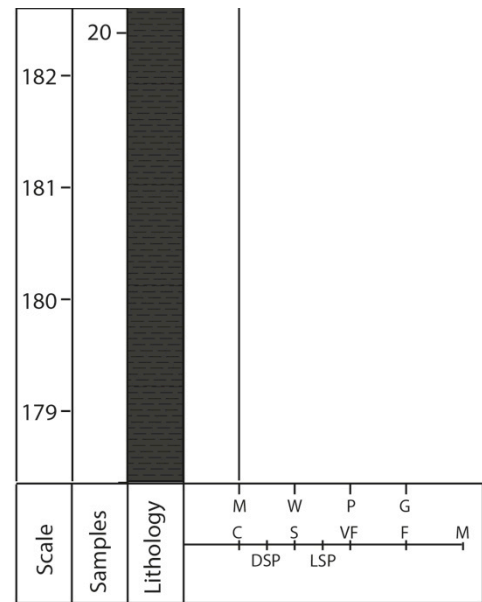


Figure 34: The most dominating outcrop of black shale (F13) is an approximately 26 m thick interval in the middle of the Kapp Starostin Formation, ranging from about 162 to 188 m in the composite log. This interval also contains a few bioclastic limestone lenses and beds. Legend is shown in Fig. 40.

Interpretation: Clay and silt-sized particles are usually deposited in low-energy environments where they fall out from suspension, such as deep-marine environments below SWWB. The presence of organic material, limited bioturbation and preservation of the lamination is also consistent with deposition in deep-marine oxygen-restricted environments. An oxygen-deficient environment also provides favourable conditions for the formation of suflide minerals such as pyrite. The black shale is therefore interpreted as the most distal facies, restricted to the outer ramp setting below the SWWB. This low-energy environment is characterized by pelagic settling of very fine-grained terrigenous material and micritic material produced by erosion of the shallower-water carbonates. In contrast, Ehrenberg et al. (2001) suggested that the close association between the shale and the bioclastic limestone of facies 9, 10 and 11 (bryozoan dominated floatstone, bryozoan-echinoderm dominated pack- to rudstone and bryozoan dominated pack- to rudstone) suggested a shallower rather than deeper depositional environment. However, the lens shaped bioclastic deposits restricted to certain horizons are most likely distal tempestites resulting from storm waves and relaxation currents. According to Ehrenberg et al. (2001), the large scale channel-structures may be a result of high accumulation rates and erosion by high-energy currents. It is uncertain whether the SE-NW oriented cross-section of the channel is parallel or perpendicular to the paleoslope. If the paleochannel was oriented

downslope, the channel may have been a conduit for storm wave-supported gravity flows, but if the paleochannel was oriented parallel to the paleoslope, the channel may be a result of deep marine contour currents flowing parallel to the slope. Such channels have been described by Surlyk et al. (2008), from the Danian Chalk Group in the German North Sea.

4.4 Facies of the Vikinghøgda Formation

Facies 14: Laminated siltstone

The following description is based on field observations of section E.

Description: This facies comprises a homogeneous brown to grey shaly siltstone with planar parallel lamination. The rock is easily weathered and has a flaky appearance in the few outcrops where it is exposed (Fig. 17c). Calcareous skeletal fossils disappears in the uppermost part of the Kapp Starostin Formation and precede the anoxic development at the base of the Vikinghøgda Formation, whereas siliceous sponges and trace fossils are abruptly eliminated at the formation boundary (Wignall et al., 1998). This is evident from the abrupt loss of chert at the boundary. No signs of subaerial exposure or prolonged non-deposition is observed at the boundary.

Occurrence and association: This facies occurs directly above the Permian-Triassic boundary (here informally placed on the formation boundary between the Kapp Starostin and Vikinghøgda formations). The lower boundary is defined where soft Triassic siltstones rest with a sharp boundary on glauconitic cherty sandstones of the Kapp Starostin Formation. This boundary was studied at section E (Fig. 17a).

Interpretation: The fine-grained texture, the laminated nature, and the lack of bioturbation suggest deposition in a low-energy anoxic environment. Sedimentation probably occurred by suspension fallout. Deposition in an anoxic environment is consistent with the gradual onset of anoxia across the Permian-Triassic boundary, reported by several authors (e.g. Dustira et al. 2013). As no direct signs of a hiatus is

observed at the boundary, the deposition may have been continuous, but very slow, as suggested by Mangerud & Konieczny (1993) and Wignall et al. (1998).

4.5 Facies of the Røye Formation

Facies 15: Light spiculite

Description: This facies is similar to the light spiculite (F7) of the Kapp Starostin Formation. The light spiculite is tightly cemented and has a grey to white colour. Some dark grey nodules occur, but they are less than 3 cm in diameter. *Nereites*, *Phycosiphon* and *Zoophycos* trace fossils are frequent throughout the spiculitic interval. Some cemented shell fragments are possibly present, but it is hard to tell without thin section analysis.

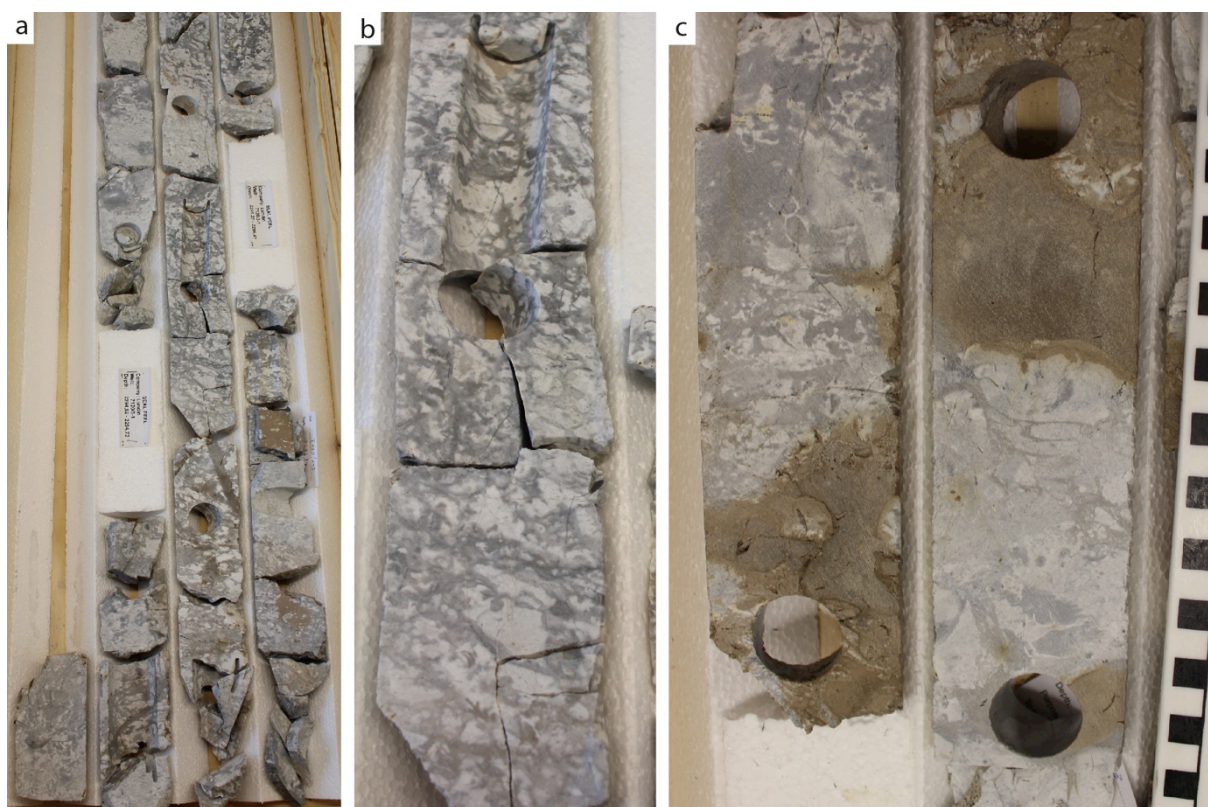


Figure 35: **a)** The light spiculite (F15) of the Gohta core is similar to the light spiculite of the Kapp Starostin Formation (F7). Depth: 2293.90-2297.00, well 7120/1-3. **b)** The light spiculite is intensely burrowed, mainly by *Nereites*, *Phycosiphon* and *Zoophycos*. Depth: 2295.30-2295.60, well 7120/1-3. **c)** The light spiculite is closely associated with the dolomitic light spiculite (F16). Depth: 2318.00-2318.27 (left) and 2319.00-2319.30 (right), well 7120/1-3. Cores are 6.5 cm in diameter.

Occurrence and association: This facies occurs in a continuous interval at the top of the core section, but also sporadically throughout the cores. The light spiculite is closely associated with the dolomitic light spiculite and black shale (F16 and F17, Table 1).

Interpretation: The light spiculite of the core section is very similar to the light spiculite of the Kapp Starostin Formation, and the depositional environments have probably also been similar. The light spiculite of the core section is thus also interpreted to having been deposited in agitated and oxygenated water conditions between the FWWB and SWWB.

Facies 16: Dolomitic light spiculite

Description: The facies consists of a light brown to brownish grey dolomitic light spiculite. The dolomitization has to great extent obliterated primary structures, but trace fossils similar to those observed in the light spiculitic intervals also occur in parts of the dolomitic light spiculite. The rock is locally brecciated with angular fragments <6 cm. The fragments are light brown to grey and are embedded in a dark brown micritic matrix. Calicte has grown as elongated fibres in fractures within the matrix. Some clasts and areas of the core are less dolomitized and still have the light grey colour characteristic of the light spiculites. It is possible that these areas are more tightly cemented and therefore not as easily pervaded by Mg-rich water. Some possible brachiopod shell fragments are also observed, but they do not react with hydrochloric acid, probably due to strong silicification.

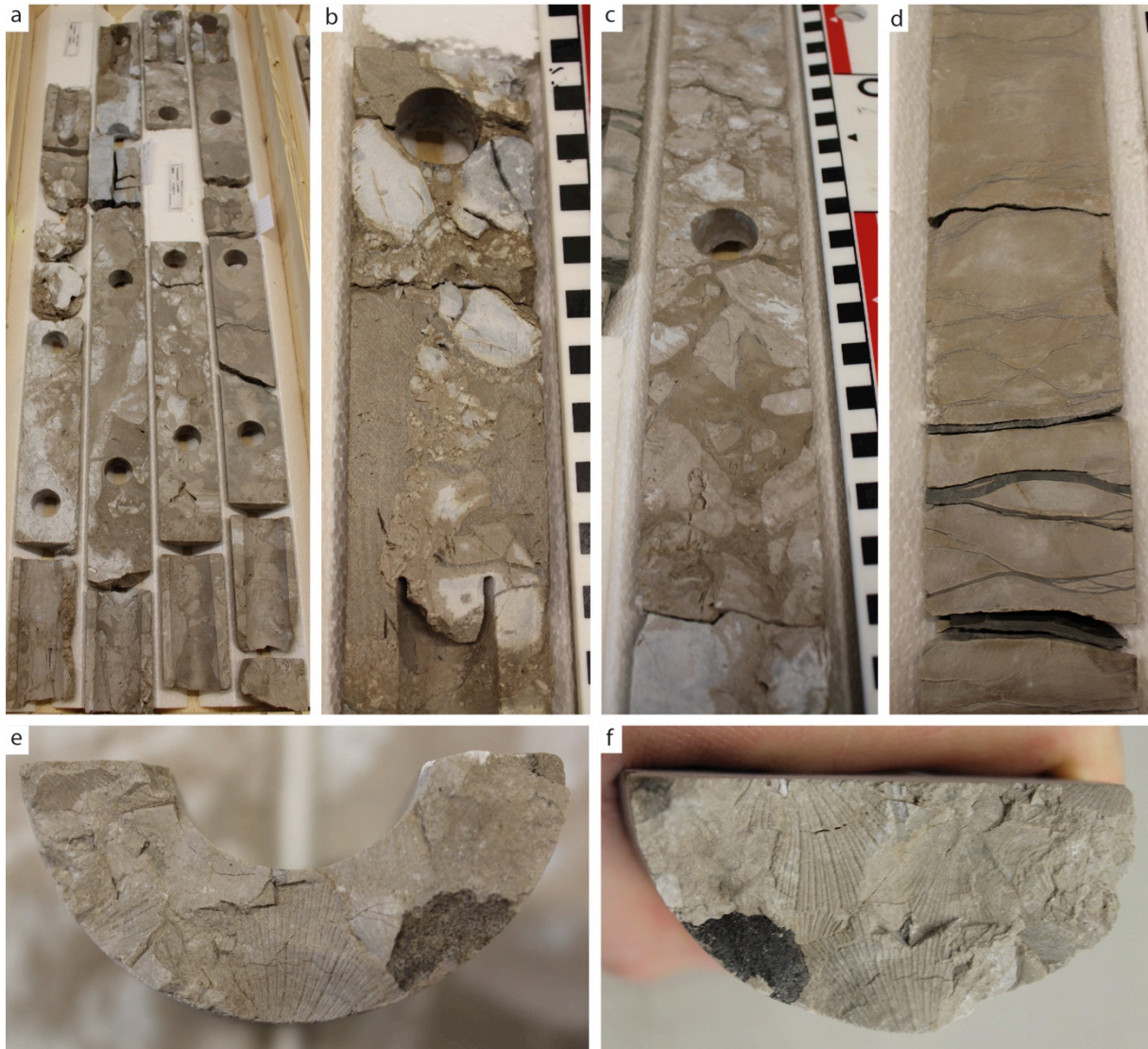


Figure 36: **a)** The dolomitic light spiculite (F16) is common throughout the Gohta core section. Depth: 2310.00-2314.00, well 7120/1-3. **b)** Dolomitization is probably related to the properties of the rock, and tightly cemented areas are not dolomitized. Depth: 2318.47-2318.67, well 7120/1-3. **c)** Brecciated section of the dolomitic light spiculite. The fragments are angular and less than 6 cm in diameter. Depth: 2303.05-2303.35, well 7120/1-3. **d)** Dolomitic light spiculite is closely associated with black shale (F17), here occurring as thin drapes and laminae. Depth: 2338.70-2338.90, well 7120/1-3. **e)** Shell fragments are not common in the core section, but are observed at two levels within one of the cores. Depth: 2310.20, well 7120/1-3. **f)** Dolomitized shell fragments. Depth: 2311.90, well 7120/1-3. Cores are 6.5 cm in diameter.

Occurrence and association: This facies occurs throughout the core section and is closely associated with light spiculite (F15, Table 1). The dolomitic light spiculite is also associated with black shale (F17), which occurs as mm-scale laminations.

Interpretation: Subsequent to deposition the spiculite was probably subjected to diagenetic alteration, in terms of silicification, dissolution and dolomitization. The mixing-zone model for dolomitization states that mixing of saline and meteoric water

lowers the salinity sufficiently so that dolomite can form (Boggs, 1995a). Although dolomitization in most cases is caused by hypersaline fluids (Stemmerik et al., 1999), it is possible that dolomite formed as a result of mixing of meteoric and saline water. This is plausible because the Loppa High was repeatedly uplifted and exposed to meteoric water during the Late Permian (Stemmerik et al., 1999; Worsley et al., 2001a).

Facies 17: Black shale

Description: This facies is similar to the black shale (F13) of the Kapp Starostin Formation. The dark grey to black laminated shale occur as thin layers (<2 cm) and laminae within the dolomitic light spiculite (F16). The bedding is heterolithic, and intervals with both flaser, wavy and lenticular lamination occur. Flaser lamination is by far the most common, and mud laminae often drape lenses of light spiculites. Some of the lens structures look like ripples, but they do not have the internal cross-stratification, and are therefore probably just lenses formed by silica growth within the mudstone matrix. *Chondrites* trace fossils are common. Pyrite crystallizations have commonly formed on the lower boundary of some mudstone layers.

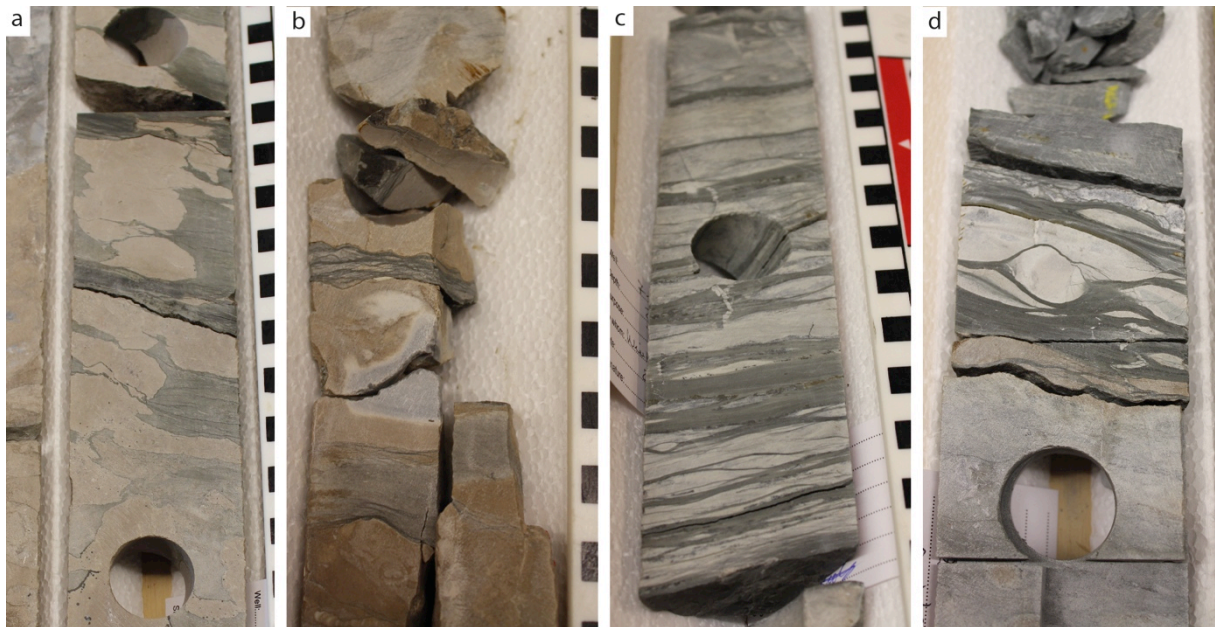


Figure 37: a) Black shale is closely associated with dolomitic light spiculite (F16), where it forms thin drapes and up to 3 cm thick laminae. Depth: 2302.47-2302.67, well 7120/1-3. **b)** The mud seems to be draping ripple-structures, however, these structures have no internal cross-lamination and are probably formed by crystallization of silica within the mud matrix. Depth: 2336.50.-2336.70, well 7120/1-3. **c)** The black shale also occurs together with light spiculite (F15), as thin laminae and drapes. Depth: 2340.10-2340.30, well 7120/1-3. **d)** The light spiculite expands due to silica crystallization, and form lenses within the shale. Depth: 2334.40-2334.60, well 7120/1-3. Cores are 6.5 cm in diameter.

Occurrence and association: The facies occurs throughout the core section and is associated with the light spiculite (F15, Table 1) and the dolomitic light spiculite (F16, Table 1).

Interpretation: The same indicators of depositional environment used for the black shale (F13) of the Kapp Starostin Formation can also be used for the shale in the core section. The fine-grained texture, dark colour (possibly due to organic content), preservation of lamination and pyrite growth all points to deposition in a deep-marine oxygen-deficient environment far below the SWWB. The shale is therefore interpreted to be a result of pelagic settling of very fine-grained terrigenous material in a low-energy environment below the SWWB.

5. Facies associations

The facies defined in the previous chapter have been grouped into facies associations based on their genetic relationship and depositional environment. The facies recognized in the Gipshuken Formation have been grouped into two facies associations, being the supratidal flat facies association (FA1) and the intertidal to subtidal flat facies association (FA2). The three facies associations constituting the Kapp Starostin Formation are the shoreface deposits of the inner ramp (FA3), the offshore transition deposits of the mid-ramp (FA4), and the deep shelf deposits of the outer ramp (FA5). The last facies association is the marine siltstone deposited on a siliciclastic shelf (FA6), belonging to the Triassic succession. The facies associations are presented in order from shallow/proximal to deep/distal. The facies included in each facies association can be seen in Table 1.

5.1 Facies association 1 (FA1) – Supratidal flat

Facies association 1 (FA1) comprises dark brown micritic mudstones deposited in the supratidal zone. The mudstones are highly fractured with calcite cement filling the fractures. As the sediments were deposited above normal high tide, they were flooded only during storms and high spring tides (Flügel, 2010). The fine-grained texture of the rocks relates to the low energy in the depositional environment, whereas the fractures relate to the desiccation in warm and arid climate. Intraclast conglomerate (F1) constitutes the only facies in this facies association and is observed at the top of the Gipshuken Formation (Fig. 16b). This facies association is related to subaerial exposure and meteoric alteration of the sediments, and is characterized by features like desiccation cracks and intraclasts. Due to deposition in a saline, subaerial environment with low degree of bioturbation, this facies association has a high preservation potential.

5.2 Facies association 2 (FA2) – Intertidal to subtidal flat

Facies association 2 (FA2) comprises mudstones deposited in intertidal and shallow marine environments. The deposits of FA2 are observed below the deposits of FA1 (at section B), indicating a regression and progradation of the sabkha deposits. Facies

association 2 comprises the microbial mudstone (F2), dolomitic mudstone (F3) and argillaceous limestone (F4). The microbial mudstone (F2) dominates the intertidal zone and is the facies connecting the supratidal flat (FA1) with the subtidal flat. The microbial mats were periodically exposed and the presence of eolian quartz grains on the algal mat surface (Fig. 15) suggests occurrence of sand dunes landward of the supratidal flat. The subtidal zone lies seaward of the intertidal zone is dominated by fine-grained carbonate mud. The dolomitic mudstone (F3) and the argillaceous limestone (F4) are interpreted to have been deposited in the shallow subtidal environment. The fine-grained texture of the rocks implies deposition in a protected, low-energy area of the shelf.

5.3 Facies association 3 (FA3) – Shoreface deposits (Inner ramp)

Facies association 3 (FA3) comprises well-sorted and well-washed deposits of the shoreface, such as glauconitic sandstone (F5) and brachiopod dominated limestone (F6), and thus comprises the shallowest facies of the Kapp Starostin Formation. The terrigenous origin of the sandstone indicates a more proximal depositional environment than the limestone. The brachiopod dominated limestone is typical for the Vøringen Member and is characterized by nearshore and thick-shelled species (mainly thick-shelled brachiopods). Although the limestones and glauconitic sandstones are found mainly in the lower and upper parts of the formation, respectively, they were both deposited in the high-energy nearshore environment of the inner ramp. The small amount of mud present in both the limestones and sandstones is typical for agitated, shallow marine environments. Erosional lower boundaries and normal grading are characteristic for storm deposits, indicating that the brachiopod limestone beds may have been deposited as proximal tempestites.

5.4 Facies association 4 (FA4) – Offshore transition deposits (Mid ramp)

Facies association 4 comprises the light spiculite (F7, F8), which was deposited in the offshore transition zone of the mid ramp. The sediments of the mid ramp were mainly affected by storm waves, but any storm-related sedimentary structures have been obliterated by bioturbation and strong silicification. The sponge spicules are larger (megascleric) than their outer ramp microscleric equivalents (dark spiculite, F12), which is typical for shallow-water species. Although the bioclastic limestones of facies 9,

10 and 11 are assigned to facies association 5, the bioclastic material was distributed both onshore and offshore during storms, so deposition of bioclastic limestones also took place on the mid ramp.

5.5 Facies association 5 (FA5) – Offshore shelf deposits (Outer ramp-basin)

Facies association 5 comprises the sediments deposited in the low-energy environments below the storm wave base and is dominated by dark spiculite (F12) and laminated black shale (F13). The bryozoan dominated floatstone (F9), bryozoan-echinoderm dominated pack-to rudstone (F10) and bryozoan dominated pack- to rudstone (F11) are also found within this facies association, and are interpreted as distal tempestites. Due to the content of organic material and low degree of bioturbation in the laminated shale, the deepest part of the outer ramp-basin environment is assumed to have been suboxic to anoxic. The shale contains a small amount of microscleric spicules, which is thought to represent a somewhat more proximal part of the outer ramp-basin environment. The black shale is therefore the most distal facies of the Kapp Starostin Formation.

6. Depositional models for the Gipshuken and Kapp Starostin formations

The facies analysis of the Permian strata in central Spitsbergen clearly shows that there was a significant change in depositional environment from the Gipshuken Formation to the Kapp Starostin Formation. The facies of the Gipshuken Formation display a marginal-marine setting of a carbonate platform in an arid to semi-arid climatic zone (Blomeier et al., 2011), whereas the overall depositional setting of the Kapp Starostin Formation is a temperate to cold, intermediate- to high energy, mixed siliceous-carbonate shelf environment (Malkowski, 1982; Ehrenberg et al., 2001; Hüneke et al., 2001; Blomeier et al., 2011; Blomeier et al., 2013).

The period when the Gipshuken Formation was deposited (Sakmarian to Artinskian) was characterized by a regional regression, which led to the development of intertidal to supratidal lagoons, mudflats and sabkhas on the platform in central and western Spitsbergen (Dallmann et al., 2015b). Blomeier et al. (2011) described a depositional model for the Gipshuken Formation in NE Svalbard, where he divided the carbonate platform into two adjacent depositional environments; the supratidal sabkha environment and the intertidal to shallow subtidal environment of the inner platform (Fig. 38). The deposits belonging to these environments are different types of mudstones, hence indicating that low-energy conditions prevailed in these areas.

The supratidal areas of the platform belong to the sabkha environment and are characterized by desiccation, meteoric alteration, dolomitization, erosion, reworking and pedogenesis (Blomeier et al., 2009; Blomeier et al., 2011). The intraclast conglomerate (F1) of facies association 1 (FA1) was deposited in this environment. Other common deposits from this environment are coarse-grained breccias (e.g. the Zeipelodden Member, Lauritzen, 1981). Carbonate breccias and karstic surfaces are described from the uppermost part of the Gipshuken Formation in central Spitsbergen (e.g. Lauritzen, 1981; Samuelsberg & Pickard, 1999; Groen, 2010) and from NE Svalbard (e.g. MFT6, Blomeier et al., 2011) and are formed due to *in situ* fragmentation of subaerially exposed carbonates. Caliche, root-traces and Microcodium are features that reflect development of palaeosols and vegetation and therefore indicate a terrestrial environment (Blomeier et al., 2009).

The inner platform comprises the peritidal to shallow subtidal areas and include the deposits in facies association 2 (FA2). The intertidal area was characterized by low-energy conditions and accumulation of fine-grained suspended matter, resulting in the formation of mudstones (F3) and microbial mudstones (F2) (Blomeier et al., 2011). The low-diversity biota represented by microbial organisms populated the intertidal and shallow subtidal areas and indicate restricted marine, and possibly hypersaline conditions within these areas (Blomeier et al., 2011). Quartz grains trapped on the algal mat surfaces probably indicate an eolian system and sand dunes in the vicinity of the inner platform.

The deposits of the Gipshuken Formation show a shallowing-upward trend through subtidal to intertidal-supratidal deposits. Small-scale shallowing upward units are common in carbonate formations and represents the periodic flooding of the platform during transgressive events (Tucker et al., 1990). The cyclicity of the Gipshuken Formation shows strong similarities to modern sabkha deposits of the Persian Gulf. Modern sabkha deposits are characterized by subtidal lime mud overlain by intertidal microbial mats and supratidal chickenwire anhydrite, whereas the ancient counterpart is characterized by subtidal fine-grained dolomites or lime mudstones overlain by dolomicrites or micritic limestones with parallel and wavy laminations (Flügel, 2010). The facies recorded in the Gipshuken Formation fit the description of ancient sabkha deposits very well, and the succession is therefore interpreted to be stacked sabkha cycles. Subaerial exposure of the Gipshuken carbonate platform during the Artinskian is evident due to the presence of caliche, root traces, *Microcodium*, carbonate breccias and karst (e.g. Blomeier et al., 2011; Groen, 2010; Lauritzen 1981; Samuelsberg & Pickard, 1999). A hiatus resulting from both subaerial exposure and transgressive erosion is thus separating the Gipshuken Formation from the Kapp Starostin Formation (Figs. 5, 8 and 13) (Blomeier et al., 2011).

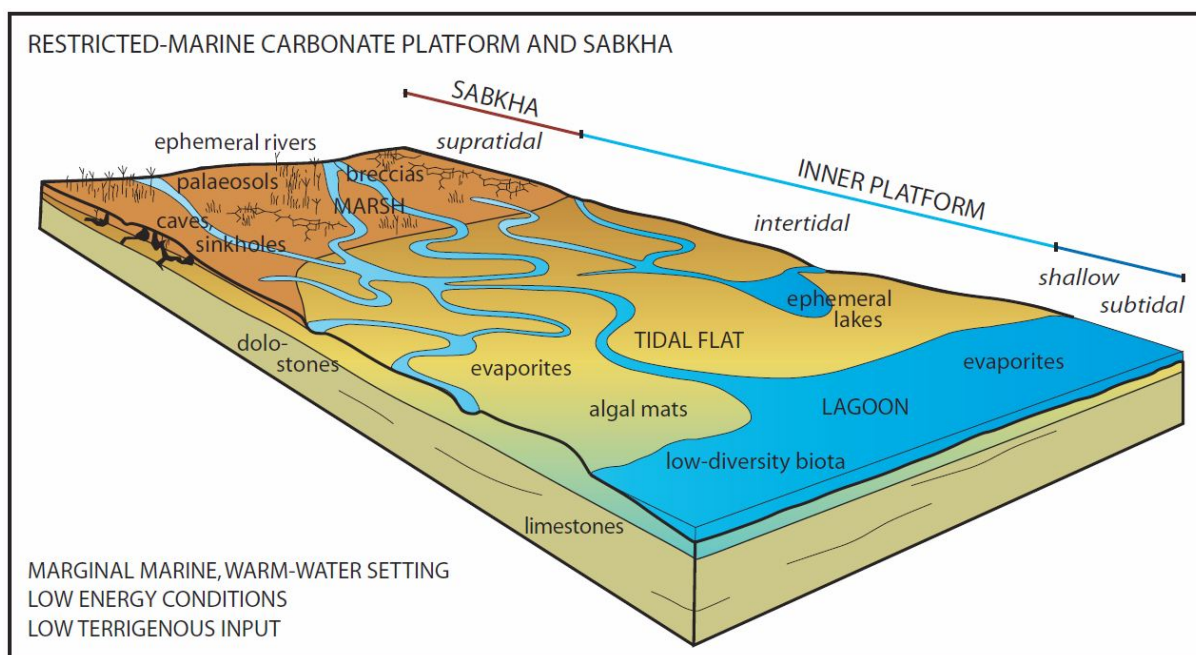


Figure 38: Depositional environment during the sedimentation of the Gipshuken Formation. The shelf is divided into a supratidal sabkha environment and an intertidal and shallow subtidal inner platform. Intraclast conglomerate (F1) was deposited in the supratidal area, microbial mudstones (F2) were deposited in the intertidal area and dolomitic mudstones (F3) and argillaceous limestones (F4) were deposited in the shallow subtidal area.

Due to northwards drift and changes in climate and oceanic circulation, the warm-water restricted carbonate platform of the Gipshuken Formation changed into an open-marine cool-water mixed siliciclastic-carbonate ramp (Blomeier et al., 2011). The ramp model proposed for the Kapp Starostin Formation by Blomeier et al. (2013) follows the definitions by Burchette & Wright (1992), and divides the shelf into an inner-, mid- and outer shelf area, each of which is characterized by specific facies associations, depositional environments, sedimentary processes and biotic assemblages (Fig. 39). Although the model addresses the Kapp Starostin Formation in NE Svalbard, it can also be applied for the strata in central Spitsbergen.

The inner ramp comprises the intertidal to shallow subtidal areas above the FWWB, and is thus constantly reworked and winnowed by currents (Fig. 39). The most proximal areas (shoreface) receive high amounts of terrigenous material and are characterized by well-washed and well-sorted sand shoals (F5). These deposits are intensely bioturbated by *Thalassinoides*, which are opportunistic bottom feeders especially active in the aftermath of storm events (Blomeier et al., 2013). Shallow-water reef builders are generally scarce on ramps (Burchette & Wright, 1992), unlike wave-reworked shell

banks, which is the dominating facies (F6) of the shoreface zone. The shell banks are dominated by shallow-shelf thick-shelled brachiopods.

The sandy brachiopod shell banks at the FWWB marks the transition to the deeper water and offshore transition of the mid-ramp (Fig. 39). Due to the location between the FWWB and SWWB, storm processes are the major factor influencing the deposition of the mid ramp. The offshore plains of the mid ramp was site of a prevalent sponge population during the Late Permian, and constituted the dominant silica factory of the shelf during the Permian Chert Event (Blomeier et al., 2013). The sponges disintegrated and accumulated on the seabed, and eventually formed the light spiculitic cherts (F7). The widespread spiculitic deposits must have demanded a major silica source, and Beauchamp & Baud (2002) have explained the chert accumulations along the northwestern margin of Pangea as a result of upwelling of cold nutrient-rich bottom waters. According to Gates et al. (2004) siliceous sponge spicules occur in two settings: 1) areas where upwelling of cold bottom waters brings nutrients onto continental slopes and 2) areas where silica content is due to runoff from land. The presence of phosphate, glauconite and silica in abundance throughout the ramp suggests upwelling of nutrient rich deep oceanic waters onto the ramp as an essential factor for chert accumulation also in central Spitsbergen (Gates et al., 2004). Around the outer mid ramp margin, colonies of robust bryozoans (mainly trepostome and and cystoporate bryozoans) and echinoderms (crinoids) thrive. During storms the skeletal debris was distributed landward across the mid- and inner ramp, and seaward onto the outer ramp. This process formed the distal tempestites and bioclastic limestones of facies 9, 10 and 11 (bryozoan dominated floatstone, bryozoan-echinoderm dominated pack- to rudstone and bryozoan dominated pack- to rudstone).

The outer ramp extends from the SWWB and comprises fine-grained siliciclastics and a low-diversity biotic association consisting mainly of siliceous sponges and some fragile fenestrate bryozoans (Fig. 39) (Blomeier et al., 2013). Dark spiculites (F12) dominates the most proximal areas of the outer ramp, whereas dark shale (F13) dominates the distal parts. The siliciclastic dark shale represents the background sedimentation and is also present within the dark spiculites. Storm-generated currents transporting bioclastic material from the mid and inner ramp is the source of the limestone beds and

lenses (F9, F10, F11) within the shale. Due to deep water and restricted circulation, suboxic to anoxic conditions probably prevailed during deposition of the organic rich black shale (F13). Suboxic or anoxic bottom waters are common in outer-ramp environments and restrict bioturbation, and thus promote deposition of organic-rich laminites, particularly during sea-level rises when the O₂/H₂S interface is raised (Johnson & Baldwin, 1996).

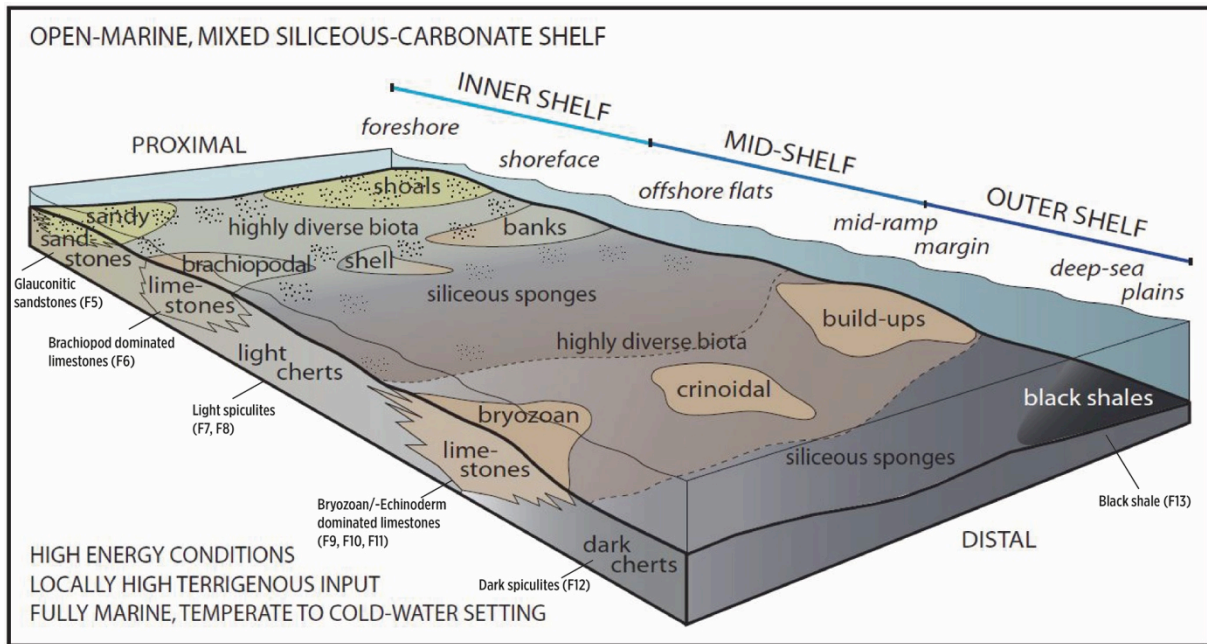


Figure 39: Shelf model for the Kapp Starostin Formation in central Spitsbergen showing the general distribution of the main facies (sandstones, limestones, light spiculites, dark spiculites and black shales) across the inner, mid and outer ramp areas. MLW= Mean low water level, FWWB/SWWB = Fair/storm-weather wave base. Modified from Blomeier et al. (2013) and Dallmann et al. (2015b).

7. Sequence stratigraphy

The cyclicity observed in the Gipshuken Formation continues throughout the Kapp Starostin Formation, and reflects the regional and global sea level fluctuations through late Palaeozoic time (Ezaki et al., 1994). Based on the facies analysis and the stacking pattern of the facies associations, three transgressive-regressive sequences have been recognised from the Kapp Starostin Formation (Figs. 40, 41). A transgressive-regressive sequence comprises the strata deposited from the time of one transgressive event to the beginning of the next (Johnson & Murphy, 1984; Johnson et al., 1985; Catuneanu et al., 2009). Such sequences are bounded by subaerial unconformities on the basin margins and marine maximum regressive surfaces further seaward (Catuneanu, 2006). In the Kapp Starostin Formation strata, the sequence boundary overlying each highstand systems tract is marked by shallow-water deposits, and not a subaerial unconformity. Each transgressive-regressive sequence thus reflects a transition from deeper-water sedimentation at the base to shallower-water sedimentation at the top. The maximum flooding surface represents the maximum extent of landward marine influence and the turnaround between transgressive and regressive strata (Miall, 2010), and is therefore used to subdivide the T-R sequences into transgressive and regressive units. The systems tracts constituting the studied succession is described below.

Highstand systems tract (HST) I

Deposition of the Gipshuken Formation occurred during the Artinskian, a time marked on Svalbard by a general regression (Lauritzen, 1981). The formation represents backbarrier facies, evident from the supra- and intertidal deposits observed in the field, and is interpreted as stacked sabkha cycles (Lauritzen, 1981). In carbonate-evaporite depositional systems, basinal evaporites are common in the lowstand systems tract, whereas shallow-water and sabkha evaporites are most common in the transgressive and highstand systems tracts (Coe et al., 2003). The regressive deposits of the Gipshuken Formation are therefore thought to represent the highstand systems tract. The highstand systems tract forms during the late stage of sea-level rise, when the rate of sea-level rise is outpaced by the rate of sedimentation (Catuneanu, 2006). The stacking pattern is thus dominated by aggradational to progradational parasequences.

Subsequent sea-level fall and subaerial exposure of the platform is evident from the calciche on the top of the Gipshuken Formation (at 90 m, Fig. 40). The changes in climatic conditions from a warm and arid sabkha environment to an open marine environment in a temperate climate is reflected in the changes in faunal assemblage from the Gipshuken Formation to the Kapp Starostin Formation (Steel & Worsley, 1984; Stemmerik & Worsley, 1989). The following transgressive systems tract (TST) is dominated by cool-water fossils, and marks a drastic change from the warm-water carbonates of the Gipshuken Formation.

Transgressive systems tract (TST) I

The transgressive systems tract (TST) I comprises the stratigraphic succession between the flooding surface (FS) at the base and the maximum flooding surface (MFS) at the top (91-106 m, Fig. 40) (Catuneanu, 2006). The transgressive systems tract forms when the rate of sedimentation is outpaced by the rate of sea-level rise (Catuneanu, 2006). The deposition of the Vøringen Member thus coincides with a regional sea-level rise. The Vøringen Member is interpreted to represent a marine shoreface facies deposited by transgression of barrier sequences across the restricted Gipshuken platform (Hellem, 1980; Steel & Worsley, 1984; Nakrem, 1994). When the shoreface migrated landward, by a barrier or shoreface retreat, the pre-existing and newly deposited sediments were truncated by wave erosion, creating a transgressive wave ravinement surface (Cattaneo & Steel, 2003). The erosive and undulating boundary between the regressive Gipshuken Formation and the overlying transgressive Vøringen Member is thus a ravinement surface and a transgressive surface (TS), a surface associated with shoreline turnaround (from regressive to transgressive) and abrupt increase in marine influence (at 91 m, Fig. 40) (Cattaneo & Steel, 2003). The transgressive Vøringen Member corresponds to the T-C lithosome of Cattaneo & Steel (2003), where the transgressive deposits develop above the wave ravinement surface in low-gradient settings as a result of shoreface erosion. The TST I is capped by a maximum flooding surface (MFS) (located at 106 m, Fig. 40).

Highstand systems tract (HST) II

The maximum flooding surface (at 106 m, Fig. 40) separates the transgressive Vøringen Member from the regressive unit of shale and spiculite above belonging to the highstand systems tract (HST) II. The flooding surface and change in lithology indicates

a termination of shallow marine shelf sedimentation, and a change to deeper water sedimentation. The highstand systems tract forms when the rate of sea level rise is outpaced by the sedimentation rate, generating a normal regression of the shoreline (Catuneanu, 2006). The HST I comprises the major part of the Svenskegg member (Fig. 40), which contains interbedded shale and spiculites, thus representing an open marine platform (Nakrem, 1994). A general upward change from dark-coloured to light-coloured spiculites indicates a system developing from aggradational to more progradational as the light spiculites become more prominent upward in the succession (Fig. 40).

Transgressive systems tract (TST) II

The flooding surface (FS) separates the underlying spiculitic deposits of the highstand systems tract II from the deposits of the transgressive systems tract II (at 164 m, Fig. 40). The flooding surface is overlain by a 25 m thick interval of black shale deposited in the outer ramp area (164-189 m, Fig. 40). Some bioclastic limestone beds and lenses are present within the shale (at 175 m, 185 m, 187 m, Fig. 40) and were probably transported from the mid-ramp by storm-induced currents. These bioclastic deposits are therefore interpreted as distal tempestites. The transgressive systems tract II was deposited when the rate of sea-level rise outpaced the rate of sediment supply (Catuneanu, 2006). This led to the formation of the thick shale unit and formation of phosphatic and glauconitic minerals (Cattaneo & Steel, 2003). The basal transgressive surface does not show any evidence of an erosional wave ravinement surface in the study area. This is probably because the wave ravinement surface is restricted to the shallow-marine areas above the FWWB, and the flooding took place in mid-ramp environment between the FWWB and SWWB (thus separating light spiculite from the shale, Fig. 40) (Cattaneo & Steel, 2003). The transgressive systems tract III therefore corresponds to the T-E lithosome of Cattaneo & Steel (2003), being transgressive deposits without evidence of ravinement surfaces. The boundary to the overlying HST III is a bit unclear, and has been placed within the upper part of the shale interval with the assumption that the HST III has a stronger aggrading than prograding component at the beginning of deposition.

Highstand systems tract (HST) III

The shale of the TST III is overlain by light spiculites (both brecciated and normal) of the HST III. Two phosphatized surfaces are observed within this HST III, at the top of the brecciated interval (at 214 m, Fig. 40) and at the top of the light spiculitic interval (at 229 m, Fig. 40). The phosphatized surfaces were probably formed during periods of slow sedimentation, when hardgrounds formed by mineralization of minerals such as iron oxides and calcium phosphates (Ehrenberg et al., 2001). A glauconitic sandstone unit occurs at the top of the HST III and indicates a regressive trend.

Transgressive systems tract (TST) III

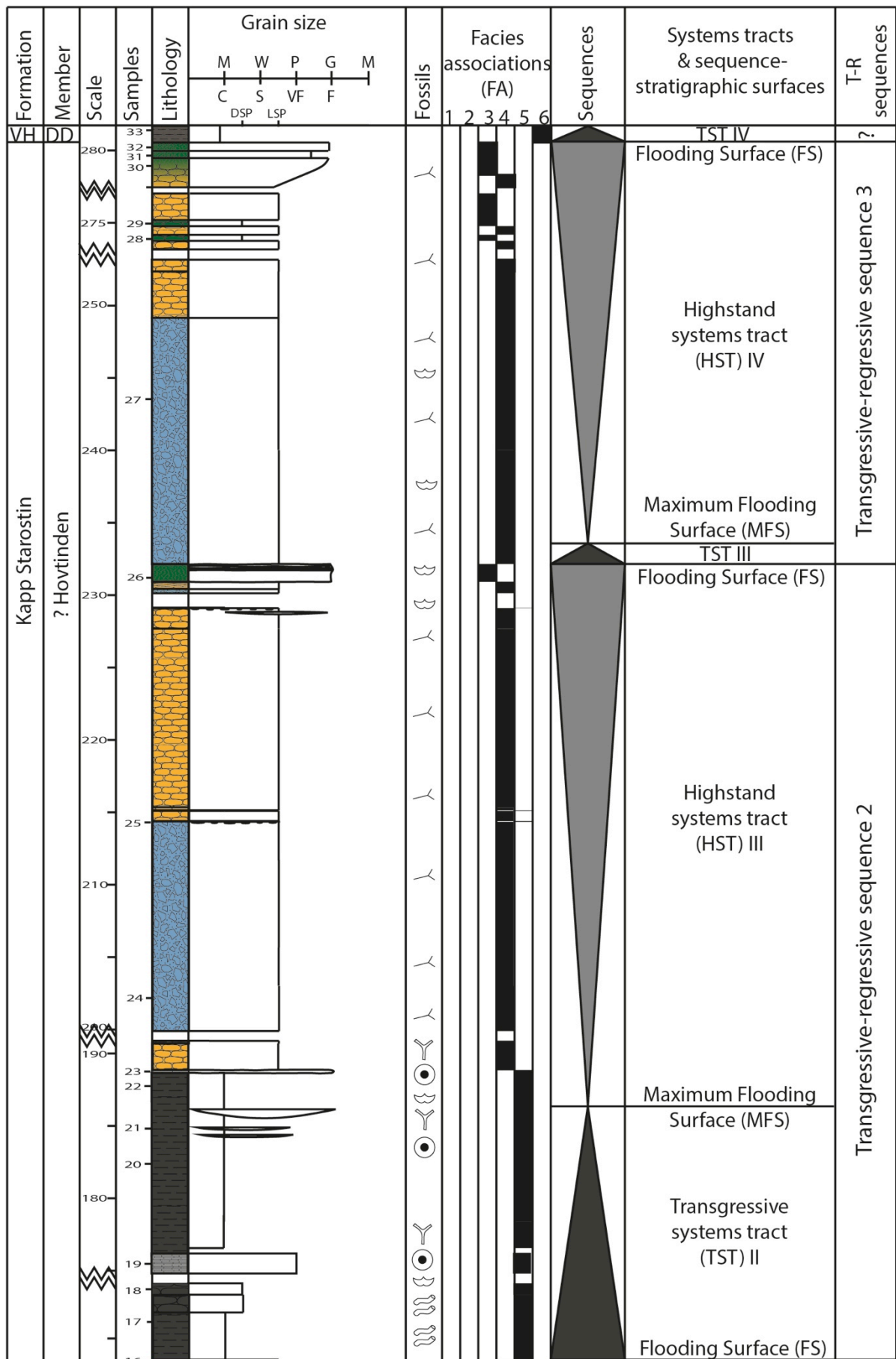
The flooding surface (FS) separating the HST III from the TST III only represents a minor flooding, from the glauconitic sandstone of FA3 to the light spiculite of FA4. The deposits included in the TST III, between the flooding surface (at 233 m, Fig. 40) and the maximum flooding surface (at 234 m, Fig. 40), are therefore not very thick. No signs of erosion or a transgressive lag is observed and the transgressive systems tract III can therefore be classified as the T-E lithosome of Cattaneo & Steel (2003), being transgressive deposits without evidence of ravinement surfaces. The exact location of the maximum flooding surface is uncertain, as this surface was not observed in the field, however, it has been interpreted to be in the lower part of the brecciated interval (at 234, Fig. 40).

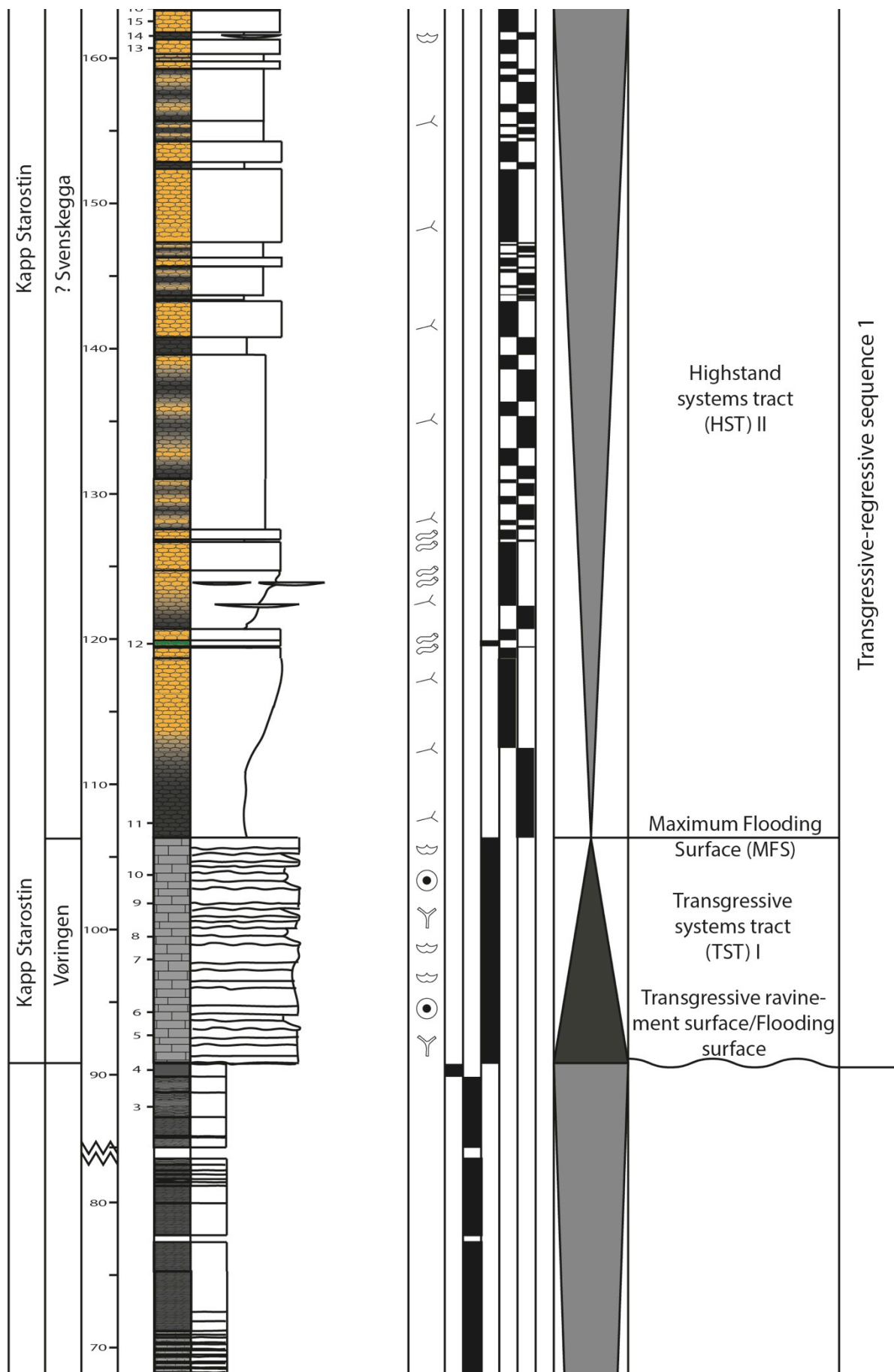
Highstand systems tract (HST) IV

As the rate of sedimentation outpaced the rate of sea level rise in the TST III, deposition of the highstand systems tract IV began. The maximum flooding surface separates the TST III from the HST IV above (at 234 m, Fig. 40). The overlying light spiculite is composed of a brecciated unit and a non-brecciated spiculitic unit, which passes gradually into glauconitic sandstone towards the top of the formation. The gradual change from spiculite to glauconitic sandstone indicates a regressive trend. The glauconitic sandstone unit is terminated at the Kapp Starostin-Vikingshøgda formation boundary, informally called the Permian-Triassic boundary (at 281 m, Fig. 40), and capped by a flooding surface.

Transgressive systems Tract (TST) IV

The Permian-Triassic boundary coincides with a major flooding surface, which separates the glauconitic sandstone of the HST IV from the marine Triassic siltstones and shales of the transgressive systems tract IV (at 281 m, Fig. 40). The boundary does not only mark a change from shallow-shelf to deeper shelf sedimentation, but also a shut-down of both the silica and carbonate factories.





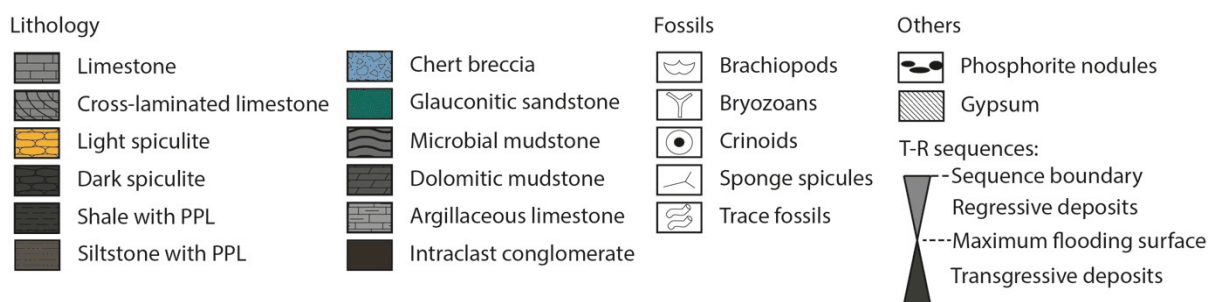
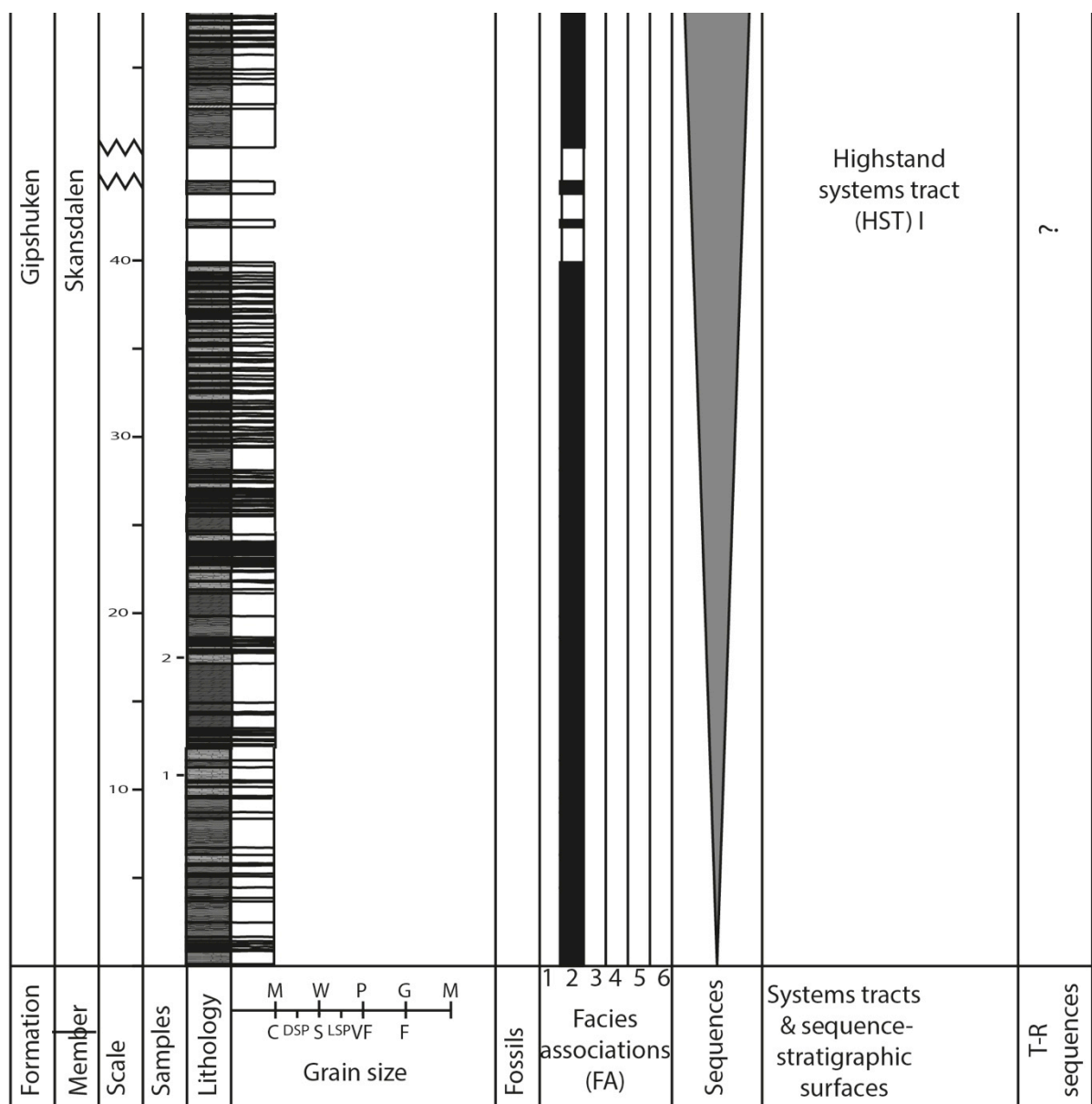


Figure 40: Composite log of the Gipshuken Formation (section A and B) and the Kapp Starostin Formation (section B, C, D and E). The sequence stratigraphic interpretation is displayed by systems tracts and their bounding surfaces. The gaps in the upper part of the Kapp Starostin Formation (between 250-280 m) might be glauconitic sandstone layers, as the talus below the outcrops were mostly consisting of glauconitic sandstone cobbles. The legend is valid for all lithostratigraphic logs.

7.1 Transgressive-regressive sequences

The Upper Carboniferous to Lower Permian strata of central Spitsbergen is composed of four long-term transgressive-regressive sequences, where each T-R sequence is defined as second-order cycles (Samuelsberg & Pickard, 1999). The Gipshuken Formation represents the regressive part of the fourth transgressive-regressive sequence (Samuelsberg & Pickard, 1999). The Gipshuken Formation in the study area is therefore also part of a transgressive-regressive sequence, although the lower sequence boundary and the transgressive part of the sequence was not studied. The formation also has a high-order internal cyclicity composed of stacked sabkha deposits. Numerous of parasequences separated by minor flooding surfaces make up the overall regressive expression of the formation.

According to Stemmerik & Worsley (2005), the Tempelfjorden Group, here represented by the Kapp Starostin Formation, represents a second a second-order cycle with a duration of 15-30 Ma. In the study area, the formation has been subdivided into three transgressive-regressive sequences (Figs. 40, 41). These T-R sequences thus represent higher than second-order cycles, most likely third-order cycles. The transgressive-regressive sequences reflect the large-scale sea-level fluctuations, and many minor sea level fluctuations are recorded within each sequence. T-R sequence 1 and 2 both have black shale (or shaly dark spiculite) at the base of the sequences, whereas T-R sequence 3 has light spiculite at the base of the sequence. The regressive parts of the sequences are generally thicker than the transgressive parts and are dominated by increasingly shallower facies, leading to an overall regressive trend.

The sequence stratigraphic architecture of the succession shows an overall change from warm-water carbonates to cool-water carbonates, and a change from a carbonate platform to a mixed carbonate-siliciclastic ramp, being increasingly more dominated by siliciclastic sediments. The general upward change from dark spiculites to light spiculites, and the change in siliciclastic lithology from shale to sandstone indicates an overall regressive trend toward the Permian-Triassic boundary (Ehrenberg et al., 2001). Several transgressive-regressive cycles, ranging from 3-6 Ma, have also been identified in the Triassic succession of the Sverdrup Basin, Svalbard and the Barents

Sea (Mørk et al., 1989). This indicates that the 3rd order sea-level cycles that were present during the Late Permian, also continued throughout the Triassic.

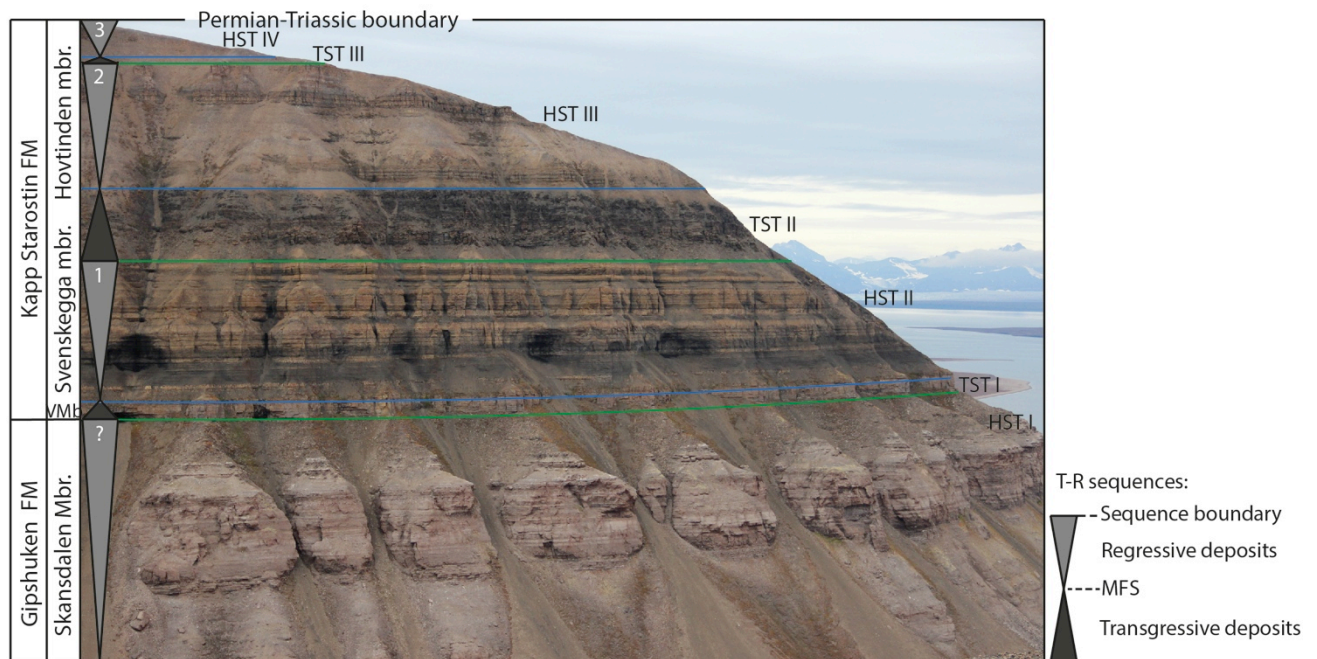


Figure 41: Sequence stratigraphic interpretation of the Gipshuken and Kapp Starostin formations. The succession consists of six systems tracts and their bounding surfaces. Minor flooding surfaces are present within each systems tract. Green lines represent main flooding surfaces (FS) and blue lines represent maximum flooding surfaces (MFS). Due to scree covered parts, the lines may not be placed at their exact level. TST: Transgressive systems tract, HST: Highstand systems tract, VMB: Vøringen Member. SW-NE view of the northern part of Heimenfjellet (see Fig. 3c for location).

8. Economic implications

Late Palaeozoic rocks constitute one of the play models in the Barents Sea, and the Permian Røye Formation represents one of the possible reservoir rocks. The Late Permian Kapp Starostin Formation on Spitsbergen is a lateral equivalent to the Røye Formation, and may therefore be an outcrop analogue of great value when it comes to improving the understanding of subsurface reservoir architectures and geometric relationships, as well as small-scale properties like facies transitions and porosities.

8.1 Diagenesis and reservoir potential

The reservoir potential of the Upper Palaeozoic succession in the Barents Sea depends on the primary mineralogy, early diagenetic processes and karstification, and the best properties are generally found in Upper Carboniferous to Lower Permian dolomitic carbonates (Stemmerik et al. 1999). Ehrenberg (2004) studied the Upper Carboniferous-Lower Permian carbonate strata of the Finnmark platform and concluded that dolomitization is necessary for high porosity in mudstones and wackestones, whereas high porosity in grain-dominated rocks depends on the paucity of burial cement. The Moscovian to early Sakmarian carbonates consists of high-Mg calcitic and aragonitic material, which is mineralogically unstable and therefore easily dissolved and dolomitized (Stemmerik et al., 1999). Dolomite forms by dissolution and reprecipitation, and can retain or create porosity and permeability to much greater burial depths than limestone (Warren, 2000). Replacement of limestone (calcite or aragonite) by dolomite reduces the mineral volume and thus increases the pore volume (porosity). This is because dolomite has a smaller molar volume than calcite and aragonite (Warren, 2000). However, dolomitization does not always improve porosity or permeability; if there is an external source of carbonate and magnesium ions overdolomitization can result in volume increase and loss of total porosity (Lucia & Major, 1994; Warren, 2000). Nevertheless, Palaeozoic dolomites are usually more porous than their associated limestones due to the ability to retain porosity during burial (Lucia, 1999).

The cherty lithologies of the Tempelfjorden Group are not nearly as dolomitized as the Moscovian-Sakmarian carbonates, and porosity is therefore mainly depending on the

size of the spicules, matrix content and presence of vugs and fractures (Ehrenberg et al., 2001). Limestones within the Tempelfjorden Group are commonly tight and strongly silicified without any significant reservoir potential. Instead, they may form regional lateral seals (Stemmerik et al., 1999). However, porosities ranging from 10% to 20% have been measured in Sakmarian to Artinskian bryozoan-*Tubiphytes* build-ups (well 7229/11-1), suggesting that shallowly buried build-ups may have retained some primary porosity or developed some secondary porosity (Stemmerik et al., 1999). In the light spiculites, porosity comprise interparticle pores that are not filled with silicified matrix and cement, fractures and vugs formed during compaction and secondary molds formed by dissolution of spicules (Ehrenberg et al., 2001). Diagenesis of biogenic siliceous sediments generally occurs by transformation of silica from opal-A to opal-CT and eventually to quartz (Ehrenberg et al., 1998). The diagenesis of the siliceous spicules involved dissolution and reprecipitation, which is evident from the replacement of spicules by chalcedony and microquartz. In the spiculitic strata on the Finnmark Platform (wells 7128/4- and 7128/6-1) high porosities (15-25%) have been correlated with low chert/chalcedony ratio, which decreases from the base toward the top of the succession (Ehrenberg et al., 1998). It is uncertain whether the higher porosities in the upper part of the spiculite is related to change in depositional lithology or is a result of subaerial exposure and leaching by meteoric water. Ehrenberg et al. (1998) suggested the moldic porosity of the spiculite to be a result of local silica redistribution during shallow phreatic diagenesis.

The best potential reservoirs of highstand deposits tend to be associated with the shoreline to shoreface depositional systems that have a low mud content (Catuneanu, 2006). This is also true for the Kapp Starostin Formation, where high porosities generally are associated with relatively proximal facies, such as light spiculite and glauconitic sandstone. Porosity measurements of the glauconitic sandstone in Dickson Land have revealed porosities ranging from 20-25% (Ehrenberg et al., 2001). The same values have also been recorded in the 25 m thick glauconitic sandstone interval at the top of the Kapp Starostin Formation in Sassendalen (Nøttvedt et al., 1993). The porosity of the light spiculite is more variable, and is ranging from 5-25% (Ehrenberg et al., 2001). Bioclastic limestones, shales and dark spiculite have no apparent reservoir potential (Ehrenberg et al., 2001). This means that the reservoir quality is linked to

facies and seabed topography; platforms and structural highs were sites of accumulation of porosity-prone light coloured spiculites during sea-level highstand and proximal shelf areas were sites of glauconitic sandstone deposition during sea-level lowstand (Ehrenberg et al., 2001). If the same properties are present in the Barents Sea equivalents (Røye and Ørret formations), glauconitic sandstone and light spiculite can be good possible reservoir rocks.

Porosity in limestones is commonly controlled by original facies types and diagenetic processes, and there are six major diagenetic processes; cementation, microbial micritization, neomorphism, dissolution, compaction and dolomitization (Tucker et al., 1990). Karstification is dissolution of limestone through chemical reactions with acidic water. Uplift in the latest Permian led to subaerially exposure of structural highs and may have led to karstification of limestones (e.g. Miseryfjellet Formation) over large areas and development of mouldic secondary porosity (Worsley et al., 2001a). Prolonged subaerial exposure of extensive areas across Svalbard during the Artinskian led to intensive weathering and karstification of the Gipsdalen Group (e.g. Kloten and Zeipelodden members) (Dallmann et al., 2015b). All these factors have led the Norwegian Petroleum Directorate (NPD) to conduct a play analysis of the Late Palaeozoic successions in the Barents Sea. The play analysis examines geological factors like source rock, migration paths, reservoir rock and traps within a geographically and stratigraphically delimited area. The Late Palaeozoic play models in the Barents Sea will be discussed in the next subchapter.

8.2 A Late Palaeozoic play model

The Palaeozoic petroleum system is mainly located on the Finnmark Platform and eastwards, however, a mixed Palaeozoic/Early-Middle Triassic system occurs in large areas of the Norwegian Barents Sea (Fig. 42). The Late Palaeozoic play models in the Barents Sea proposed by the Norwegian Petroleum Directorate are confined to structurally high areas like the Finnmark Platform, Loppa and Stappen highs (Figs. 42, 43).

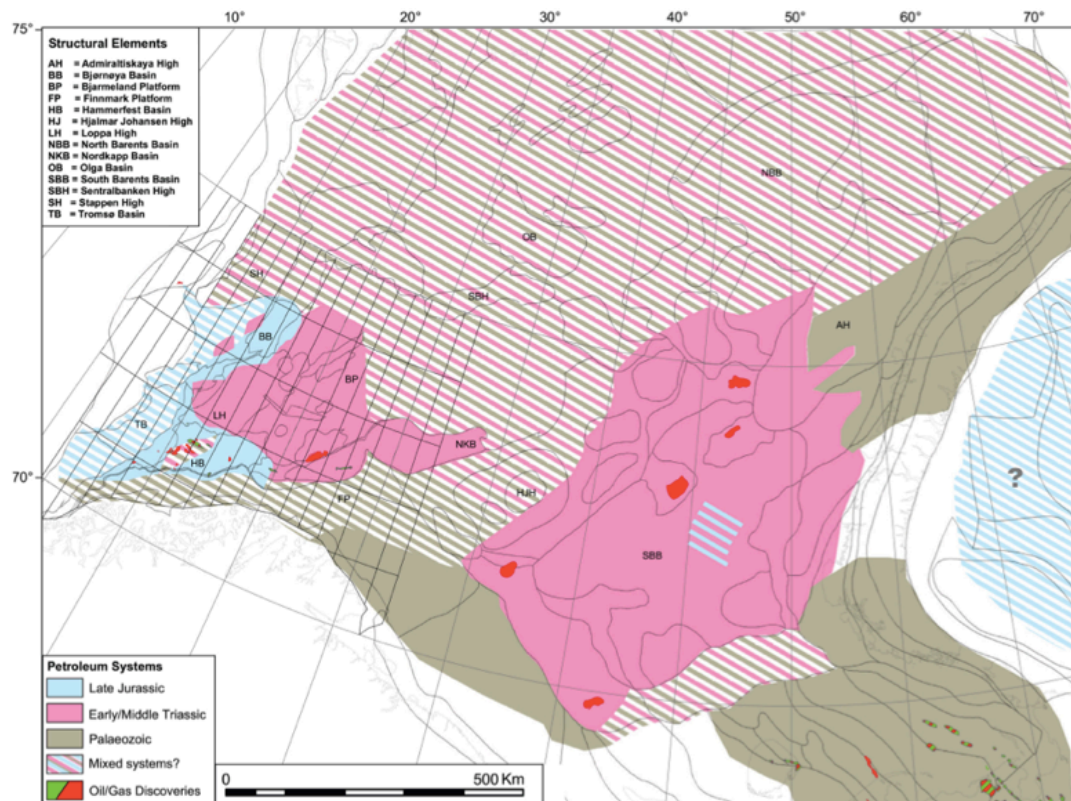


Figure 42. The main petroleum systems of the Barents Sea. The Palaeozoic petroleum system dominates on the Finnmark Platform and in the eastern Barents Sea. However, the mixed Palaeozoic-Triassic system that is present across large parts of the Norwegian Barents is also present on structurally high areas, such as the Loppa and Stappen highs. Henriksen et al. (2011b).

The Stappen High trends N-S from 73°30' N to about 75°30' N with Bjørnøya forming its highest point. The proposed plays consist of Middle Bashkirian to Late Wordian reservoir rocks (e.g. the Gipsdalen Group with Landnørdingsvika, Kapp Kåre, Kapp Hanna and Kapp Duner formations) with Upper Devonian to Lower Carboniferous shales as source rocks, and Late Cisuralian to Guadalupian mixed siliciclastic-bioclastic reservoir rocks with coal and carbonaceous shales of the Billefjorden Group or shales of the Tempelfjorden Group as source rocks. These plays are relevant for the Stappen High, but have not yet been confirmed.

The Finnmark Platform is the site of several possible plays. Possible reservoir rocks are late Bashkirian to late Sakmarian limestones and dolomites, late Bashkirian to late Sakmarian sandstone, Sakmarian to Artinskian limestones and dolomites and late Cisuralian to Guadalupian silicified carbonates and sandstones. Common to all the plays on the Finnmark Platform is that they all have Lower Carboniferous coal (Billefjorden Group) and Upper Permian shales (Tempelfjorden Group) as probable source rocks.

Several wells have been drilled on the Finnmark Platform (e.g. wells 7122/7-3, 7120/12-4, 7120/12-2, 7128/4-1, 7128/6-1, 7130/4-1, Fig. 43). Well 7128/6-1 cored almost half of the 900 m thick Upper Palaeozoic succession, which showed oil stains in the Upper Carboniferous carbonates (Ehrenberg et al., 1998a), whereas a noncommercial oil and gas discovery was made in the Permian Røye Formation in well 7128/4-1 and in the Carboniferous Seldog Formation in well 7130/4-1.

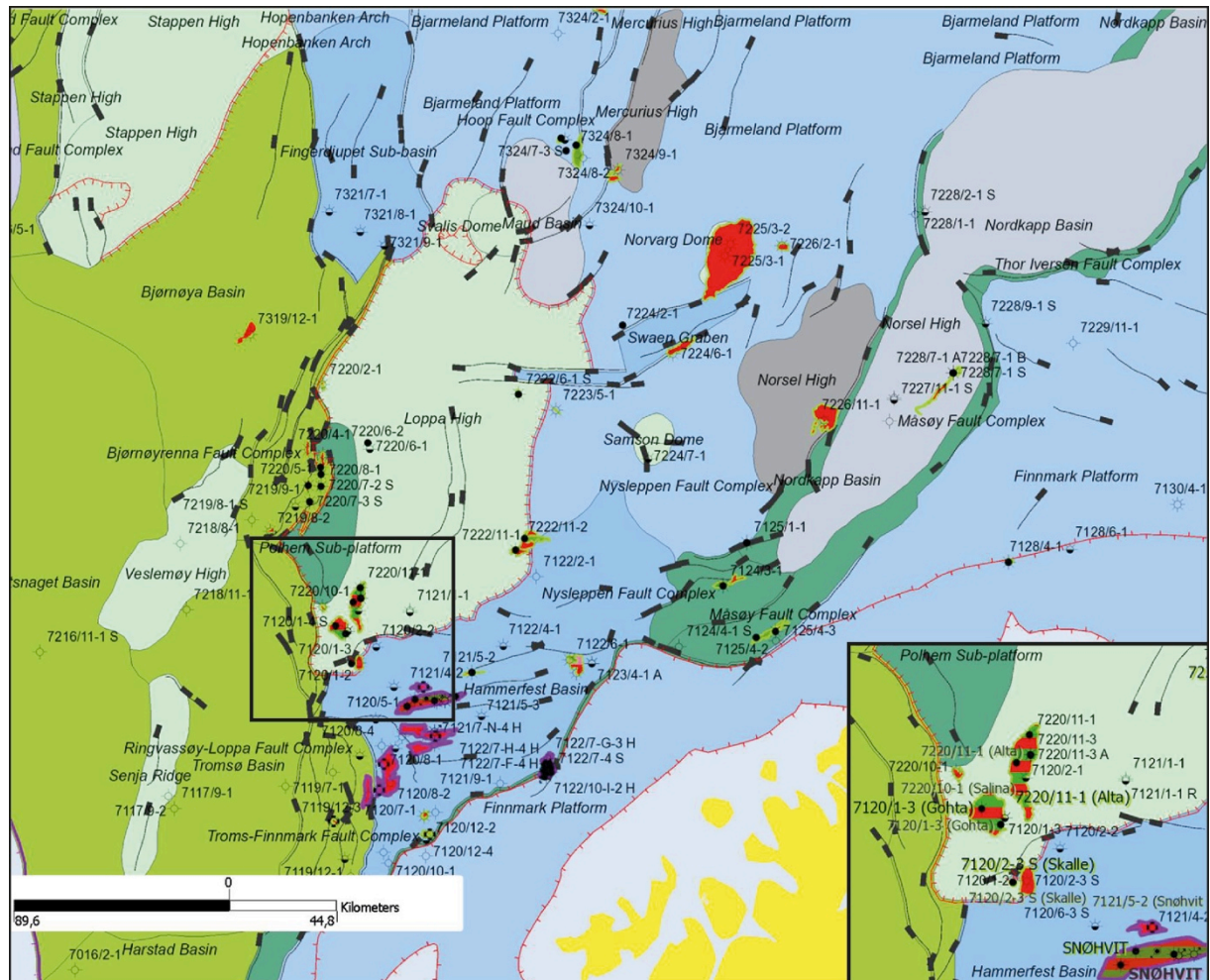


Figure 43: The Late Palaeozoic (Carboniferous and Permian) plays in the Barents Sea are located on the Stappen High, Loppa High and on the Finnmark Platform. The map shows all wellbores (exploration, development and active exploration) and all discoveries, whether they are being developed or not. The Gohta (well 7120/1-3) and Alta (well 7220/11-1) discoveries are located on the southern end of the Loppa High. Modified from NPD's FactMaps http://gis.npd.no/factmaps/sl_20/?Viewer=FactMaps_20.

The Loppa High is located between 71°50'N 20°E and 75°55'N, 22°40' E, and 72°55'N, 24°10'E and 73°20'N, 23°E, near the southwestern margin of the Norwegian Barents Sea and exhibits a Mid-Carboniferous rift topography (Fig. 43). The rifts were filled and draped by Upper Palaeozoic siliciclastic deposits, evaporites and carbonates that pinch

out westwards due to Late Permian and early Triassic uplift and erosion (Fig. 44) (Stemmerik et al., 1999). The high is separated from Bjørnøya and the Tromsø basins in the west by the Bjørnøyrenna and Ringvassøy-Loppa fault complexes, and from the Hammerfest Basin in the south by the Asterias Fault complex. Eastwards, the high grades into the Bjarmeland Platform (Fig. 43). The play models on the Loppa High comprise reservoirs of Late Bashkirian to Late Sakmarian sandstones, Late Bashkirian to Late Sakmarian limestones and dolomites, and Sakmarian to Artinskian limestones and dolomites. The main source rocks are Lower Carboniferous coal and shales of the Billefjorden Group and Upper Permian shales of the Tempelfjorden Group. Palaeoaplysinid-phyllloid algal build-ups have been identified on parts of the high (Smelror et al., 2009). The high has been uplifted and exposed a number of times, and it is estimated that carbonate build-ups may have undergone as much as 25 Ma of subaerial exposure in a temperate and possible humid climate (Stemmerik et al., 1999). During sea-level lowstands, the exposed high was subjected to dissolution and karstification (Smelror et al., 2009). The Upper Palaeozoic succession on the Loppa High has been encountered by several wells, e.g. wells 7120/1-1, 7120/2-1, 7220/6-1, 7120/1-3 and 7220/11-1. Two significant discoveries have been made; the Alta discovery (well 7220/11-1) and the Gohta discovery (well 7120/1-3) (Fig. 43).

Well 7120/1-3 (Gohta) was drilled on the southern end of the Loppa High in 2013 and encountered Triassic sandstones of the Snadd Formation and Permian karstified carbonates of the Røye Formation. The karstified carbonates were penetrated at 2281 m depth, where the well encountered a gas column of 34 m (GOC at 2310.3 m) and an oil column of 76 m (OWC at 2389 m). The well was terminated in the Røye Formation at a depth of 2512 m. Although the Snadd target proved water filled, the Røye Formation had oil shows throughout the reservoir. The recoverable oil and gas has been estimated to be 13.98 mill Sm³ oil and 10.95 mill Sm³ gas. Six cores, and a total of 50.3 m, were recovered from the interval 2288.5 to 2346.8 in the karstified carbonates. A drill stem test of the interval 2336.8 to 2377.3 m in the Røye Formation confirmed good production properties of the reservoir; a production rate of 683 Sm³ oil and 222000 Sm³ gas per day through a 44/64 inch nozzle.

The Alta discovery (well 7220/11-1) was made in 2014 and is located 20 km northeast of the Gohta discovery (well 7120/1-3). The well encountered Triassic sandstones of the Kobbe Formation (Sassendalen Group) and chalk of the Permian Ørn Formation (Gipsdalen Group). An oil column of 45 m and a gas column of 10 m was penetrated in carbonate rocks of the Gipsdalen Group. These rocks showed good reservoir- and flow properties. The discovery is estimated to contain 26.10 mill Sm³ recoverable oil and 9.70 mill Sm³ recoverable gas.

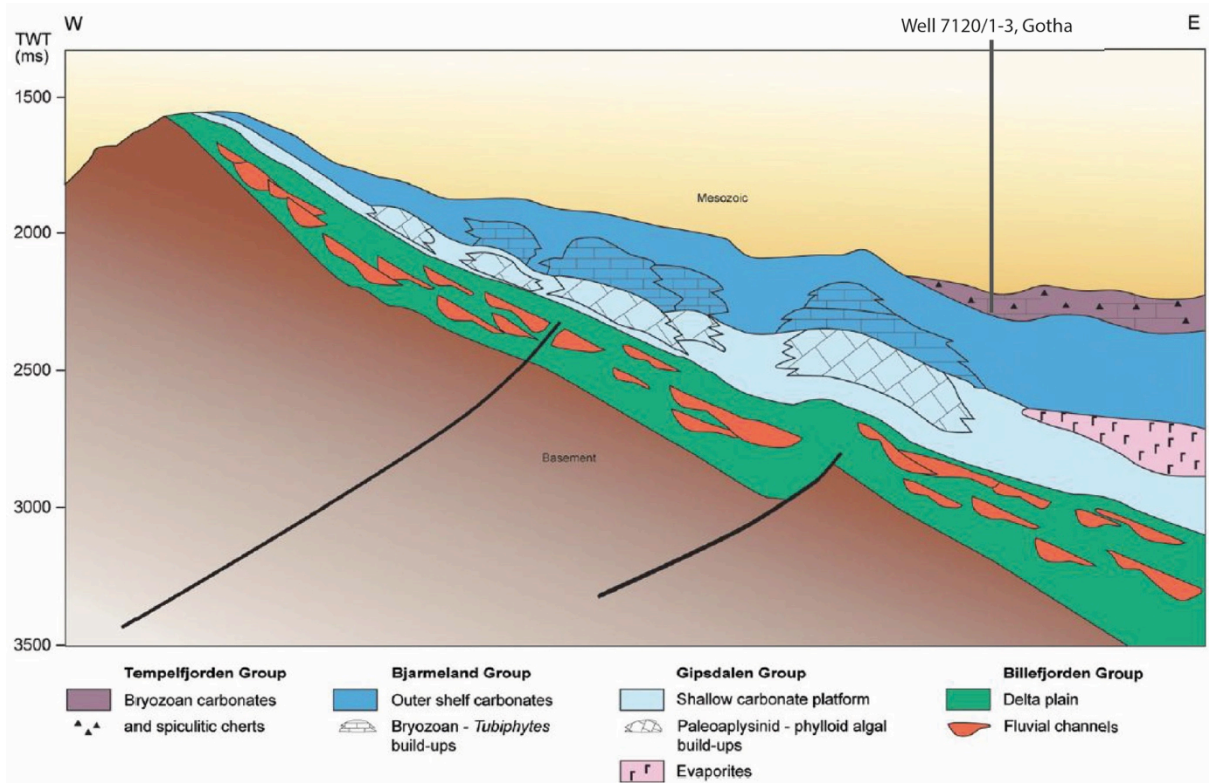


Figure 44: Distribution of the Upper Palaeozoic strata on the Loppa High. The strata pinch out westwards due to Late Permian-Early Triassic uplift and erosion. The Gohta discovery (well 7120/1-3) was made in spiculitic deposits of the Røye Formation. Modified from Henriksen et al. (2011b).

8.3 The Kapp Starostin Formation as an outcrop analogue for the Røye Formation

Comparison of the Kapp Starostin Formation in central Spitsbergen with a core section of the Røye Formation from well 7120/1-3 in the Barents Sea proved that both similarities and differences are present. Both the Kapp Starostin Formation and the Røye Formation consists mainly of siliceous sponge spicules. The light spiculite of the Kapp Starostin Formation (F8) and the light spiculite from the Røye Formation (F15) are both strongly silicified and heavily bioturbated by *Nereites* and *Zoophycos*. One noticeable difference is that the light spiculite of the Røye Formation is much more

dolomitized than the light spiculites on Spitsbergen, hence the definition of an additional facies – dolomitic light spiculite (F16). Black shale is also a common lithology and occurs as facies 13 in the Kapp Starostin Formation and as facies 17 in the Røye Formation. The black shale occurs as thin beds and laminas in both formations, but also constitutes thicker intervals in the Kapp Starostin Formation (e.g. 164-189 m, Fig. 40 and TST II, Fig. 41). Unfortunately, no thin sections were made from the Røye Formation and it is therefore difficult to say whether these facies have the same microscopical properties. The top of the Røye formation/ Tempelfjorden Group was reached at 2281 m depth and penetrated to a total depth of 2542 m. However, only 50.3 m of the 261 m penetrated strata was cored, which makes the stratigraphical development of the group hard to interpret. As the cores were taken in the interval 2288.5 m to 2345.3 m depth, the upper 7.5 m and the lower 196,7 m of the formation have not been looked at. However, different well logs (e.g. gamma ray, resistivity, neutron, density and sonic) were measured throughout the wellbore, and can therefore give information about lithology in the non-cored intervals, and thus also the sequence stratigraphic development of the formation. The different degree of dolomitization of the Kapp Starostin and Røye formations may be due to differences in their geological histories, in terms of uplift and erosion. The Loppa High has been tectonically active and subjected to subaerial exposure and erosion a number of times throughout it's geological history, e.g. during the Late Permian (Wordian), Early Triassic, Late Triassic-Early Jurassic (Hettangian), Late Jurassic (Tithonian) and Late Pliocene-Pleistocene (Smelror et al., 2009). The highly dolomitized spiculite is therefore most probably a result of prolonged subaerial exposure and meteoric diagenesis.

9. Summary and conclusions

The main objective of this thesis was to investigate the sedimentology and the sequence stratigraphic architecture of the Kapp Starostin Formation and present the field observations in a digital lithostratigraphic log. The outcrop-data was thereafter compared with a core section from the Gohta discovery (Røye Formation, well 7120/1-3) in the Barents Sea. Based on the fieldwork in Dickson Land, the thin section analysis and comparison with the core section, the following conclusions can be drawn:

- Deposition of the Gipshuken Formation occurred on a protected warm-water carbonate platform with low-energy conditions favourable for mud accumulation. The climate was warm and arid, which resulted in desiccation and allowed formation of evaporites. Gradual northwards drift of the area and changing oceanic circulation led to a change faunal assemblage and sedimentary facies. The Kapp Starostin Formation was deposited in open-marine cool-water conditions of a mixed carbonate-siliciclastic ramp. The Permian-Triassic environmental crisis led to a shutdown of both carbonate and silica factories, and the Vikinghøgda Formation was therefore deposited on a siliciclastic shelf.
- Fourteen depositional facies (F1-F14) were distinguished from the succession investigated in Dickson Land, and another three facies (F14-F17) were distinguished from the core section. Intraclast conglomerate (F1), microbial mudstone (F2), dolomitic mudstone (F3) and argillaceous limestone (F4) constitutes the Gipshuken Formation. The Kapp Starostin Formation comprises the glauconitic sandstone (F5), brachiopod dominated pack- to rudstone (F6), light spiculite (F7), chert breccia (F8), bryozoan dominated floatstone (F9), bryozoan-echinoderm dominated pack- to rudstone (F10), bryozoan dominated pack- to rudstone (F11), dark spiculite (F12) and black shale (F13). Siltstone (F14) constitutes the Vikinghøgda Formation. From the core section (Røye Formation) three facies were defined; light spiculite (15), dolomitic light spiculite (F16) and black shale (F17).
- The facies can be grouped into six facies associations where FA1-FA2 comprises the supratidal to intertidal deposits of the Gipshuken Formation, FA3-FA5 comprises the

shoreface to deep shelf deposits of the Kapp Starostin Formation, and FA6 comprises the marine siltstone of the Vikinghøgda Formation.

- A depositional model with a supratidal sabkha environment and an intertidal- to shallow subtidal inner platform can be applied for the Gipshuken Formation. The sabkha environment comprises the supratidal deposits of FA1 (F1), and the intertidal- to shallow subtidal areas comprises mudstones of FA2 (F2, F3 and F4). For the Kapp Starostin Formation, a depositional model with an inner- middle and outer ramp area can be applied. The inner ramp area (above FWWB) comprises wave-reworked sand shoals and shell banks (F5 and F6), the mid ramp area (between FWWB and SWWB) comprises light spiculite (F7 and F8), whereas the outer ramp area (below SWWB) comprises dark spiculite and black shale (F12 and 13) and storm-deposited bioclastic beds and lenses (F9, F10 and F11).
- Based on the facies analysis and the stacking pattern, three transgressive-regressive sequences were identified in the Kapp Starostin Formation (Figs. 40, 41). These T-R sequences probably represent third order cycles. The formation also shows an overall regressive trend influenced by a second order sea-level cycle towards the Permian-Triassic boundary.
- The Røye Formation on the Loppa High (well 7120/1-3) is much more dolomitized than the Kapp Starostin Formation on Spitsbergen, probably due to longer subaerial exposure of the high. Secondary porosity in spiculites mainly depends on spicule dissolution and matrix dolomitization. The reservoir potential of spiculitic deposits will therefore generally be better on structural highs and platforms that have been subaerially exposed.

9.1 Outlook

The core section from the Røye Formation on the Loppa High (well 7120/1-3) is still quite new and there are few, if any, published papers on the microscopic properties of the formation. A microfacies analysis should be conducted and supplemented with porosity and permeability measurements. Very interesting are the vertical changes in degree of cementation and primary and secondary porosity. A microfacies analysis can

enhance the understanding of the diagenetic history and porosity development in the formation. On a larger scale, the sequence stratigraphic development of the formation could be interpreted by the use of high-resolution seismic and well log information, and correlated to the age-equivalent successions of the Tempelfjorden Group.

References

- Ahlborn, M., L. Stemmerik, and T.-K. Kalstø, 2014, 3D seismic analysis of karstified interbedded carbonates and evaporites, Lower Permian Gipsdalen Group, Loppa High, southwestern Barents Sea: *Marine and Petroleum Geology*, v. 56, p. 16-33.
- Beauchamp, B., and A. Baud, 2002, Growth and demise of Permian biogenic chert along northwest Pangea: evidence for end-Permian collapse of thermohaline circulation: *Palaeogeography, Palaeoclimatology, Palaeoecology*, v. 184, p. 37-63.
- Beauchamp, B., and A. Desrochers, 1997, Permian warm- to very cold water carbonates and cherts in northwest Pangea, *in* N. P. James, and J. A. D. Clarke, eds., *Cool-Water Carbonates*, v. 56, p. 327-347.
- Beauchamp, B., J. C. Harrison, J. Utting, T. A. Brent, and S. Pinard, 2001, Carboniferous and Permian subsurface stratigraphy, Prince Patrick Island, Northwest Territories, Canadian Arctic: *Geological Survey of Canada, Bulletin* 565, p. 93.
- Becker, L., R. J. Poreda, A. G. Hunt, T. E. Bunch, and M. Rampino, 2001, Impact Event at the Permian-Triassic Boundary: Evidence from Extraterrestrial Noble Gases in Fullerenes: *Science*, v. 291, p. 1530-1533.
- Bergh, S. G., A. Braathen, and A. Andresen, 1997, Interaction of basement-involved and thin-skinned tectonism in the Tertiary fold-thrust belt of central Spitsbergen, Svalbard: *AAPG Bulletin*, v. 81, p. 637-661.
- Blomeier, D., A. Dustira, H. Forke, and C. Scheibner, 2011, Environmental change in the Early Permian of NE Svalbard: from a warm-water carbonate platform (Gipshuken Formation) to a temperate, mixed siliciclastic-carbonate ramp (Kapp Starostin Formation): *International Journal of Paleontology, Sedimentology and Geology*, v. 57, p. 493-523.
- Blomeier, D., A. Dustira, H. Forke, and C. Scheibner, 2013, Facies analysis and depositional environments of a storm-dominated, temperate to cold, mixed siliceous-carbonate ramp: the Permian Kapp Starostin Formation in NE Svalbard: *Norw. J. Geol.*, v. 93, p. 75-93.
- Blomeier, D., C. Scheibner, and H. Forke, 2009, Facies arrangement and cyclostratigraphic architecture of a shallow-marine, warm-water carbonate platform: the Late Carboniferous Ny Friesland Platform in eastern Spitsbergen (Pyefjellet Beds, Wordiekammen Formation, Gipsdalen Group): *International Journal of Paleontology, Sedimentology and Geology*, v. 55, p. 291-324.
- Blomeier, D., M. Wisshak, W. Dallmann, E. Volohonsky, and A. Freiwald, 2003, Facies analysis of the old Red Sandstone of Spitsbergen (Wood Bay Formation): Reconstruction of the depositional environments and implications of basin development: *International Journal of Paleontology, Sedimentology and Geology*, v. 49, p. 151-174.
- Boggs, S., 1995a, Carbonate Sedimentary Rocks, *in* A. Dunaway, ed., *Principles of Sedimentology and Stratigraphy*, Pearson, p. 135-167.
- Boggs, S., 1995b, Siliciclastic Sedimentary Rocks, *in* A. Dunaway, ed., *Principles of Sedimentology and Stratigraphy*, Pearson, p. 101-134.
- Bond, D. P. G., and P. B. Wignall, 2010a, Pyrite framboid study of marine Permian--Triassic boundary sections: a complex anoxic event and its relationship to contemporaneous mass extinction.(Author abstract)(Report): *The Geological Society of America Bulletin*, v. 122, p. 1265.

- Bond, D. P. G., and P. B. Wignall, 2010b, Pyrite framboid study of marine Permian–Triassic boundary sections: a complex anoxic event and its relationship to contemporaneous mass extinction: *Geological Society of America Bulletin*, v. 122, p. 1265-1279.
- Bottolfsen, I., 1994, En sedimentologisk og diagenetisk undersøkelse av Kapp Starostinformasjonen (Øvre Perm), på nordsiden av Marmierfjellet, indre Isfjorden, Spitsbergen: Candidatus Scientiarum thesis thesis, Tromsø University, 150 p.
- Bugge, T., G. Mangerud, G. Elvebakk, A. Mork, I. Nilsson, S. Fanavoll, and J. O. Vigran, 1995, The upper Palaeozoic succession on the Finnmark Platform, Barents Sea: *Norsk Geologisk Tidsskrift*, v. 75, p. 3-30.
- Buggisch, W., D. Blomeier, and M. M. Joachimski, 2012, Facies, diagenesis and carbon isotopes of the Early Permian Gipshuken Formation (Svalbard): *Z. dt. Ges. Geowiss.*, v. 3, p. 309-321.
- Burchette, T. P., and V. P. Wright, 1992, Carbonate ramp depositional systems: *Sedimentary Geology*, v. 79, p. 3-57.
- Burov, Y. P., B. P. Gavrilov, B. A. Klubov, A. V. Pavlov, and V. N. Ustritsky, 1965, New data on the Upper Permian deposits of Spitsbergen, *in* W. B. Harland, ed., *Geology of Spitsbergen*, 1965, English transln. published by National Lending Library, Boston Spa, 1970, p. 116-130.
- Carmohn, A. M., 2007, Facies analysis of the Gipshuken and Kapp Starostin formations (Permian), NE Spitsbergen: Paleoenvironmental evolution and cyclicity, Bremen University, Bremen, 106 p.
- Carozzi, A. V., and M. S. Gerber, 1978, Synsedimentary chert breccia: a Mississippian tempestite: *J. Sediment. Petrol.*, v. 48, p. 705-708.
- Cattaneo, A., and R. J. Steel, 2003, Transgressive deposits: a review of their variability: *Earth Science Reviews*, v. 62, p. 187-228.
- Catuneanu, O., 2006, *Principles of Sequence Stratigraphy: Developments in sedimentology*: Burlington, Elsevier Science.
- Catuneanu, O., V. Abreu, J. P. Bhattacharya, M. D. Blum, R. W. Dalrymple, P. G. Eriksson, C. R. Fielding, W. L. Fisher, W. E. Galloway, M. R. Gibling, K. A. Giles, J. M. Holbrook, R. Jordan, C. G. S. C. Kendall, B. Macurda, O. J. Martinsen, A. D. Miall, J. E. Neal, D. Nummedal, L. Pomar, H. W. Posamentier, B. R. Pratt, J. F. Sarg, K. W. Shanley, R. J. Steel, A. Strasser, M. E. Tucker, and C. Winker, 2009, Towards the standardization of sequence stratigraphy: *Earth Science Reviews*, v. 92, p. 1-33.
- Coe, A. L., D. W. J. Bosence, K. D. Church, S. S. Flint, J. A. Howell, and R. C. L. Wilson, 2003, *The Sedimentary record of sea-level change*: Cambridge, Cambridge University Press.
- Colpaert, A., N. Pickard, J. Mienert, L. B. Henriksen, B. Rafaelsen, and K. Andreassen, 2007, 3D seismic analysis of an Upper Palaeozoic carbonate succession of the Eastern Finnmark Platform area, Norwegian Barents Sea: *Sedimentary geology*, v. 197, p. 79-98.
- Cutbill, J. L., and A. Challinor, 1965, Revision of the stratigraphical scheme for the Carboniferous and Permian rocks of Spitsbergen and Bjornoya: *Geological Magazine*, v. 102, p. 418-439.
- Cutler, M. A., 1981, The Middle Carboniferous-Permian stratigraphy of Midterhuken Peninsula, Spitsbergen : a thesis submitted in partial fulfillment for the degree of Master of Science (Geology): Madison, University of Wisconsin.

- Dallmann, W. K., D. Blomeier, and S. Elvevold, 2015a, Geoscience atlas of Svalbard: Norsk polarinstitutt.
- Dallmann, W. K., D. Blomeier, S. Elvevold, S.-A. Grundvåg, A. Mørk, S. Olaussen, D. Bond, and A. Hormes, 2015b, Historical Geology, Geoscience atlas of Svalbard: Tromsø, Norsk Polarinstitutt, p. 89-132.
- Dallmann, W. K., S. Stratigrafisk komité for, and p. Norsk, 1999, Lithostratigraphic lexicon of Svalbard : review and recommendations for nomenclature use : Upper Palaeozoic to Quaternary bedrock: Tromsø, Norsk polarinstitutt.
- Doré, A. G., 1995, Barents Sea Geology, Petroleum Resources and Commercial Potential: Arctic, v. 48, p. 207-221.
- Dunham, R. J., 1962, Classification of carbonate rocks according to depositional texture, *in* W. E. Ham, ed., Classification of carbonate rocks, v. 1, AAPG Memoir, p. 108-121.
- Dustira, A. M., P. B. Wignall, M. Joachimski, D. Blomeier, C. Hartkopf-Fröder, and D. P. G. Bond, 2013, Gradual onset of anoxia across the Permian–Triassic Boundary in Svalbard, Norway: Palaeogeography, Palaeoclimatology, Palaeoecology, v. 374, p. 303-313.
- Ehrenberg, S., N. Pickard, L. Henriksen, T. A. Svana, P. Gutteridge, and D. Macdonald, 2001, A depositional and sequence stratigraphic model for cold-water, spiculitic strata based on the Kapp Starostin Formation (Permian) of Spitsbergen and equivalent deposits from the Barents Sea: AAPG Bull., v. 85, p. 2061-2087.
- Ehrenberg, S. N., 2004, Factors controlling porosity in Upper Carboniferous–Lower Permian carbonate strata of the Barents Sea: AAPG Bulletin, v. 88, p. 1633-1676.
- Ehrenberg, S. N., E. B. Nielsen, T. A. Svånå, and L. Stemmerik, 1998, Diagenesis and reservoir quality of the Finnmark carbonate platform, Barents Sea ; results from wells 7128/6-1 and 7128/4-1: Norsk geologisk tidsskrift, v. 78, p. 225-252.
- Ehrenberg, S. N., E. B. Nielsen, T. A. Svånå, and L. Stemmerik, 1998a, Depositional evolution of the Finnmark carbonate platform, Barents Sea ; results from wells 7128/6-1 and 7128/4-1: Norsk geologisk tidsskrift.
- Eliassen, A., and M. R. Talbot, 2003b, Sedimentary facies and depositional history of the Mid-Carboniferous Minkinfjellet Formation, central Spitsbergen, Svalbard: Norsk Geologisk Tidsskrift, v. 83, p. 299-318.
- Elvebakk, G. G., D. W. D. Hunt, and L. L. Stemmerik, 2002, From isolated buildups to buildup mosaics: 3D seismic sheds new light on upper Carboniferous–Permian fault controlled carbonate buildups, Norwegian Barents Sea: Sedimentary geology, v. 152, p. 7-17.
- Embry, A. F., and J. E. A. Klován, 1972, Absolute water depth limits of late devonian paleoecological zones: Geologische Rundschau, v. 61, p. 672-686.
- Erwin, D. H., 2006, Extinction : how life on Earth nearly ended 250 million years ago: Princeton, Princeton University Press.
- Ezaki, Y., T. Kawamura, and K. Nakamura, 1994, Kapp Starostin Formation in Spitsbergen: A sedimentary and faunal record of late Permian palaeoenvironments in an Arctic region.
- Faleide, J. I., E. Våagnes, and S. T. Gudlaugsson, 1993, Late Mesozoic-Cenozoic evolution of the south-western Barents Sea in a regional rift-shear tectonic setting: Marine and Petroleum Geology, v. 10, p. 186-214.
- Faleide, J. I. J., S. T. S. Gudlaugsson, and G. G. Jacquart, 1984, Evolution of the western Barents Sea: Marine and petroleum geology, v. 1, p. 123-150.

- Flügel, E., 2010, *Microfacies of Carbonate Rocks: Analysis, Interpretation and Application: Analysis, Interpretation and Application*: Berlin, Heidelberg, Springer Berlin Heidelberg: Berlin, Heidelberg.
- Franseen, E. K., 2006, Mississippian (Osagean) shallow-water, mid-latitude siliceous sponge spicule and heterozoan carbonate facies; an example from Kansas with implications for regional controls and distribution of potential reservoir facies: *Bulletin - Kansas Geological Survey*, v. 252.
- Fredriksen, K. R., 1988, *Sedimentologiske og diagenetiske undersøkelser av Kapp Starostinformasjonen på Akseløya og Mariaholmen, Bellsund, Svalbard: Candidatus Scientiarum thesis thesis*, Tromsø University, 286 p.
- Gammon, P. R., and N. P. James, 2001, Palaeogeographical influence on Late Eocene biosiliceous sponge - rich sedimentation, southern Western Australia: *Sedimentology*, v. 48, p. 559-584.
- Gates, L. M., N. P. James, and B. Beauchamp, 2004, A glass ramp: shallow-water Permian spiculitic chert sedimentation, Sverdrup Basin, Arctic Canada: *Sedimentary Geology*, v. 168, p. 125-147.
- Gee, E. R., W. B. Harland, and J. R. H. McWhae, 1952, *Geology of Central Vestspitsbergen : Part I. Review of the geology of Spitsbergen, with special reference to Central Vestspitsbergen : Part II. Carboniferous to Lower Permian of Billefjorden*: Royal Society of Edinburgh. Transactions, v. B.LXII, Part II, No.9, 1951-52: Edinburgh, Oliver & Boyd.
- Gjelberg, J., and R. Steel, 1981, An outline of Lower-Middle Carboniferous sedimentation on Svalbard: effects of tectonic, climatic and sea level changes in rift basin sequences.
- Golonka, J., N. Y. Bocharova, D. Ford, M. E. Edrich, J. Bednarczyk, and J. Wildharber, 2003, Paleogeographic reconstructions and basins development of the Arctic: *Marine and petroleum geology*, v. 20, p. 211-248.
- Golonka, J., M. Ross, and C. Scotese, 1994, Phanerozoic paleogeographic and paleoclimatic modeling maps.
- Goode, T. W., 2013, *Palaeoenvironmental and palaeogeographic reconstruction of the Permian Kapp Starostin Formation in central and western Spitsbergen*, Southampton, University of Southampton.
- Groen, R. D., 2010, *From a restricted carbonate platform to a tempearate, storm-dominated ramp: The onset of the Permian Chert Event in central Spitsbergen*, VU University Amsterdam, 100 p.
- Grundvåg, S.-A., 2008, *Facies analysis, sequence stratigraphy and geochemistry of the middle-upper Permian Kapp Starostin Formation, central Spitsbergen*, Tromsø, S.-A. Grundvåg.
- Gudlaugsson, S., J. Faleide, S. Johansen, and A. Breivik, 1998, Late Palaeozoic structural development of the South-western Barents Sea, *Mar. Pet. Geol.*, p. 73-102.
- Harland, W. B., L. M. Anderson, and D. Manasrah, 1997, *The geology of Svalbard: Memoirs of the Geological Society of London*, v. 17.
- Hellem, T., and D. Worsley, 1978, An outcrop of the Kapp Starostin Formation at Austjøkeltinden, Sørkaplandet, *Norsk Polarinstitutt Årbok 1977*, p. 340-343.
- Hellem, T. A., 1980, En sedimentologisk og diagenetisk undersøkelse av utvalgte profiler fra Tempelfjordengruppen (Perm) i Isfjordenområdet, Spitsbergen, Oslo, T.A. Hellem.
- Henriksen, E., H. M. Bjornseth, T. K. Hals, T. Heide, T. A. Kiryukhina, O. S. Klovjan, G. B. Larssen, A. E. Ryseth, K. Ronning, K. Sollid, A. V. Stoupakova, A. M. Spencer, A. F.

- Embry, D. L. Gautier, A. V. Stoupakova, and K. Sorensen, 2011a, Uplift and erosion of the greater Barents Sea; impact on prospectivity and petroleum systems, London, London, United Kingdom: Geological Society of London, p. 271-281.
- Henriksen, E., A. E. Ryseth, G. B. Larssen, T. Heide, K. Ronning, K. Sollid, A. V. Stoupakova, A. M. Spencer, A. F. Embry, D. L. Gautier, A. V. Stoupakova, and K. Sorensen, 2011b, Tectonostratigraphy of the greater Barents Sea; implications for petroleum systems, London, London, United Kingdom: Geological Society of London, p. 163-195.
- Henriksen, L. B., 1988, En sedimentologisk og diagenetisk undersøkelse av Kapp Starostinformasjonen på Akseløya og Mariaholmen, Svalbard, Tromsø, L. B. Henriksen.
- Hjelle, A., and A. Brekke, 1993, Geology of Svalbard, Svalbards geologi: Polarhåndbok (online), Oslo, Norsk polarinstitutt.
- Hüneke, H., M. Joachimski, W. Buggisch, and H. Lützner, 2001, Marine carbonate facies in response to climate and nutrient level: The upper carboniferous and permian of central spitsbergen (Svalbard): *International Journal of Paleontology, Sedimentology and Geology*, v. 45, p. 93-135.
- Johannessen, E. P., and R. J. Steel, 1992, Mid-Carboniferous extension and rift-infill sequences in the Billefjorden Trough, Svalbard: *Norsk geologisk tidsskrift*.
- Johnson, H. D., and C. T. Baldwin, 1996, Shallow clastic seas, *in* H. G. Reading, ed., *Sedimentary Environments: Processes, Facies and Stratigraphy*, Blackwell, p. 232-280.
- Johnson, J. G., G. Klapper, and C. A. Sandberg, 1985, Devonian eustatic fluctuations in Euramerica: *Geological Society of America Bulletin*, v. 96, p. 567-587.
- Johnson, J. G., and M. A. Murphy, 1984, Time-rock model for Siluro-Devonian continental shelf, western United States: *Geological Society of America Bulletin*, v. 95, p. 1349-1359.
- Kaiho, K., Y. Kajiwarra, T. Nakano, and Y. Miura, 2001, End-Permian catastrophe by a bolide impact: Evidence of a gigantic release of sulfur from the mantle: *Geology*, v. 29, p. 815-818.
- Kendall, A. C., and G. M. Harwood, 1996, Marine evaporites: arid shorelines and basins, *in* H. G. Reading, ed., *Sedimentary Environments: Processes, Facies and Stratigraphy*, Blackwell, p. 281-324.
- Kolodny, Y., 1969, Petrology of siliceous rocks in the Mishash Formation (Negev, Israel): *Journal of Sedimentary Petrology*, v. 39, p. 165-175.
- Kozur, H. W., 1998, Some aspects of the Permian-Triassic boundary (PTB) and of the possible causes for the biotic crisis around this boundary: *Palaeogeography, Palaeoclimatology, Palaeoecology*, v. 143, p. 227-272.
- Larssen, G., G. Elvebakk, L. B. Henriksen, S. Kristensen, I. Nilsson, T. Samuelsberg, T. Svånå, L. Stemmerik, and D. Worsley, 2002, Upper Palaeozoic lithostratigraphy of the Southern Norwegian Barents Sea: *Norwegian Petroleum Directorate Bulletin*, v. 9, p. 76.
- Larssen, G. B., G. Elvebakk, L. B. Henriksen, S.-E. Kristensen, I. Nilsson, T. J. Samuelsberg, T. A. Svånå, L. Stemmerik, and D. Worsley, 2005, Upper Palaeozoic lithostratigraphy of the southern part of the Norwegian Barents Sea: *Norges Geologiske Undersøkelse Bulletin*, v. 444, p. 3-45.
- Lauritzen, Ø., 1981, Investigations of Carboniferous and Permian sediments in Svalbard, v. 176.
- Lucia, F. J., 1999, Carbonate reservoir characterization: Berlin, Springer.

- Lucia, F. J., and R. P. Major, 1994, Porosity evolution through hypersaline reflux dolomitization, *in* B. H. Purser, M. E. Tucker, and D. H. Zenger, eds., *Dolomites : A Volume in Honour of Dolomieu. Spec. Publ.-Int. Assoc. Sedimentol*, v. 21: Cambridge, Blackwell Scientific Publications, p. 325-341.
- Maher, H. D., and A. Braathen, 2011, Løvehovden fault and Billefjorden rift basin segmentation and development, Spitsbergen, Norway: *Geol. Mag.*, v. 148, p. 154-170.
- Malkowski, K., 1982, Development and stratigraphy of the Kapp Starostin Formation (Permian) of Spitsbergen: *Palaeontologia Polonica*, v. 43, p. 69-81.
- Malkowski, K., and A. Hoffman, 1979, Semi-quantitative facies model for the Kapp Starostin Formation <Permian>, Spitsbergen.
- Mangerud, G., 1994, Palynostratigraphy of the Permian and lowermost triassic succession, Finnmark Platform, Barents sea: Review of Palaeobotany and Palynology, v. 82, p. 317-349.
- Mangerud, G., and R. M. Konieczny, 1993, Palynology of the Permian succession of Spitsbergen, Svalbard: *Polar Research*, v. 12, p. 65-93.
- Miall, A. D., 2010, *The Geology of Stratigraphic Sequences*: Dordrecht, Springer.
- Mørk, A., G. Elvebakk, A. W. Forsberg, M. W. Hounslow, H. A. Nakrem, J. O. Vigran, and W. Weitschat, 1999, The type section of the Vikinghøgda Formation: a new Lower Triassic unit in central and eastern Svalbard: *Polar Research*, v. 18, p. 51-82.
- Mørk, A., A. F. Embry, and W. Weitschat, 1989, Triassic transgressive-regressive cycles in the Sverdrup Basin, Svalbard and the Barents Shelf, *in* J. D. Collinson, ed., *Correlation in hydrocarbon exploration : proceedings of the conference Correlation in Hydrocarbon Exploration organized by the Norwegian Petroleum Society and held in Bergen, Norway, 3-5 October 1988*: London, Graham & Trotman for the Norwegian Petroleum Society, p. 113-130.
- Mork, M. B. E., 1999, Compositional variations and provenance of Triassic sandstones from the Barents Shelf: *Journal of Sedimentary Research*, v. 69, p. 690-710.
- Nakamura, K., G. Kimura, and T. S. Winsnes, 1987, Brachiopod zonation and age of the Permian Kapp Starostin Formation (Central Spitsbergen: *Polar Research*, v. 5, p. 207-219.
- Nakrem, H. A., 1988, Permian bryozoans from southern Spitsbergen and Bjørnøya. A review of bryozoans described by J. Malecki (1968, 1977: *Polar Research*, v. 6, p. 113-121.
- Nakrem, H. A., 1991, Conodonts from the Permian succession of Bjørnøya (Svalbard): *Norsk geologisk tidsskrift*.
- Nakrem, H. A., 1994, Bryozoans from the Lower Permian Vøringen Member (Kapp Starostin Formation), Spitsbergen, Svalbard.
- Nakrem, H. A., I. Nilsson, and G. Mangerud, 1992, Permian biostratigraphy of Svalbard (Arctic Norway) A review: *International Geology Review*, v. 34, p. 933-959.
- Nilsson, I., 1988, Carboniferous - permian fusulinids on the Nordfjorden block, Spitsbergen (Svalbard), Oslo, I. Nilsson.
- Nilsson, I., 1993, Upper Palaeozoic fusulinid stratigraphy of the Barents Shelf and surrounding areas : dissertation for the degree of doctor scientiarum, University of Tromsø, Tromsø.
- Nordenskiöld, A. E., 1863, Geografisk och geognostisk beskrifning öfver nordöstra delarne af Spetsbergen och Hinlopen Strait, v. Ny följd 4(7), Kungl. svenska vetenskapsakademien, 25 p.

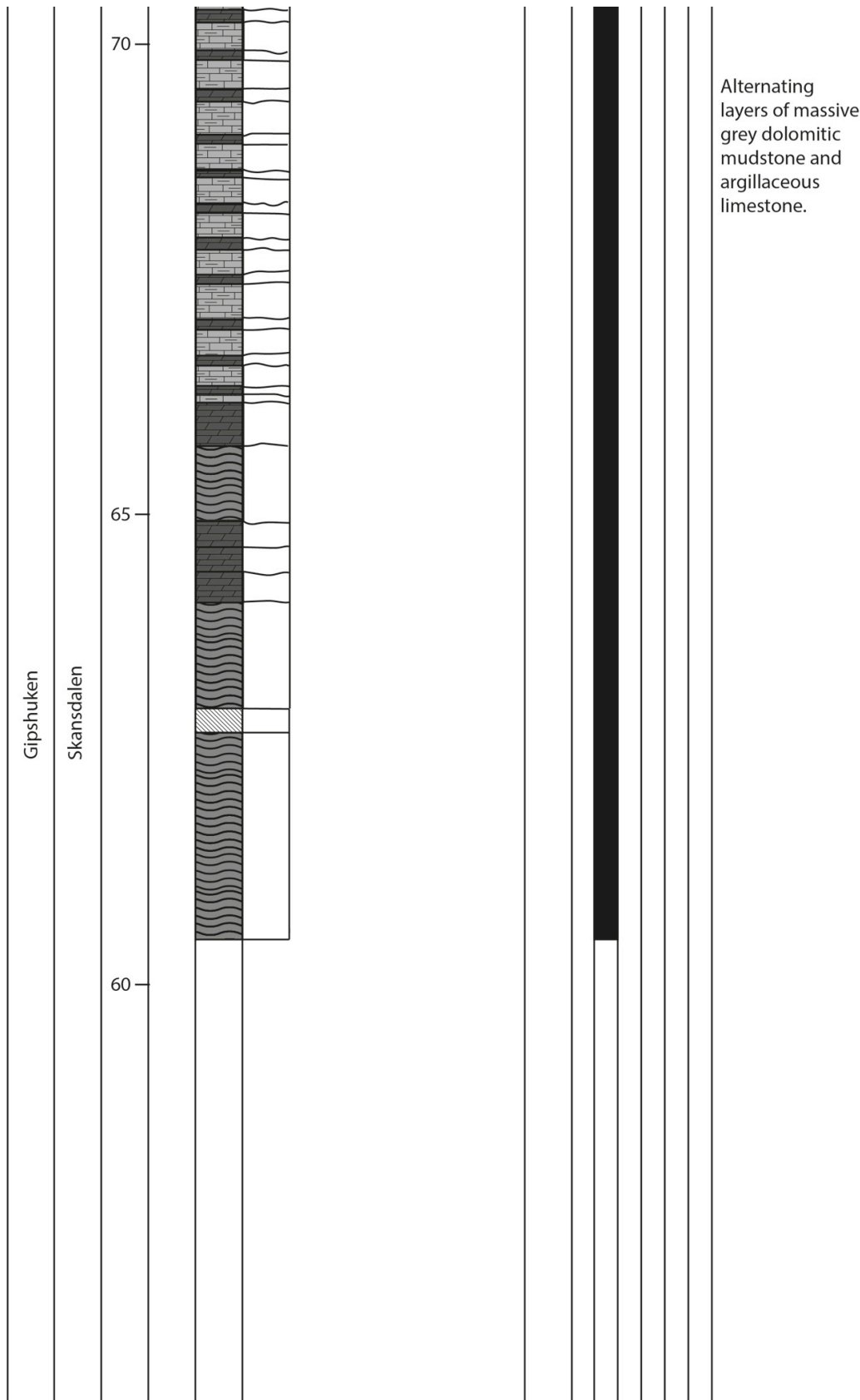
- Nøttvedt, A., F. Livbjerg, P. S. Midbøe, and E. Rasmussen, 1993, Hydrocarbon potential of the Central Spitsbergen Basin, v. 2, 333-361 p.
- Odin, G. S., and A. Matter, 1981, De glauconiarum origine: *Sedimentology*, v. 28, p. 611-641.
- Pettijohn, F. J., P. E. Potter, and R. Siever, 1972, *Sand and sandstone*: Berlin, Springer.
- Piasecki, S., 1984, Preliminary palynostratigraphy of the Permian-Lower Triassic sediments in Jameson Land and Scoresby Land, east Greenland: *Bulletin of the Geological Society of Denmark*, v. 32, p. 139-144.
- Ramaker, E. M., R. H. Goldstein, E. K. Franseen, and W. L. Watney, 2014, What controls porosity in cherty fine-grained carbonate reservoir rocks? Impact of stratigraphy, unconformities, structural setting and hydrothermal fluid flow: Mississippian, SE Kansas: Geological Society, London, Special Publications, p. SP406.2.
- Reichow, M. K., A. D. Saunders, R. V. White, M. S. Pringle, A. I. Medvedev, and N. P. Kirda, 2002, 40 Ar/ 39 Ar Dates from the West Siberian Basin: Siberian Flood Basalt Province Doubled: *Science*, v. 296, p. 1846-1849.
- Reid, C. M., N. P. James, B. Beauchamp, and T. K. Kyser, 2007, Faunal turnover and changing oceanography: Late Palaeozoic warm-to-cool water carbonates, Sverdrup Basin, Canadian Arctic Archipelago: *Palaeogeography, Palaeoclimatology, Palaeoecology*, v. 249, p. 128-159.
- Renne, P. R., Z. Zichao, M. A. Richards, M. T. Black, and A. R. Basu, 1995, Synchrony and Causal Relations Between Permian-Triassic Boundary Crises and Siberian Flood Volcanism: *Science*, v. 269, p. 1413-1416.
- Samuelsberg, T. J., G. Elvebakk, and L. Stemmerik, 2003, Late Palaeozoic evolution of the Finnmark Platform, southern Norwegian Barents Sea: *Norsk Geologisk Tidsskrift*, v. 83, p. 351-362.
- Samuelsberg, T. J., and N. A. H. Pickard, 1999, Upper Carboniferous to Lower Permian transgressive-regressive sequences of central Spitsbergen, Arctic Norway: *Geological Journal*, v. 34, p. 393-411.
- Scholle, P. A., and D. S. Ulmer-Scholle, 2003, *A Color guide to the petrography of carbonate rocks : grains, textures, porosity, diagenesis*: AAPG memoir, v. 77: Tulsa, Okla, American Association of Petroleum Geologists.
- Scotese, C. R., and W. S. McKerrow, 1990, Revised World maps and introduction: Geological Society, London, *Memoirs*, v. 12, p. 1-21.
- Siedlecka, A., 1970, Investigations of Permian cherts and associated rocks in southern Spitsbergen: *Skrifter (Norsk polarinstitutt)*, Oslo, Norsk polarinstitutt.
- Smelror, M., V. A. Basov, and u. Norges geologiske, 2009, *Atlas : geological history of the Barents Sea*: Trondheim, Geological Survey of Norway.
- Stanley, S. M., 1984, Temperature and biotic crises in the marine realm: *Geology*, v. 12, p. 205-7613-12-4-205-5435.
- Steel, R. J., and D. Worsley, 1984, Svalbard's post-Caledonian strata - an atlas of sedimentational patterns and palaeographic evolution, *in* A. M. S. e. al, ed., *Petroleum Geology of the North European Margin*, Norwegian Petroleum Society (Graham & Trotman), p. 109-135.
- Stemmerik, L., 1988, Discussion. Brachiopod zonation and age of the Permian Kapp Starostin Formation (Central Spitsbergen: *Polar Research*, v. 6, p. 179-180.
- Stemmerik, L., 1996, High frequency sequence stratigraphy of a siliciclastic influenced carbonate platform, lower Moscovian, Amdrup Land, North Greenland: Geological Society, London, Special Publications, v. 104, p. 347-365.

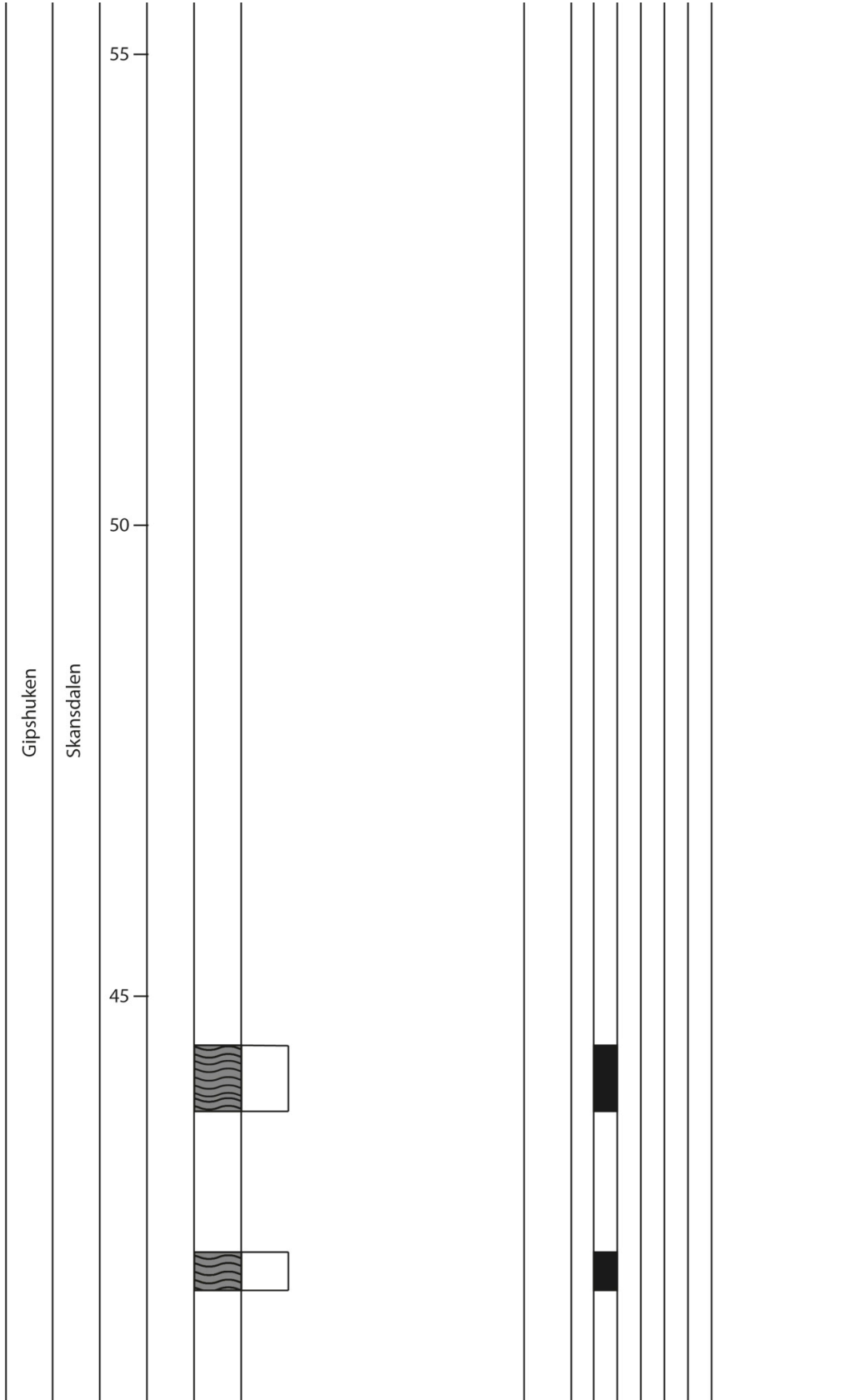
- Stemmerik, L., 1997, Permian (Artinskian-Kazanian) cool-water carbonates in North Greenland, Svalbard and the western Barents Sea, *in* N. P. James, and J. A. D. Clarke, eds., *Cool-Water Carbonates*, v. 56, p. 349--364.
- Stemmerik, L., G. L. Elvebakk, and D. L. Worsley, 1999, Upper Palaeozoic carbonate reservoirs on the Norwegian arctic shelf; delineation of reservoir models with application to the Loppa High: *Petroleum geoscience*, v. 5, p. 173-187.
- Stemmerik, L., I. Nilsson, and G. Elvebakk, 1995, Gzelian-Asselian depositional sequences in the western Barents Sea and North Greenland: *Norwegian Petroleum Society Special Publications*, v. 5, p. 529-544.
- Stemmerik, L., J. Os Vigran, and S. Plasecki, 1991, Dating of late Paleozoic rifting events in the North Atlantic: new biostratigraphic data from the uppermost Devonian and Carboniferous of east Greenland: *Geology*, v. 19, p. 218.
- Stemmerik, L., and D. Worsley, 1989, Late Palaeozoic sequence correlations, North Greenland, Svalbard and the Barents Shelf, *Correlation in hydrocarbon exploration*, Springer, p. 99-111.
- Stemmerik, L., and D. D. Worsley, 2005, 30 years on - Arctic Upper Palaeozoic stratigraphy, depositional evolution and hydrocarbon prospectivity: *Norwegian Journal of Geology*, v. 85, p. 151-186.
- Stemmerik, L. L., 2000, Late Palaeozoic evolution of the North Atlantic margin of Pangea: *Palaeogeography, palaeoclimatology, palaeoecology*, v. 161, p. 95-126.
- Stevens, C. H., 1977, Was development of brackish oceans a factor in Permian extinctions?: *Geological Society of America Bulletin*, v. 88, p. 133-7606-88-1-133-17289.
- Surlyk, F., 1997, A cool-water carbonate ramp with bryozoan mounds: Late Cretaceous-Danian of the Danish Basin, *in* J. A. D. Clarke, ed., *Cool-water carbonates*, v. 56, SEPM Special Publication, p. 293-307.
- Surlyk, F., S. Kolbye Jensen, and M. Engkilde, 2008, Deep channels in the Cenomanian-Danian Chalk Group of the German North Sea sector: Evidence of strong constructional and erosional bottom currents and effect on reservoir quality distribution: *AAPG Bulletin*, v. 92, p. 1565-1586.
- Suter, J. R., 2006, Clastic shelves, *in* H. W. Posamentier, and G. Roger, eds., *Facies models revisited*, v. 84, SEPM Society for Sedimentary Geology.
- Torsvik, T. H., D. Carlos, J. Mosar, L. R. M. Cocks, and T. Malme, 2002, Global reconstructions and North Atlantic paleogeography 440 Ma to Recent, *in* E. A. Eide, ed., *BATLAS – Mid Norway plate reconstructions atlas with global and Atlantic perspectives*: Trondheim, Geological Survey of Norway, p. 18-39.
- Tucker, M. E., V. P. Wright, and J. A. D. Dickson, 1990, *Carbonate sedimentology*, Chichester, Wiley.
- Warren, J., 2000, Dolomite: occurrence, evolution and economically important associations: *Earth Science Reviews*, v. 52, p. 1-81.
- Watney, W. L., J. G. Willard, and A. P. Byrnes, 2001, Characterization of the Mississippian chat in south-central Kansas: *AAPG Bulletin*, v. 85.
- Wignall, P. B., and A. Hallam, 1992, Anoxia as a cause of the Permian/Triassic mass extinction: facies evidence from northern Italy and the western United States: *Palaeogeography, Palaeoclimatology, Palaeoecology*, v. 93, p. 21-46.
- Wignall, P. B., R. Morante, and R. Newton, 1998, The Permo-Triassic transition in Spitsbergen: 13 C org chemostratigraphy, Fe and S geochemistry, facies, fauna and trace fossils: *Geol. Mag.*, v. 135, p. 47-62.

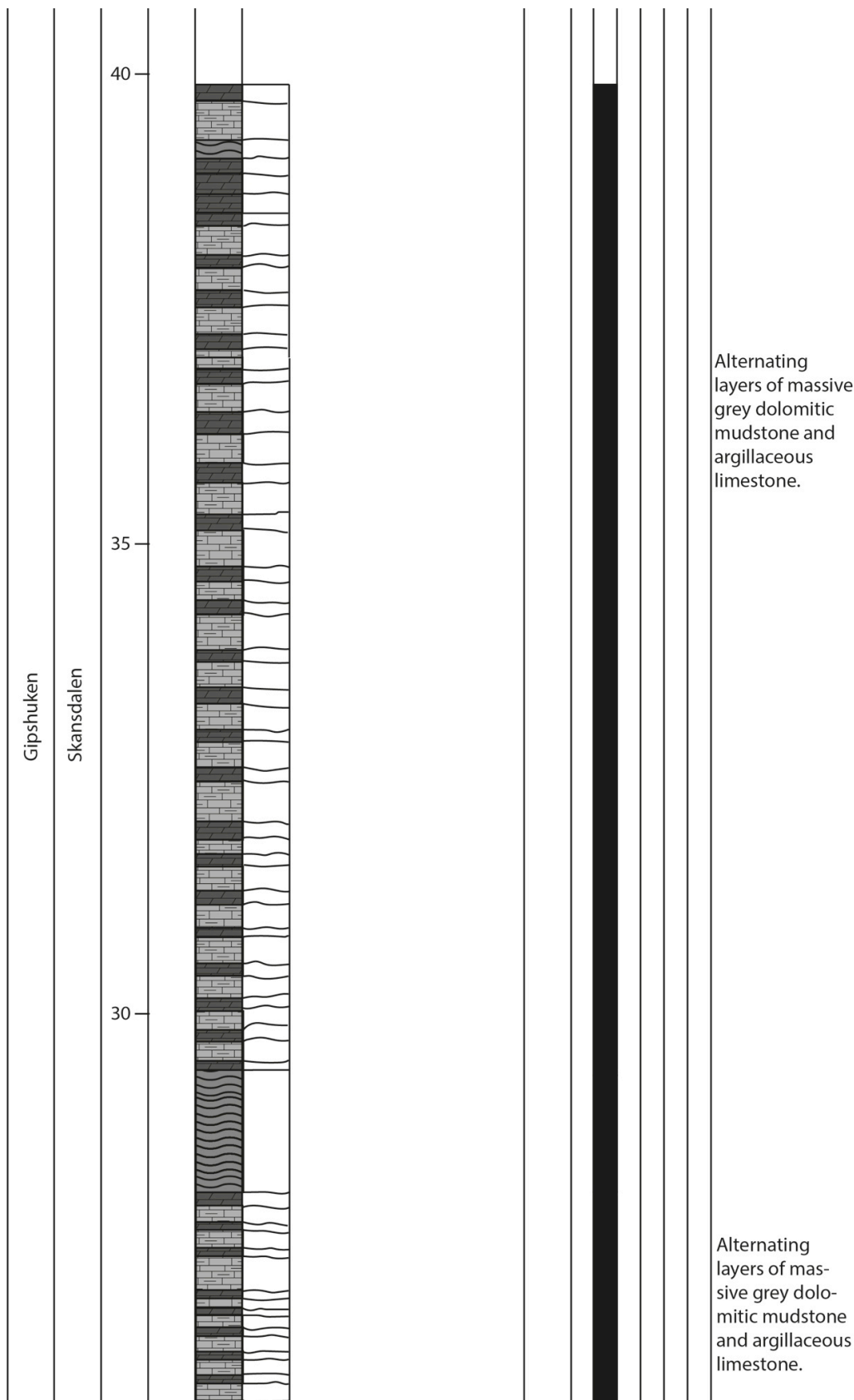
- Wignall, P. B., and R. Newton, 2003, Contrasting Deep-water Records from the Upper Permian and Lower Triassic of South Tibet and British Columbia: Evidence for a Diachronous Mass Extinction, p. r Permian and Lower Triassic of South Tibet and British Columbia: Evidence for a Diachronous Mass Extinction. *Palaios*, 18 (2). pp. 153-167. ISSN 0883-1351.
- Wignall, P. B., and R. J. Twitchett, 1996, Oceanic Anoxia and the End Permian Mass Extinction: *Science*, v. 272, p. 1155-1158.
- Worsley, D., 2008, The post - Caledonian development of Svalbard and the western Barents Sea: *Polar Research*, v. 27, p. 298-317.
- Worsley, D., O. J. Aga, A. Dalland, A. Elverhøi, and A. Thon, 1986, The geological history of Svalbard : evolution of an arctic archipelago: Stavanger, Den norske stats oljeselskap a.s., 121 p.
- Worsley, D., T. Agdestein, J. G. Gjelberg, K. Kirkemo, A. Mork, I. Nilsson, S. Olaussen, R. J. Steel, and L. Stemmerik, 2001a, The geological evolution of Bjornoya, Arctic Norway; implications for the Barents Shelf: *Norsk Geologisk Tidsskrift*, v. 81, p. 195-234.
- Worsley, D., T. Agdestein, J. G. Gjelberg, K. Kirkemo, A. Mørk, I. Nilsson, S. Olaussen, R. J. Steel, and L. Stemmerik, 2001b, The geological evolution of Bjørnøya, Arctic Norway: implications for the Barents Shelf: *Norsk geologisk tidsskrift*, v. 81, p. 195-234.
- Worsley, D., and A. Nøttvedt, 2008, Carboniferous and Permian in the North; 359–251 Million years ago, *in* I. B. Ramberg, ed., *The Making of a land : geology of Norway: Trondheim*, The Norwegian Geological Association, p. 304-329.

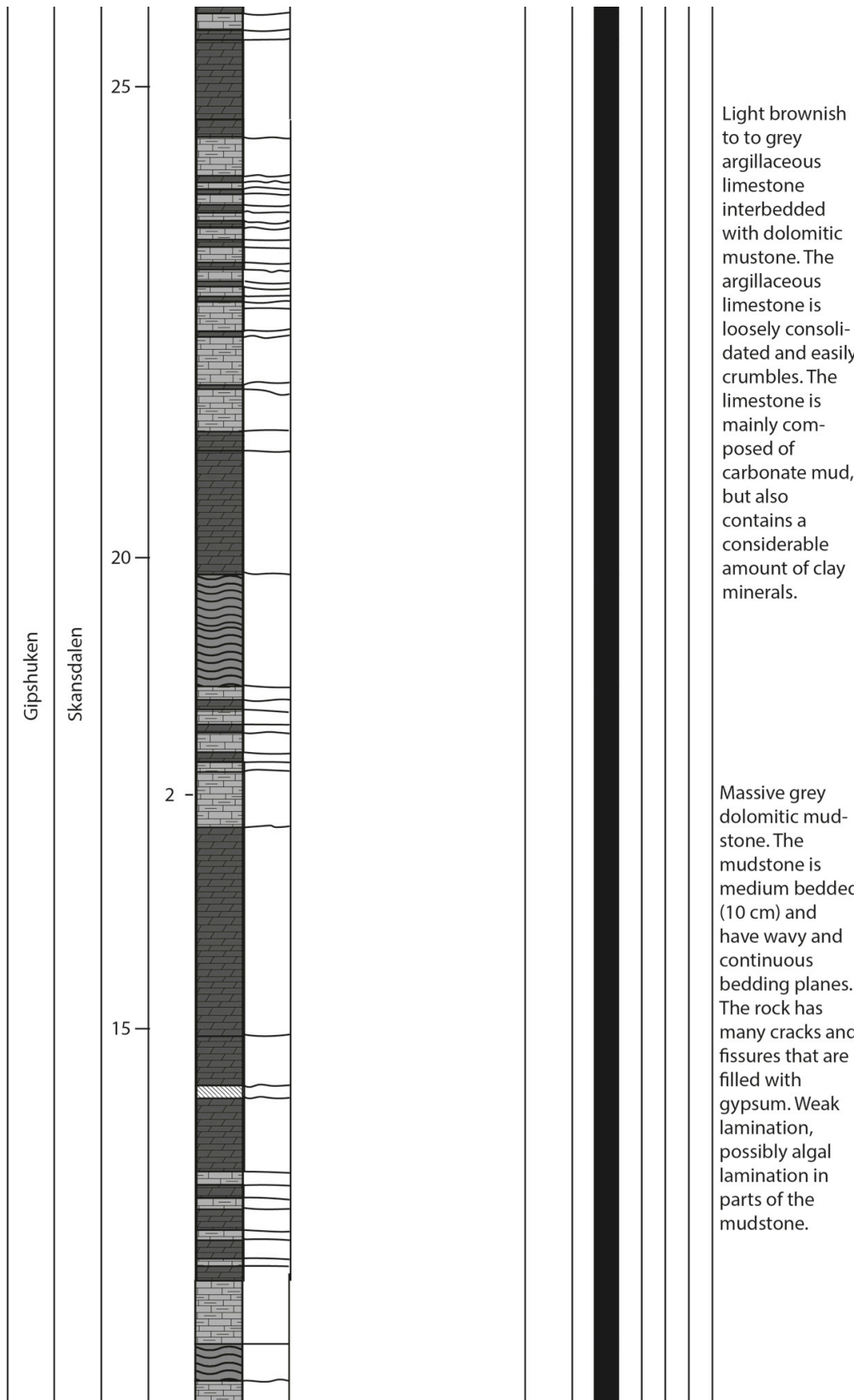
UTM E509900 N8727080

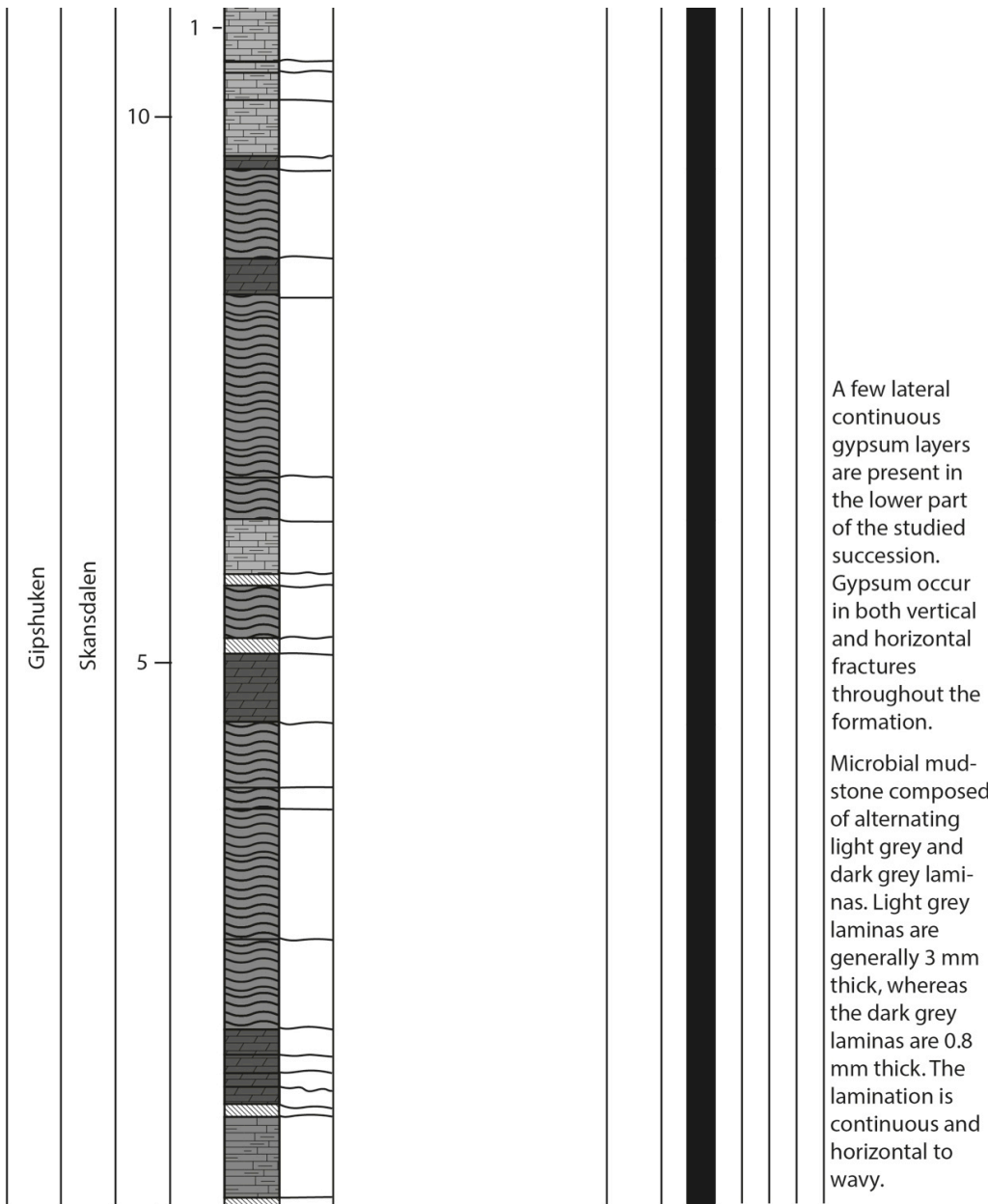
118







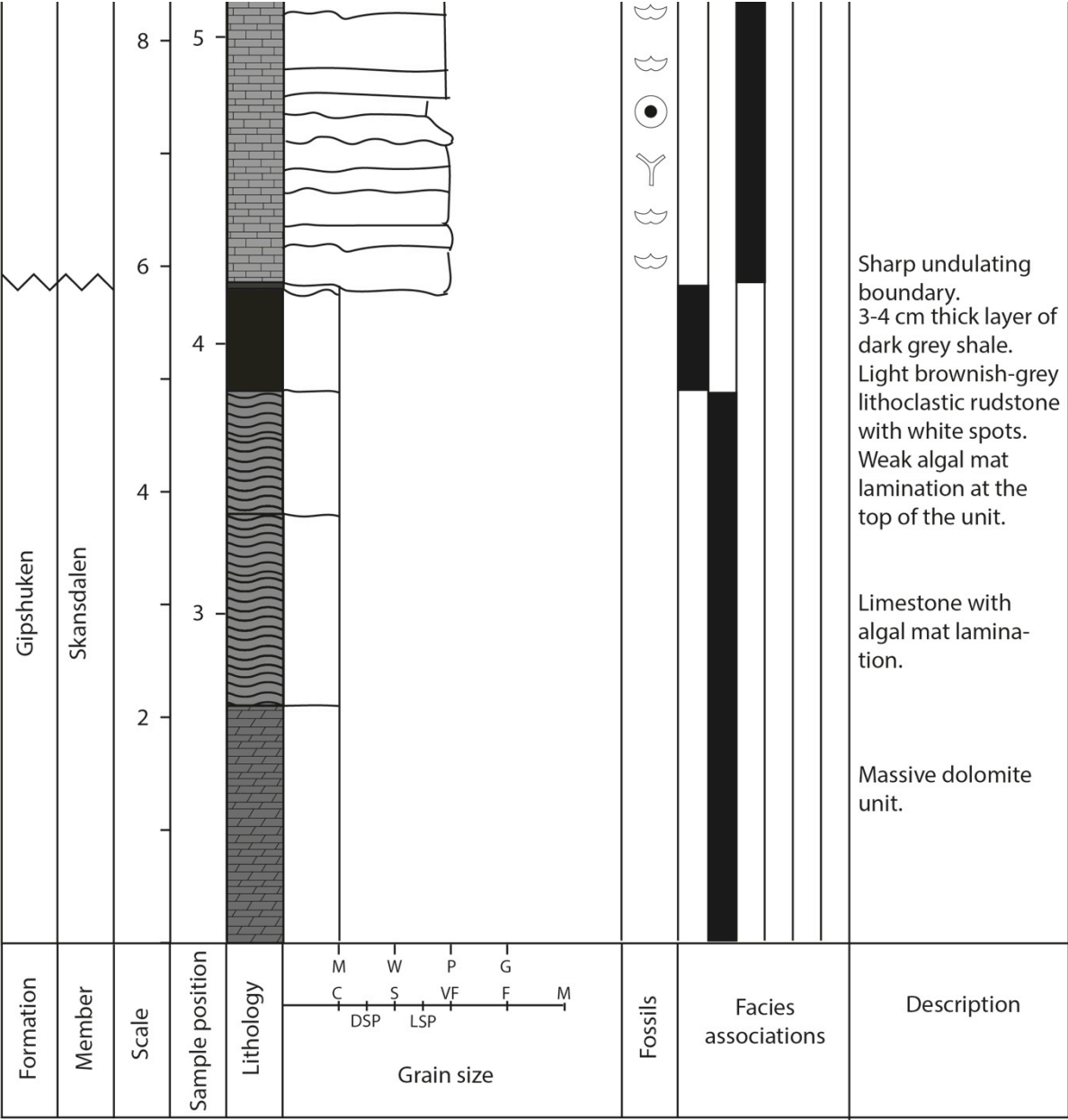




Section B

UTM 33X E507430 N8725080

Formation	Member	Scale	Sample position	Lithology	Grain size	Fossils	Facies associations						Description
							1	2	3	4	5	6	
Kapp Starostin	Vøringen	20											Grey bioclastic limestones with a fossil assemblage dominated by brachiopods. Bryozoans and crinoids are also present. Many beds have erosive lower boundaries and are normal graded. The limestones are highly silicified and contain dark grey silica nodules. Yellowish-beige weathering colour.
Kapp Starostin	Vøringen	18											Grey bioclastic limestones with a fossil assemblage dominated by brachiopods. Bryozoans and crinoids are also present. Many beds have erosive lower boundaries and are normal graded. The limestones are highly silicified and contain dark grey silica nodules. Yellowish-beige weathering colour.
Kapp Starostin	Vøringen	16											Grey bioclastic limestones with a fossil assemblage dominated by brachiopods. Bryozoans and crinoids are also present. Many beds have erosive lower boundaries and are normal graded. The limestones are highly silicified and contain dark grey silica nodules. Yellowish-beige weathering colour.
Kapp Starostin	Vøringen	14											Grey bioclastic limestones with a fossil assemblage dominated by brachiopods. Bryozoans and crinoids are also present. Many beds have erosive lower boundaries and are normal graded. The limestones are highly silicified and contain dark grey silica nodules. Yellowish-beige weathering colour.
Kapp Starostin	Vøringen	12											Grey bioclastic limestones with a fossil assemblage dominated by brachiopods. Bryozoans and crinoids are also present. Many beds have erosive lower boundaries and are normal graded. The limestones are highly silicified and contain dark grey silica nodules. Yellowish-beige weathering colour.
Kapp Starostin	Vøringen	10											Grey bioclastic limestones with a fossil assemblage dominated by brachiopods. Bryozoans and crinoids are also present. Many beds have erosive lower boundaries and are normal graded. The limestones are highly silicified and contain dark grey silica nodules. Yellowish-beige weathering colour.



Section C

UTM 33X E510240 N8727180

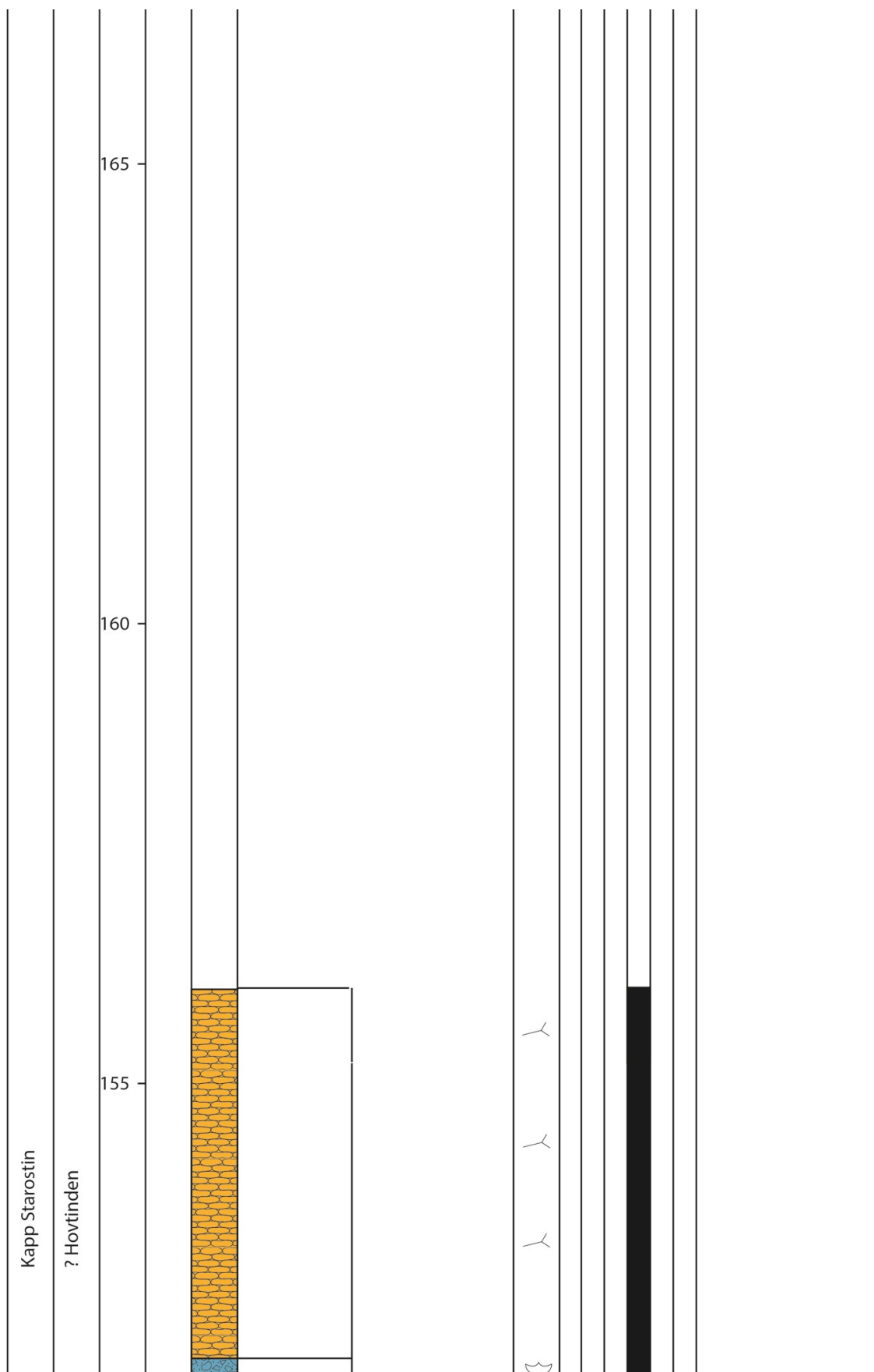
Formation	Member	Scale	Sample position	Lithology	Grain size	Fossils	Facies associations	Description
							1 2 3 4 5 6	
Kapp Starostin	Vøringen	6 7 8	8 7 4 2					<p>Grey bioclastic limestone with yellowish-beige weathering colour. The fossil assemblage is dominated by thick-shelled brachiopods. Many beds are normal graded and have erosive lower boundaries. Rare cross-bedding with skeletal fragments aligned on the bedding planes. Some dark grey silica concretions.</p>
Formation	Member	Scale	Sample position	Lithology	Grain size	Fossils	Facies associations	Description

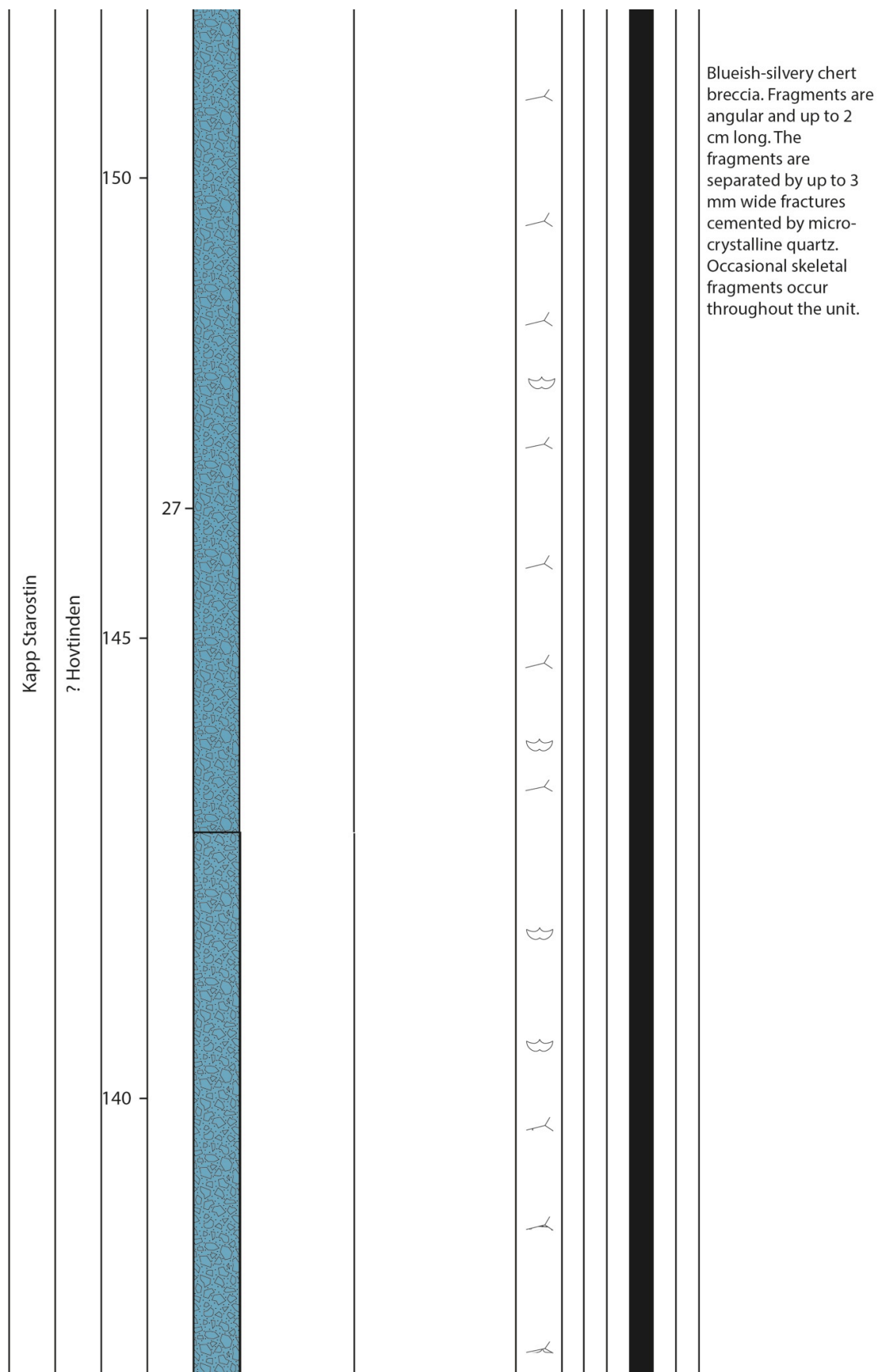
Section D-D'

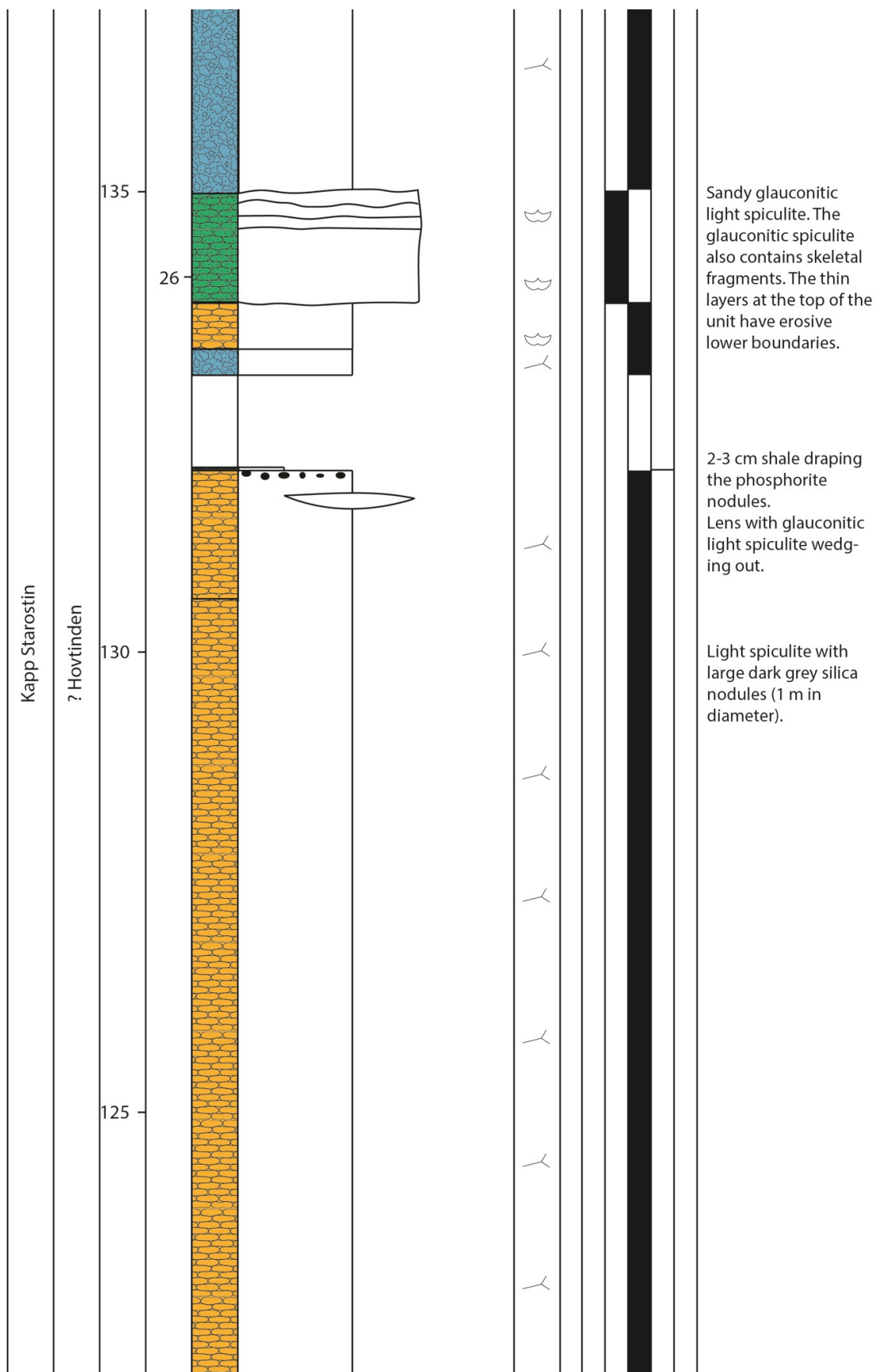
Start: UTM 33X E509620 N8726540

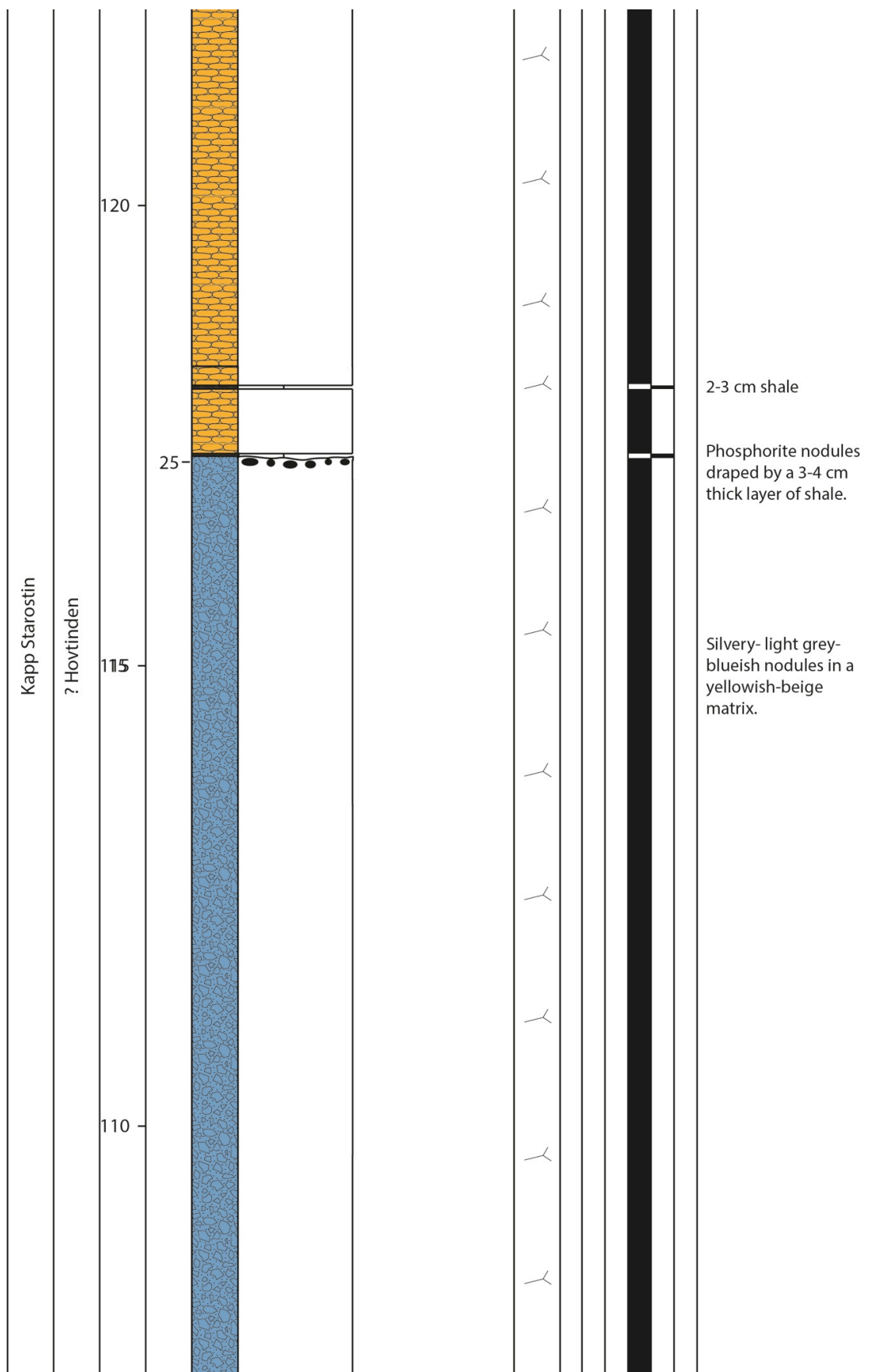
End: UTM 33X E510200 N8726040

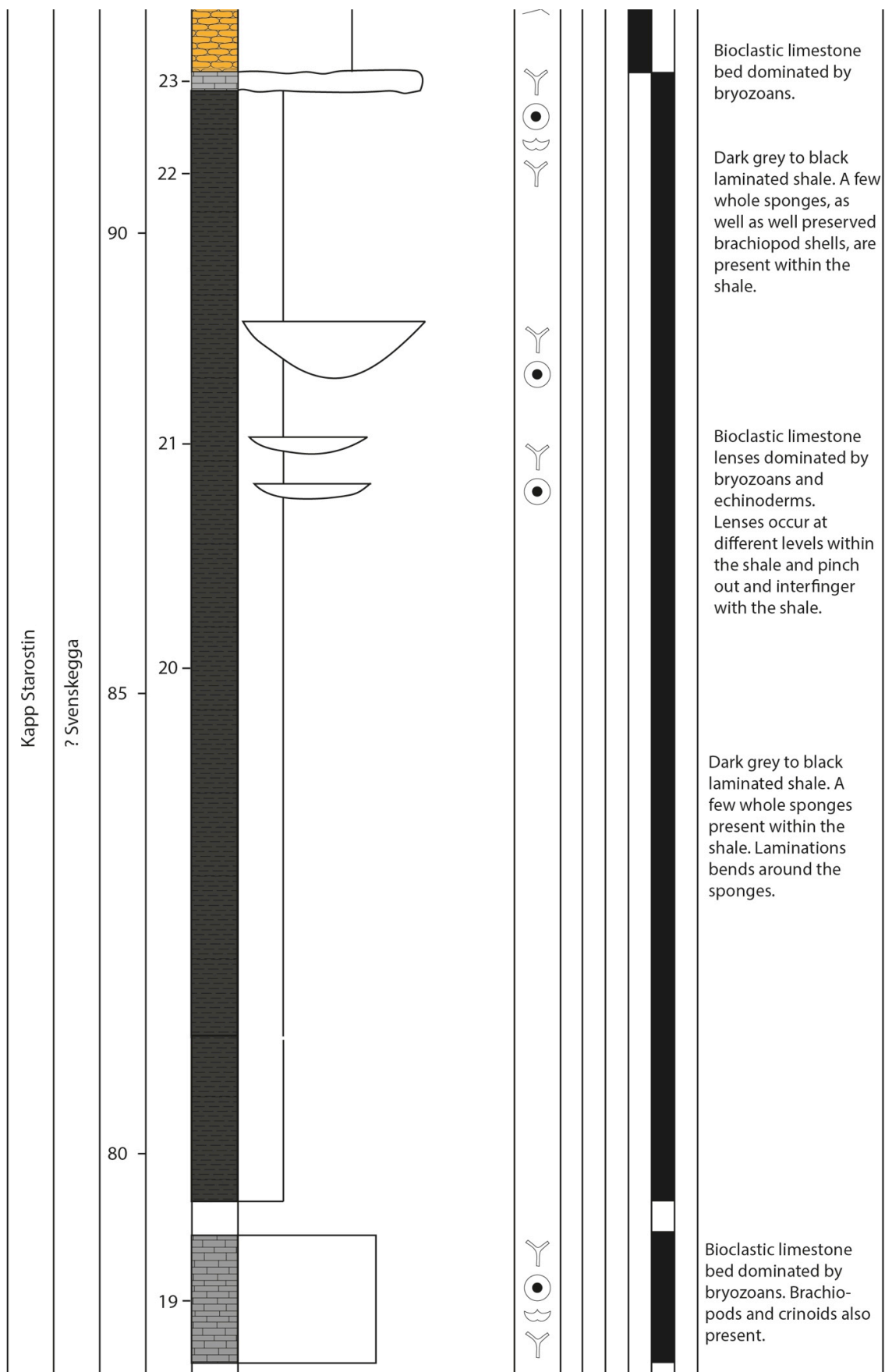
Formation	Member	Scale	Samples	Lithology	Grain size		Fossils	Facies associations	Description
					C	S			
Kapp Starostin	? Hovtinden	175	29	[Orange pattern]	DSP	LSP	[Fossil symbols]	[Facies patterns]	Light nodular spiculite with dark grey silica nodules.
					M	W			
Kapp Starostin	? Hovtinden	170	28	[Orange pattern]	P	G	[Fossil symbols]	[Facies patterns]	<p>Glaucopitic nodular dark spiculite.</p> <p>Light nodular spiculite with dark grey silica nodules.</p> <p>Glaucopitic nodular dark spiculite.</p> <p>Light nodular spiculite with dark grey silica nodules.</p>

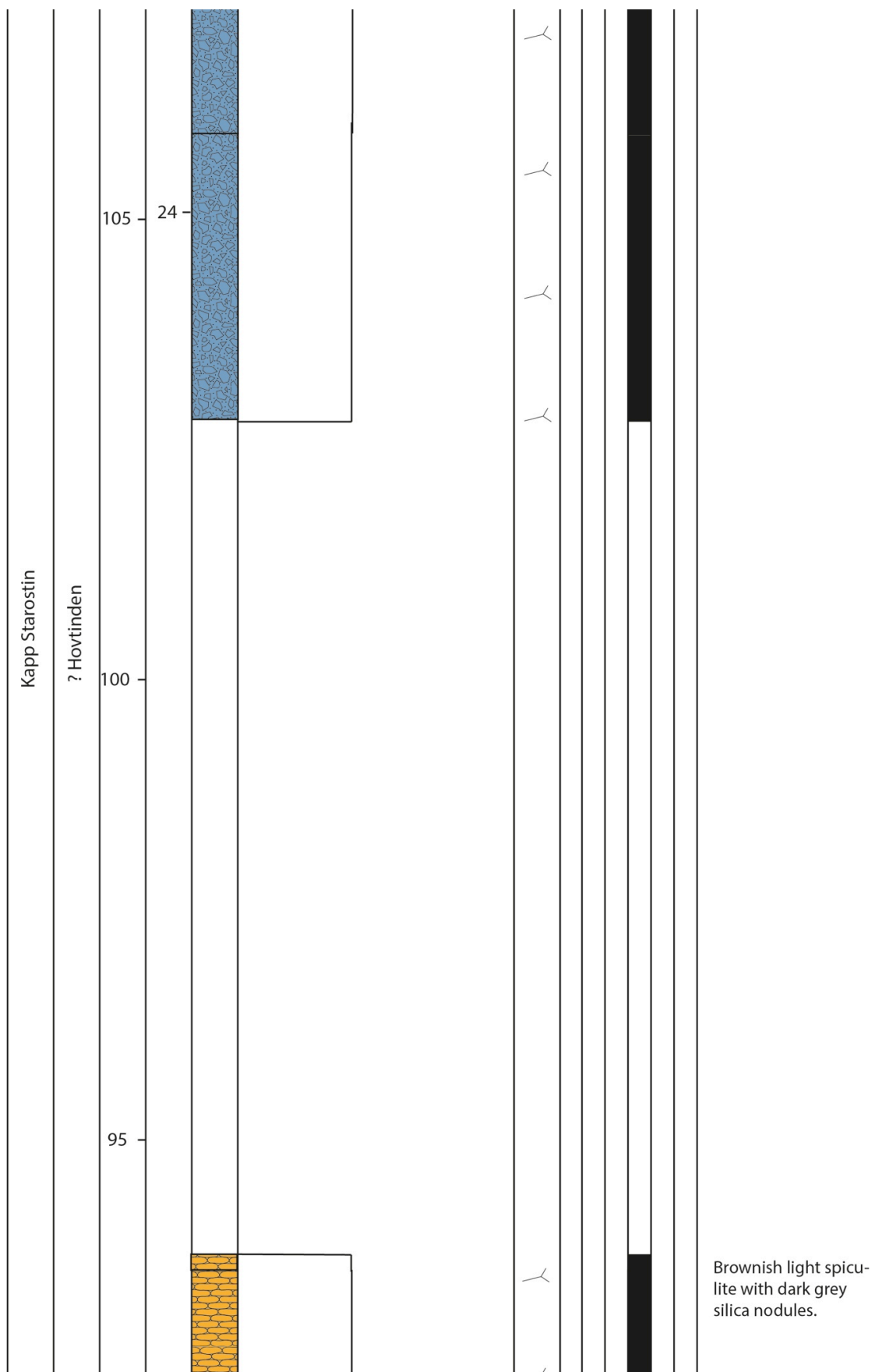


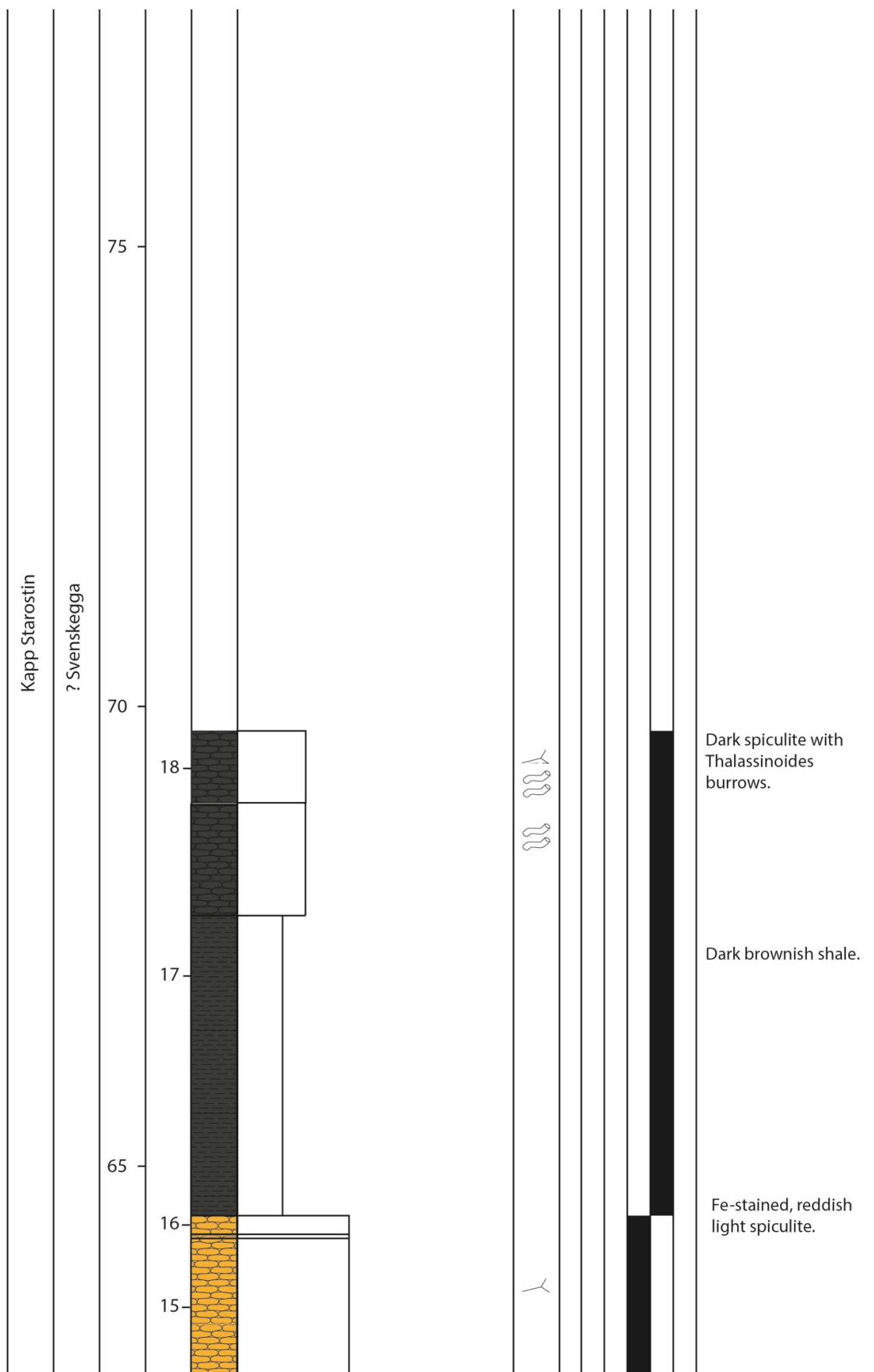


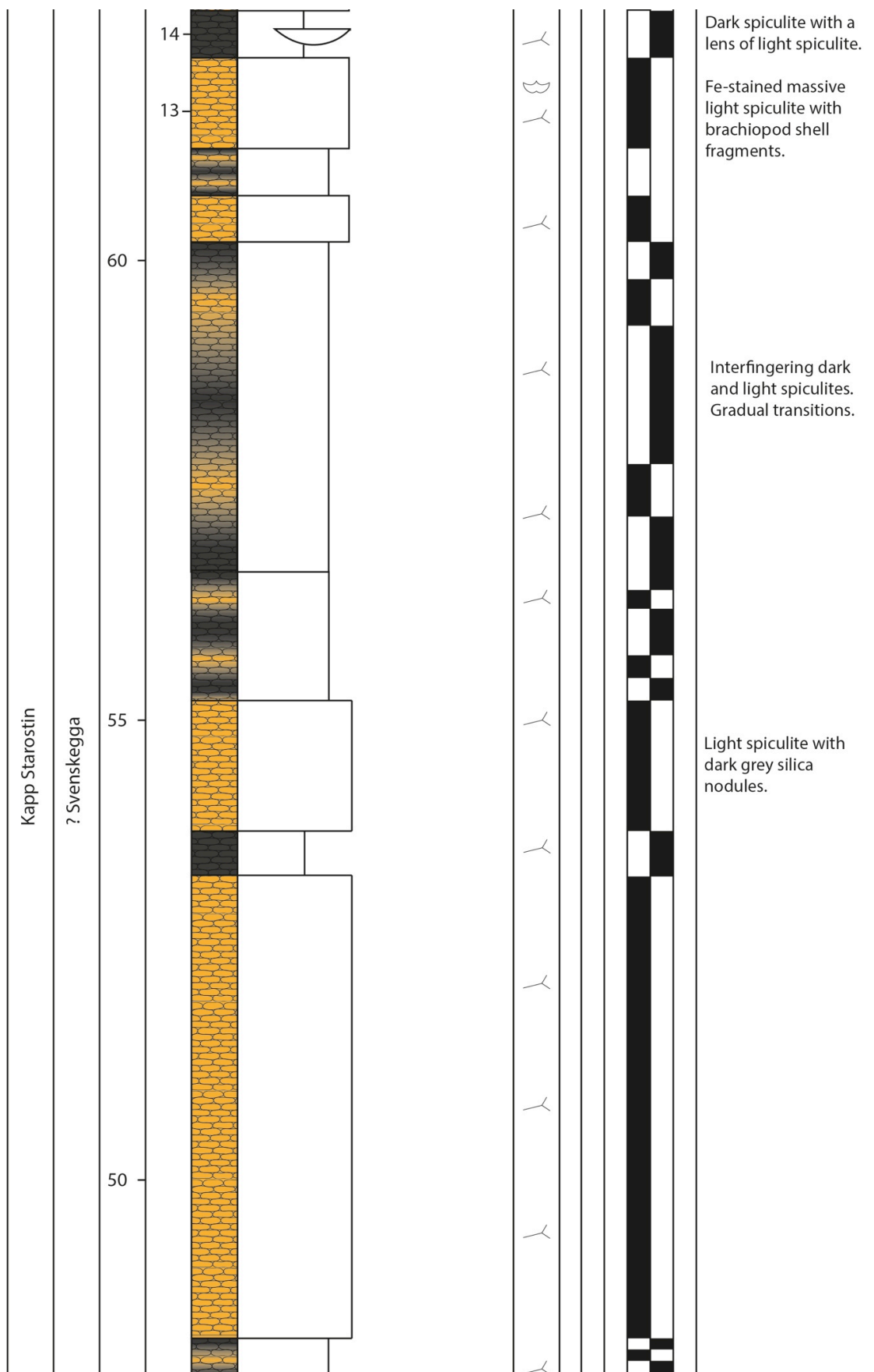




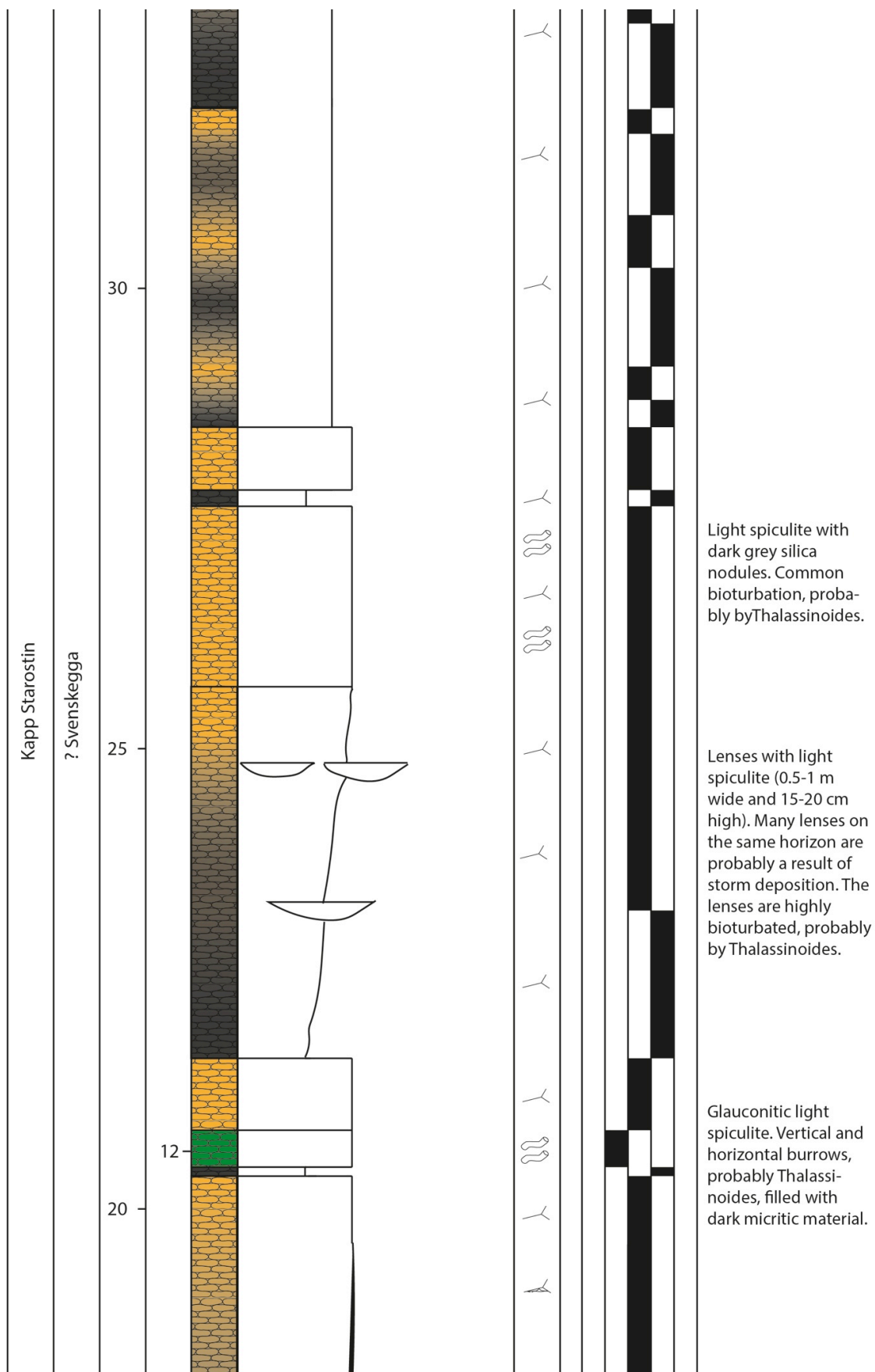


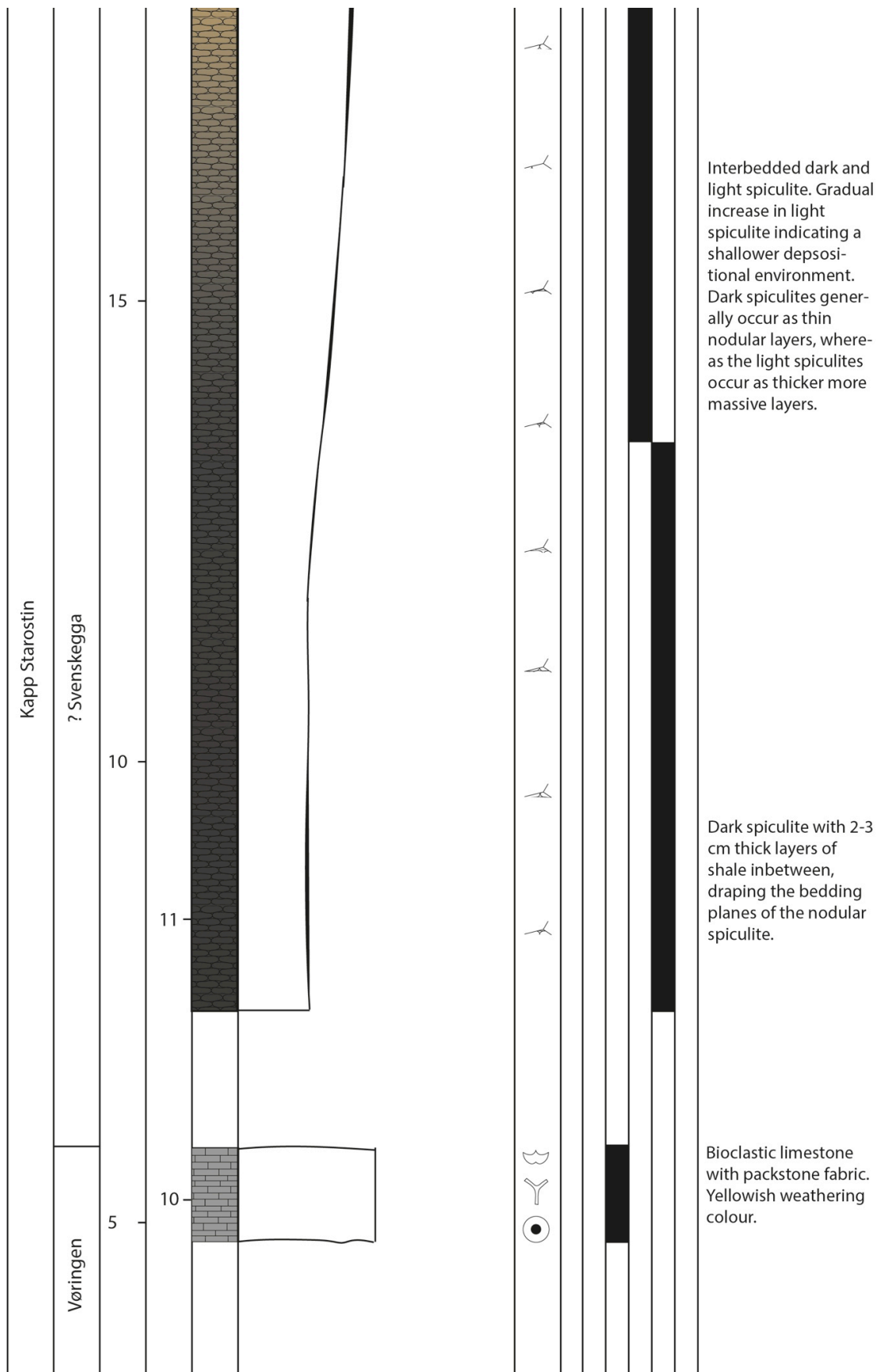


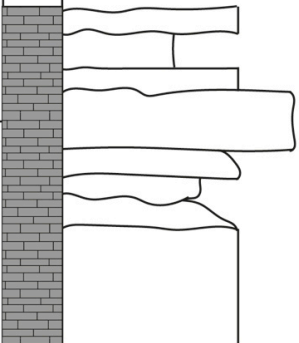
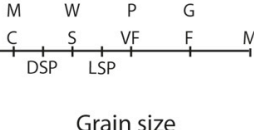
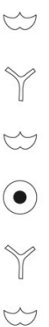







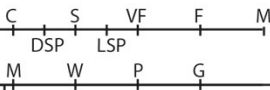
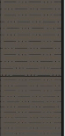


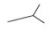


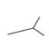




Kapp Starostin	Vøringen		9					Bioclastic limestone beds with a heterozoan fossil assemblage. Brachiopods dominate. Lower boundaries are often erosive. Some beds are normal graded. The limestones are strongly silicified and contain dark grey silica nodules. Yellowish-beige weathering colour.
Formation	Member	Scale	Sample position	Lithology	Grain size	Fossils	Facies associations	Description

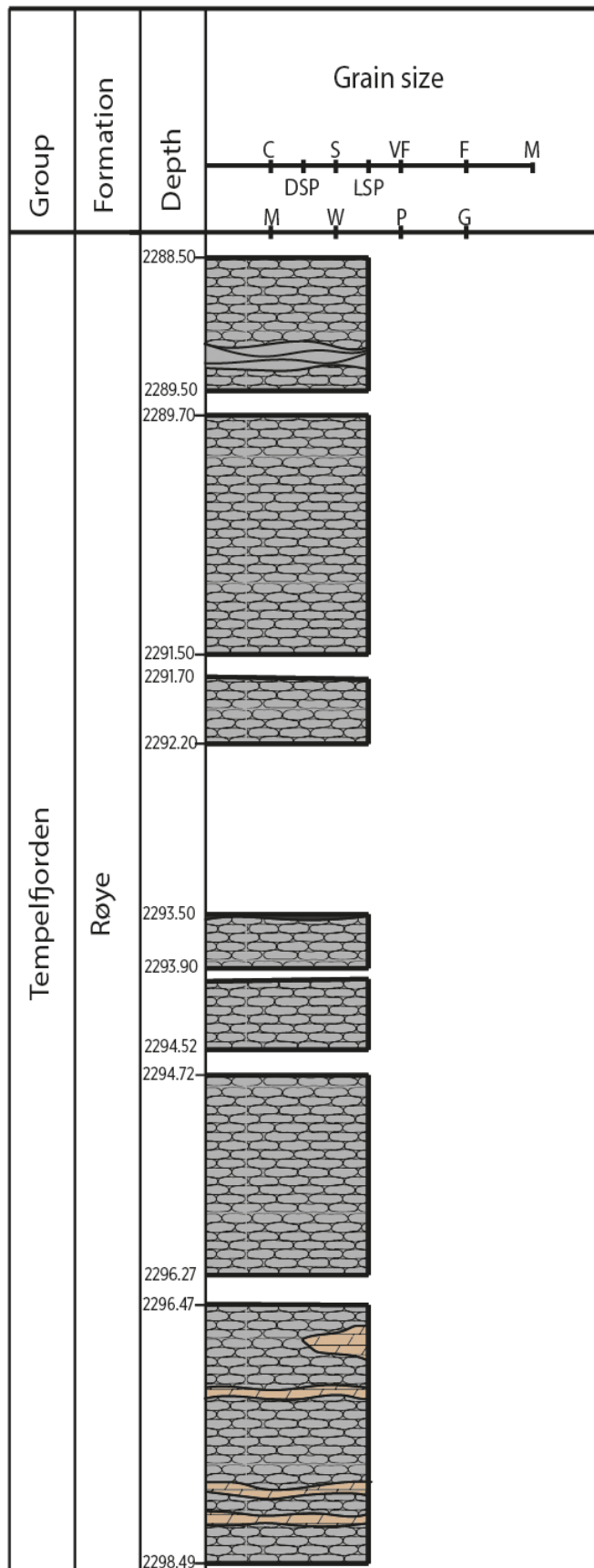
Section E

UTM 33X E510020 N8724120

Formation	Member	Scale	Samples	Lithology	Grain size	Fossils	Facies association	Description
							1 2 3 4 5 6	
Vikingshøgda	Deltadalen	8	33					Brownish-grey shaly siltstone.
Kapp Starostin	Hovtinden	6	32					Sharp contact marking the Permian-Triassic boundary.
		4	31					Glauconitic green sandstone.
		2	30					Light spiculite interfingering with glauconitic sandstone. Lenses with shale inbetween.
								Light spiculite.

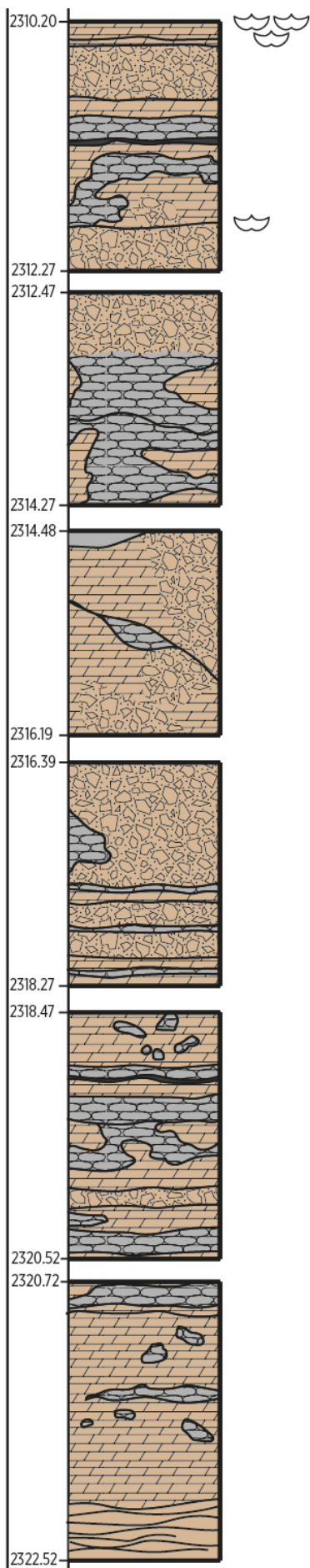
Gothta core section, Well 7120/1-3

Depth: 2288.50 m - 2345.15 m



Tempelfjorden

Røye



Tempelfjorden

Røye

